NATIONAL COOPERATIVE
HIGHWAY RESEARCH PROGRAM REPORT **318**

ROADSIDE SAFETY DESIGN FOR SMALL VEHICLES

TRANSPORTATION RESEARCH BOARD
NATIONAL RESEARCH COUNCIL

NATIONAL COOPERATIVE HIGHWAY RESEARCH PROGRAM REPORT **318**

ROADSIDE SAFETY DESIGN FOR SMALL VEHICLES

H. E. ROSS, JR., H. S. PERERA, D. L. SICKING
and R. P. BLIGH
Texas Transportation Institute
Texas A&M Research Foundation
The Texas A&M University System
College Station, Texas

RESEARCH SPONSORED BY THE AMERICAN ASSOCIATION OF STATE HIGHWAY AND TRANSPORTATION OFFICIALS IN COOPERATION WITH THE FEDERAL HIGHWAY ADMINISTRATION

AREAS OF INTEREST:

Transportation Safety
Vehicle Characteristics
(Highway Transportation)

TRANSPORTATION RESEARCH BOARD
NATIONAL RESEARCH COUNCIL
WASHINGTON, D.C.

MAY 1989

NATIONAL COOPERATIVE HIGHWAY RESEARCH PROGRAM

Systematic, well-designed research provides the most effective approach to the solution of many problems facing highway administrators and engineers. Often, highway problems are of local interest and can best be studied by highway departments individually or in cooperation with their state universities and others. However, the accelerating growth of highway transportation develops increasingly complex problems of wide interest to highway authorities. These problems are best studied through a coordinated program of cooperative research.

In recognition of these needs, the highway administrators of the American Association of State Highway and Transportation Officials initiated in 1962 an objective national highway research program employing modern scientific techniques. This program is supported on a continuing basis by funds from participating member states of the Association and it receives the full cooperation and support of the Federal Highway Administration, United States Department of Transportation.

The Transportation Research Board of the National Research Council was requested by the Association to administer the research program because of the Board's recognized objectivity and understanding of modern research practices. The Board is uniquely suited for this purpose as: it maintains an extensive committee structure from which authorities on any highway transportation subject may be drawn; it possesses avenues of communications and cooperation with federal, state, and local governmental agencies, universities, and industry; its relationship to the National Research Council is an insurance of objectivity; it maintains a full-time research correlation staff of specialists in highway transportation matters to bring the findings of research directly to those who are in a position to use them.

The program is developed on the basis of research needs identified by chief administrators of the highway and transportation departments and by committees of AASHTO. Each year, specific areas of research needs to be included in the program are proposed to the National Research Council and the Board by the American Association of State Highway and Transportation Officials. Research projects to fulfill these needs are defined by the Board, and qualified research agencies are selected from those that have submitted proposals. Administration and surveillance of research contracts are the responsibilities of the National Research Council and the Transportation Research Board.

The needs for highway research are many, and the National Cooperative Highway Research Program can make significant contributions to the solution of highway transportation problems of mutual concern to many responsible groups. The program, however, is intended to complement rather than to substitute for or duplicate other highway research programs.

NCHRP REPORT 318

Project 22-6 FY'85

ISSN 0077-5614

ISBN 0-309-04615-7

L. C. Catalog Card No. 89-80139

Price $10.00

NOTICE

The project that is the subject of this report was a part of the National Cooperative Highway Research Program conducted by the Transportation Research Board with the approval of the Governing Board of the National Research Council. Such approval reflects the Governing Board's judgment that the program concerned is of national importance and appropriate with respect to both the purposes and resources of the National Research Council.

The members of the technical committee selected to monitor this project and to review this report were chosen for recognized scholarly competence and with due consideration for the balance of disciplines appropriate to the project. The opinions and conclusions expressed or implied are those of the research agency that performed the research, and, while they have been accepted as appropriate by the technical committee, they are not necessarily those of the Transportation Research Board, the National Research Council, the American Association of State Highway and Transportation officials, or the Federal Highway Administration, U.S. Department of Transportation.

Each report is reviewed and accepted for publication by the technical committee according to procedures established and monitored by the Transportation Research Board Executive Committee and the Governing Board of the National Research Council.

Special Notice

The Transportation Research Board, the National Research Council, the Federal Highway Administration, the American Association of State Highway and Transportation Officials, and the individual states participating in the National Cooperative Highway Research Program do not endorse products or manufacturers. Trade or manufacturers' names appear herein solely because they are considered essential to the object of this report.

Published reports of the

NATIONAL COOPERATIVE HIGHWAY RESEARCH PROGRAM

are available from:

Transportation Research Board
National Research Council
2101 Constitution Avenue, N.W.
Washington, D.C. 20418

Printed in the United States of America

FOREWORD

By Staff
Transportation
Research Board

This report is recommended to highway design engineers, safety engineers, maintenance engineers, researchers, and others concerned with the performance of highway appurtenances and roadside features when impacted by small vehicles. Rigid and flexible longitudinal barriers, breakaway luminaire supports, breakaway and base-bending sign supports, crash cushions, guardrail terminals, and roadside features such as slopes, ditches, driveways, and curbs were evaluated under a full-scale crash test program coupled with extensive computer analyses. Emphasis was placed on the evaluation of the impact performance of widely used roadside safety elements for 1,500-lb vehicles and the identification of potential modifications to existing hardware and roadside features that would accommodate vehicles weighing as little as 1,250 lb.

The size and weight of passenger vehicles on the nation's highways have decreased during the 1980s. However, most highway appurtenances and roadside features were designed to safely accommodate passenger vehicles with weights in the range of 2,250 to 4,500 lb. In the last few years some crash tests have been conducted on roadside elements with lighter weight vehicles. The results of these tests indicate that many of the impacts involving small vehicles are more hazardous than similar crashes with larger vehicles. Some of the roadside hardware have been modified to improve the impact performance with vehicles as light as 1,800 lb.

Prior to the research effort performed under NCHRP Project 22-6, "Roadside Safety Design for Small Vehicles," little was known about the impact performance of appurtenances and roadside features with vehicles lighter than 1,800 lb. The objectives of this project were to assess the performance of selected highway safety appurtenances and roadside features with passenger vehicles below 1,800 lb and to project the limits of vehicle characteristics that can be safely accommodated through improvements in current hardware and roadside features.

The researchers identified problem areas with many of the highway appurtenances in common use, described the variables involved in the vehicle-appurtenance interaction and, in most cases, suggested modifications to extend the impact performance of the systems and features evaluated to safely accommodate vehicles as light as 1,250 lb. For those highway appurtenances that could not be modified to accommodate these small vehicles, the researchers identified safe vehicle weight limits. Specific findings are provided for concrete safety shape barrier; G4(1S) roadside barrier; breakaway luminaire supports with transformer and slip bases; breakaway sign supports; GREAT, Hi-Dri, and sand-filled plastic barrel crash cushions; breakaway cable terminals (BCT) and guardrail extruder terminals (GET); roadside slopes, ditches and driveways; and AASHTO curb types C, E, and G.

The researchers concluded with specific recommendations that should be considered in the modification of national roadside design and barrier performance standards to accommodate small vehicles.

CONTENTS

ACKNOWLEDGMENTS

The research reported herein was performed under NCHRP Project 22-6 by the Texas Transportation Institute (TTI), Texas A&M University, and Cranfield Institute of Technology (CIT), Bedford, England. TTI was the contractor for this study. The work undertaken at CIT was under a subcontract with TTI.

Hayes E. Ross, Jr., Professor of Civil Engineering and Head, Structural Research Division, TTI, was the principal investigator. The other authors of this report are: Huron S. Perera, Engineering Research Associate, TTI; Dean L. Sicking, Assistant Research Engineer, TTI; and Roger P. Bligh, Engineering Research Associate, TTI.

The work was done under the general supervision of Professor Ross. The work at CIT was done under the supervision of Professor John Robertson.

The authors are indebted to Asif Qureshy, Earl Worthington, Narayana Sripadanna, Rebecca Kubena, Doris Calhoun, and Patrick McConal for their assistance in preparing the report. The able assistance of TTI Proving Ground personnel, including Wanda Campise, James Bradley, and Richard Zimmer, is also appreciated.

ROADSIDE SAFETY DESIGN FOR SMALL VEHICLES

SUMMARY

Most roadside safety elements have been designed for vehicles weighing 2,250 lb or more. An effort has been made since the publication of *NCHRP Report 230* in 1981 to modify existing designs and to develop new designs to accommodate an 1,800-lb design vehicle. The trend is toward even smaller, more fuel efficient vehicles. At the time of this writing there were at least four minicars on the U.S. markets, two of which have a curb weight of approximately 1,500 lb.

This project had two basic objectives; (1) to evaluate the impact performance of widely used roadside safety elements for a 1,500-lb vehicle, using *NCHRP Report 230* performance guidelines, and (2) to identify potential modifications that would enable existing roadside safety elements to accommodate a design vehicle weighing as little as 1,250 lb. A full-scale crash test program coupled with an extensive computer analysis study were used to accomplish the objectives.

Specific roadside safety elements (roadside hardware and roadside features) analyzed and conclusions reached about each follow.

Concrete Safety-Shaped Barriers (CSSB). Barrier performance is acceptable for cars weighing as little as 1,250 lb based on *NCHRP Report 230* performance guidelines. However, modifications may be needed to reduce overturn accidents associated with nontracking or high angle impacts. It is estimated that approximately 50 percent of inadvertent run-off-the-road vehicular encroachments occur in a nontracking mode.

G4(1S) Roadside Barriers. Barrier performance is acceptable for cars weighing as little as 1,250 lb. Minor modifications may be needed to minimize wheel snag.

Breakaway Luminaire Supports. Most supports with transformer bases are not in compliance with existing performance guidelines for an 1,800-lb vehicle. It is doubtful that the transformer base can be modified to accommodate a vehicle weighing 1,500 lb. Moderate size steel or aluminum supports with the slip-base design are acceptable for a 1,500-lb vehicle. For taller supports, acceptable performance can be achieved if aluminum or lightweight materials are used, provided a slip base is used.

Breakaway Sign Supports. Most sign supports with the slip-base design, or an equivalent design, will be acceptable for vehicles weighing 1,500 lb or more.

Base-Bending Sign Supports. A 4-lb/ft rail steel, single U-post is marginally acceptable for a 1,200-lb vehicle. Improvement in the performance of the U-post can be achieved by the use of a two-piece support with a short bolted splice at ground level.

Crash Cushions. None of the current crash cushions would be acceptable for a 1,500-lb vehicle. The sand-filled plastic barrel system can easily be designed to accommodate a 1,300-lb vehicle. The GREAT and Hi-Dri systems could be modified to accommodate a 1,500-lb vehicle.

Guardrail Terminals. Performance of the "eccentric loader" breakaway cable terminal (BCT) is not acceptable for a 1,500-lb vehicle. Performance can be improved by reducing the mass of the nose and by further reducing the force needed to buckle or collapse the W-beam. A new "guardrail extruder terminal" (GET) shows promise as a cost-effective design and could possibly be modified for minicar criteria. The SENTRE system could be modified to accommodate a 1,500-lb vehicle.

Slopes, Ditches, and Driveways. The behavior of sub-1,800-lb cars on these features is similar to larger cars for encroachments on smooth, well-compacted terrain. However, soft terrain or terrain irregularities, such as large rocks or eroded areas, pose an increased risk to occupants of a small car. It was shown that terrain objects that would not trip a large vehicle would trip and overturn a smaller one. It is not clear if current design guidelines for the above features should be changed to accommodate sub-1,800-lb vehicles. At a minimum, more care would have to be exercised in their construction and maintenance to avoid an increase in overturn accidents.

Curbs. Six-inch high curbs can easily be traversed by a 1,250-lb car if it impacts the curb in a tracking (nonskidding) condition. For nontracking impacts a small car will overturn more easily than a larger car. To minimize overturn accidents of nontracking minicars, the face of the curb should be sloped as flat as possible. AASHTO curb types C, E, and G or similarly sloped designs are preferred.

CHAPTER ONE

INTRODUCTION AND RESEARCH APPROACH

PROBLEM STATEMENT

Spurred by Federal regulation and consumer demand, auto manufacturers have reduced the weight and size of passenger vehicle models and are developing even smaller models. Consumers are purchasing the smaller sized models in increasing numbers. Several cars weighing less than 1,800 lb are now being marketed in the United States, and others are planned for the near future. Table 1 lists cars in this classification now on the U.S. market.

Most current roadside safety features were designed and tested with passenger vehicles ranging from 4,500 lb down to 2,250 lb. Research is currently in progress to develop hardware and roadside features for vehicles in the 1,800-lb range. Under some conditions, impacts with safety features become increasingly hazardous for smaller vehicles; however, little is known about the performance of current hardware and roadside safety features with vehicles weighing less than 1,800 lb. Research is needed to gain insight on the effectiveness of hardware and roadside features for these vehicles and to determine how small the vehicles can become before the development of effective safety design is no longer feasible.

OBJECTIVES

The objectives of this project are (1) to assess the performance of selected existing highway safety appurtenances and roadside features with passenger vehicles below 1,800 lb and (2) to project the limits of vehicle characteristics that can be safely accommodated through improvements in current hardware and roadside features.

SCOPE

This project consisted of two phases. In Phase I the following tasks were addressed:

Task 1—Review, evaluate, and document foreign and domestic information on the performance of safety appurtenances and roadside features with passenger vehicles weighing 1,800 lb and less.

Task 2—Identify all types of 4-wheel sedans below 1,800 lb that may constitute a significant portion of the vehicle fleet in the United States within the next 10 years. For the vehicle types identified, acquire, measure, or, where necessary, estimate the dynamic properties and other characteristics required for the computerized simulation of their reactions with safety hardware and roadside features.

Task 3—Select specific appurtenances for study in this project. Special emphasis shall be given to systems presently being installed in significant numbers and having a reasonable probability of successful impact performance with small cars. The following items shall be included: a rigid longitudinal barrier; a flexible longitudinal barrier; a breakaway support; a base-bending support; an impact attenuator; and a guardrail terminal.

Task 4—Select specific roadside features for study to identify performance limits when traversed by small cars. As a minimum, these features shall include slopes, ditches, and curbs.

Task 5—Using available data from crash tests with the lightest vehicles tested, calibrate selected existing computer programs for simulation of impact performance, and use the calibrated programs to simulate occupant-risk tests for the selected hardware and roadside features with a 1,500-lb sedan.

Task 6—Prepare an interim report on the findings of Tasks 1 through 5. This report shall contain a detailed working plan for the remainder of the study. NCHRP approval of the interim report will be required before initiation of Phase II.

Phase II tasks included the following:

Task 7—Conduct full-scale crash tests using vehicles in the 1,200 to 1,500-lb range to recalibrate the model and to demonstrate the validity of the computerized simulation to be carried out concurrently in Task 8.

Task 8—Using existing simulation models for a variety of appurtenances and roadside features (including potential improvements), vehicle types (including projections down to the lowest conceivable weight range), and crash test conditions, delineate the limiting values of particular vehicle characteristics for which feasible designs are capable of providing satisfactory performance according to the guidelines in *NCHRP Report 230* (*1*). When these evaluation criteria are not satisfied, determine the changes in impact conditions that would be required to achieve compliance.

Task 9—Based on this research, identify design modifications to hardware and roadside features to improve performance for vehicles at the low end of the weight spectrum. Such modification shall be supported by computerized simulation.

Task 10—Prepare a final report.

RESEARCH APPROACH

Collection of information on vehicles weighing 1,800 lb or less was pursued through the Transportation Research Information Service (TRIS) computerized information retrieval system, through direct contact with researchers in the United States and foreign countries, and through a survey mailed to individuals and agencies worldwide. The researchers also relied heavily on international automobile trade magazines and publications to secure small car information.

The Texas Transportation Institute (TTI) subcontracted with Cranfield Institute of Technology (CIT) in Bedford, England, to acquire and measure the properties of under 1,800-lb automobiles. CIT was chosen for this task because of the large variety of small cars in use in England and because CIT had a test facility to measure the various vehicle properties needed for computer simulation. A total of ten cars was purchased and shipped to TTI. It is noted that at the time the project began (1985) there were no under 1,800-lb cars available in the United States. In the latter part of the project a Chevrolet Sprint, weighing approximately 1,500 lb, was purchased locally and crash tested. Its dimensions and inertia properties were measured at TTI.

Selection was made of roadside safety hardware for study in the project after a review of the candidate systems. Each item selected satisfied three criteria: (1) it met current safety performance standards, (2) it was widely used, and (3) there was a reasonably good probability that it would be successful for impacts with under 1,800-lb cars. Rigid and flexible longitudinal barriers were selected, as were breakaway sign and luminaire supports, a base-bending sign support, crash cushions, and a guardrail terminal.

Roadside geometric features were also selected for study. These included fill and cut slopes, ditch sections, curbs, and driveways. Typical slopes, fill heights, ditch depths, and cross-section combinations were selected.

Simulations of vehicle impacts with roadside safety hardware were made with the GUARD program (*2*) and a modified version of the HVOSM program (*3*). Simulations of vehicle encroachments on roadside geometric features were made with the HVOSM (Highway Vehicle-Object Simulation) program. In Phase I of the project these programs were calibrated with existing data from full-scale crash tests of small cars. Practically all of the test data involved vehicles weighing approximately 1,800 lb. In Phase II the programs were recalibrated with data derived from the Phase II full-scale crash tests.

A total of seven different roadside features were subjected to a series of full-scale crash tests. They were: (1) concrete safety-shaped barrier; (2) strong-post, W-beam guardrail on steel posts; (3) luminaire support mounted on a frangible transformer base; (4) base-bending small sign support; (5) eccentric-loader" end treatment for W-beam guardrail; (6) AASHTO type "B" curb, 6 in. high; and (7) side-slope, driveway slope combination. These tests provided valuable insight on the performance of under 1,800-lb cars impacting widely used roadside safety features. They also provided a data base from which the aforementioned computer programs could be further calibrated for minicar simulation.

CHAPTER TWO

FINDINGS

MINICAR DATA

At the beginning of this project in 1985, only one under 1,800-lb car was available in the United States and it was being test marketed in the western states. At the time of this writing (early 1988), four such cars are now being sold nationwide (see Table 1). Worldwide, the minicar has been prevalent for several years,

Table 1. Under 1,800-lb cars sold in the United States (1987–1988 model year).

NAME	APPROXIMATE CURB WEIGHT (lb)	APPROXIMATE WHEEL BASE (in.)	BEGINNING MARKET DATE
Chevrolet Sprint	1600	88.4	1985-86
Daihatsu Charade	1780	91.3	1987-88
Subaru Justy	1660	90.0	1987-88
Ford Festiva	1710	90.2	1987-88

especially in European and Asian countries. A review of the literature and trade magazines revealed that there are in excess of 50 models of under 1,800-lb cars on the world market. A compilation of minicars sold worldwide was presented in the Phase I interim report (*4*).

While minicars have been used extensively in other countries, there is a sparsity of data on their impact performance as related to roadside safety features. A number of tests have been conducted in recent years in the United States with cars in the 1,700-lb to 2,000-lb range. These tests have followed and are a consequence of the publication of *NCHRP Report 230* (*1*) in 1981, the adoption of the 1,800-lb vehicle as a standard by the FHWA upon publication of *NCHRP Report 230,* and the adoption of the 1,800-lb test vehicle in the 1985 AASHTO specifications for structural supports for luminaires, signs, and traffic signals (*5*). Shown in the tables of Appendix A is a compilation of tests with minicars to date.

A review of studies summarized in Appendix A indicated there were potential problem areas in the impact performance of roadside safety features for small vehicles. These are summarized as follows:

1. *Longitudinal Barriers:*
   a. Wheel snag—There is a tendency for the front, impact side, wheel to snag on barrier posts, particularly for impact angles of 20 deg or greater. This is attributed to (a) structural aspects of front-wheel drive vehicles, including the tire and wheel diameters and the wheel design, (b) close proximity of front wheel to front bumper, and (c) close proximity of front wheel to outside edge of fender sheet metal.
   b. Stability—The small car appears to have a greater propensity for overturn following impact with the concrete safety shaped barrier. This is attributed to tire climb and the relative instability of the small car.

2. *Longitudinal Barrier End Treatments:*
   a. Stability—The small car has a greater propensity for overturn, especially for the turned-down W-beam treatment. Overturns have also occurred following off-center impacts with the breakaway cable terminal (BCT).
   b. Velocity change—Excessive occupant impact velocities have occurred following impact with the BCT. This is due to the lower mass of the small car.

3. *Luminaire and Sign Supports*:
   a. Stability—The small car has a greater propensity for overturn after impact with a support, especially for an off-center impact. An off-center impact causes the vehicle to yaw (spin), and if the yaw is excessive, the tires can engage terrain irregularities and soft soil that can result in an overturn.
   b. Velocity change—For a given luminaire or sign support system, the change in vehicular velocity increases as the mass of the vehicle decreases. In turn, the occupant impact velocity increases.

4. *Crash Cushions*:
   a. Velocity Change—For a given crash cushion, the change in vehicular velocity increases as the mass of the vehicle decreases. In turn, the occupant impact velocity increases.

SELECTION OF MINICARS AND MEASUREMENT OF THEIR PROPERTIES

A review of the literature produced very little in-depth data on under 1,800-lb cars suitable for use in computer simulation programs. Data on suspension properties, mass distribution, and inertia properties are difficult to measure and are not readily available from automobile manufacturers.

In the absence of data, TTI subcontracted with the Cranfield Institute of Technology (CIT), Bedford, England, to acquire and measure properties of selected autos. Use of under 1,800-lb cars is widespread in the United Kingdom, and the researchers had a number of models from which to choose.

Several factors were used in the selection process. First, it was decided that the cars selected should encompass the size and weight range of interest, i.e., one car should weigh less than 1,300 lb, one should be in the 1,300-lb to 1,500-lb weight range, and one should be in the 1,550-lb to 1,800-lb range. Further, it was desirable that the cars be representative of the type of cars that may constitute a meaningful portion of the USA market in the near future. And, lastly, it was desirable that a reasonable number of cars be purchased within the project budget for crash test purposes. Using these criteria, the following cars were purchased:

Name	Approximate Curb Weight (lb)	No. Purchased
Daihatsu Domino (1983)	1,250	1
Fiat Uno*	1,500	8
Ford Fiesta (1982)	1,600	1

*Seven Unos were 1985 models and one was a 1983 model.

Photos of the above three cars are shown in Figure 1, together with a 1979 Honda Civic for comparison. Note that the steering wheel is on the right side of each car. For purposes of comparison, the rear bumpers are aligned parallel so that the overall lengths can be compared in the front profile view. The Honda Civic has been widely used in the United States in recent years as a test vehicle to represent the small car population. Manufacturers' specifications for the cars were given in the Phase I report (*4*). The Fiat Uno was chosen to represent the mid-range of the under 1,800-lb cars in this project for purposes of crash testing and for most of the computer simulation work. It was used to examine the impact performance of each major roadside feature. The other two cars were used to examine the limits of performance of selected roadside features.

Dimensions, inertia properties, and suspension properties of the Daihatsu, one of the 1985 Fiats, and the Ford were measured by CIT. A complete report of the CIT work was included in the Phase I report (*4*). Data from CIT, suitable for use in computer simulation programs HVOSM, GUARD, and BARRIER VII, are summarized in Appendix B.

In the latter part of the project, a 1985 Chevrolet Sprint was also purchased and crash tested. Dimensions and inertia properties of the Sprint, as measured at TTI, are also given in Appendix B.

Table 2 is a summary of the properties of the four cars used in the present project, together with the properties of three other small cars. The Honda Civic has been widely used in the United States as a test vehicle to measure impact severity of most roadside safety features. It can be seen that properties of the

Honda Civic compare reasonably well with the other small cars. The source (*6*) for data on "Vehicle 1" and "Vehicle 2" did not reveal the make or model for these cars.

A key but unknown property of the four cars evaluated in the project was the frontal crush characteristic. The Daihatsu Domino, Fiat Uno, and Ford Fiesta are European cars with bumper standards different from those in the United States. The European cars do adhere to a "front and rear protective device (bumpers, etc.)" standard developed in 1980. In summary, the cars are subjected to a 2.5-mph "impactor" test on the front and rear bumpers. The standard does not necessarily require a damage-free vehicle after the test. The requirements state that certain items on the vehicle must be functional after the test, such as lighting and signaling devices, hood and doors, fuel and cooling systems.

It is noted that the U.S. Department of Transportation, National Highway Traffic Safety Administration, has recently reduced the requirements for car bumpers. According to the latest standards, a vehicle should be able to sustain a 2.5-mph front or rear impact with no damage. The authors have serious doubts that certain cars in Table 1, and now on the U.S. market, will meet the 2.5-mph standard. Further discussions of the structural design and crush properties of small cars and the effect these factors have on the performance of roadside safety features are given in subsequent sections.

PERFORMANCE OF SELECTED ROADSIDE SAFETY ELEMENTS FOR MINICARS

In accordance with project requirements, specific roadside safety hardware and geometric features were selected for study. Emphasis was given to widely used systems having a reasonable probability of success when impacted by small cars. A three-step procedure was followed in evaluating the hardware and

Figure 1. 1983 Daihatsu, 1985 Fiat Uno, 1982 Ford Fiesta, and 1979 Honda Civic: (a) front profile; (b) rear profile.

Table 2. Comparison of vehicle properties.

PROPERTY	1983 DAIHATSU DOMINO	1985 FIAT UNO	1982 FORD FIESTA	1985 CHEVROLET SPRINT	1978 HONDA CIVIC[b]	VEHICLE 1[a]	VEHICLE 2[a]	RANGE OF VALUES
Curb Weight (lb)	1,250	1,477	1,613	1,554	1,699	1,244	1,355	1,250 - 1,699
Wheelbase (in.)	84.7	93.0	89.8	88.3	86.3	N/A	N/A	84.7 - 93.0
Front Track (in.)	49.9	52.8	53.2	52.4	51.1	N/A	N/A	49.9 - 53.2
Rear Track (in.)	48.6	51.2	52.4	51.2	51.1	N/A	N/A	48.6 - 52.4
Overall Length (in.)	124.3	143.5	142.5	143.5	140.25	N/A	N/A	124.3 - 143.5
Overall Width (in.)	54.5	60.3	61.5	60.0	59.4	N/A	N/A	54.5 - 61.5
Tire Size	145SR10	145SR13	145R12	145PR12	155SR12	N/A	N/A	-
C.G. Position (in.)[d]								
Above Ground	20.2	21.7	21.2	20.2	20.4	22.9	20.8	20.2 - 22.9
Aft of Front Axle	32.3	30.4	33.2	33.0	31.8	N/A	N/A	30.4 - 33.2
Moment of Inertia (lb-in.-sec^2)								
Roll	1196[c]	1677[c]	1528[c]	1426[c]	1569[c]	2000[d]	1800[d]	1196[c] - 1677[c]
Pitch	5130[c]	7259[c]	7209[c]	6826[c]	7107[c]	4180[d]	4790[d]	5130[c] - 7259[c]
Yaw	4815[c]	6634[c]	6854[c]	6858[c]	5013[c]	4960[d]	5740[d]	4815[c] - 6858[c]

[a]From Reference 6
[b]From Reference 7
[c]Values are for sprung mass.
[d]Values are for total mass.

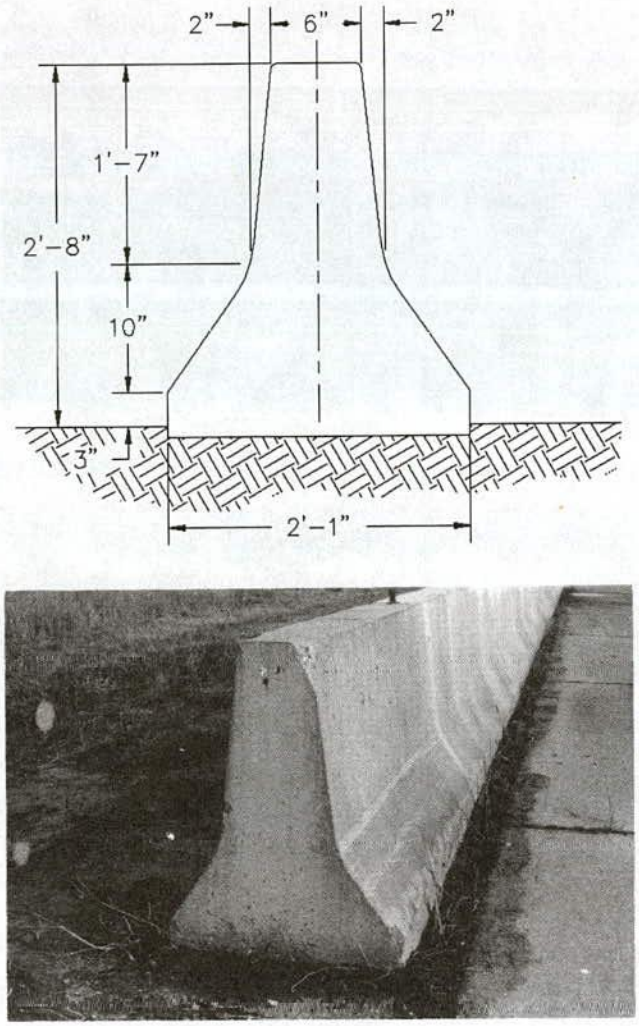

Figure 2. Concrete safety-shaped barrier.

features. In the first step, computer programs GUARD (*2*) and HVOSM (*3*) were calibrated with available small car crash test data. The programs were then used to simulate impacts by a 1,500-lb car with the hardware and to simulate encroachments by a 1,500-lb car on the geometric features. In the second, a series of full-scale crash tests were conducted using under 1,800-lb cars. The purpose of these tests was to gain further insight on the performance of selected safety hardware and roadside geometric features for small car impacts. The tests also provided a valuable data base from which the computer programs could be recalibrated. The third and final step involved the recalibration of the computer programs to verify, and improve where necessary, the original simulation.

Impact performance of the hardware was judged in terms of the evaluation criteria of *NCHRP Report 230* (*1*). Performance of the roadside geometric features was judged primarily in terms of vehicle stability. In most cases, a roadside geometric feature such as a ditch, embankment, or driveway will have acceptable performance if the encroaching vehicle can traverse the feature without overturning. The feature is judged to have unacceptable performance if the vehicle overturns or if it experiences excessive decelerations.

Roadside Hardware

Rigid Longitudinal Barriers

The concrete safety-shaped barrier (CSSB) with the "New Jersey" shape was selected because it is a widely used rigid longitudinal barrier. It is designed as "MB5" in the AASHTO Barrier Guide (*10*). A cross section of the barrier is shown in Figure 2. Although the CSSB was initially used as a median barrier, it is now widely used as a roadside barrier, as a bridge railing, and as a temporary barrier in construction or work zones.

Based on a series of computer simulations and five full-scale crash tests, the impact performance of the CSSB was judged to be in compliance with the recommended evaluation criteria of *NCHRP Report 230* (*1*) for all under 1,800-lb cars investigated including a car weighing only 1,250 lb. This included evaluations according to test S12 in the "minimum test matrix" and test S13 in the "supplemental test matrix."

It is important at this point to discuss the impact conditions recommended in *NCHRP Report 230* to evaluate occupant risk for a longitudinal barrier. The vehicle is directed into the barrier in a tracking (no cornering or skidding) mode at 60 mph at an impact angle of 15 deg for test S12 and 20 deg for test S13. As stated above, under these conditions the CSSB exhibited acceptable performance for the minicars.

Council, et al. (*11*) recently completed a study in which small car accident data from a variety of studies were examined. It was found that small vehicles have an increased propensity to overturn in almost all types of accidents, including impacts with the CSSB. An ongoing study at TTI is also addressing rollover problems with the CSSB (*64*). Because simulations and crash tests of the CSSB, conducted in accordance with *NCHRP Report 230* recommendations, gave no indication of increased overturn propensity for minicars, an attempt was made to investigate the disparity between results of this project and evidence from accident studies. As reported in Ref. 23, a large percentage of single-vehicle accidents involves a skidding or nontracking vehicle. A nontracking vehicle, as used herein, is one in which there is some lateral component of vehicular velocity at impact or at the time of encroachment on the roadside. A series of computer runs were made to study the impact behavior of minicars, as well as larger cars, for nontracking impacts with the CSSB. Results of those runs, although somewhat tentative and subject to verification, clearly point to greater overturn propensity of the minicars for these impact conditions.

Computer simulations were also made to study tracking impacts at lower speeds and at higher impact angles than recommended in *NCHRP Report 230*. For these conditions the minicars also had a greater propensity for overturn than did the larger cars.

These results offer some insight into possible reasons minicars have a greater overturn propensity in CSSB accidents. The results also raise interesting questions about the degree to which current impact performance tests reflect critical real-world accident conditions.

As will be discussed later, the nature of the pavement surface and roadside surface over which the vehicle travels before and after impact is also a factor in the vehicle's stability.

Flexible Longitudinal Barriers

The G4(1S) (*10*) roadside barrier was selected as a representative, flexible longitudinal barrier. A cross section of the barrier is shown in Figure 3. The steel W-beam is supported by steel posts spaced 6.25 ft apart. This system, together with the G4(2W) (*10*), is the most widely used roadside barrier in the United States. Tests have shown that they have similar impact behavior for given impact conditions.

On the basis of a series of computer simulations and two full-scale crash tests, the impact performance of the G4(1S) was judged to be in compliance with the recommended evaluation criteria of *NCHRP Report 230* for all under 1,800-lb cars investigated. This included evaluations according to tests S12 and S13.

It is noted that in one of the two crash tests, the vehicle ultimately overturned. This result, however, was not attributed to improper barrier performance. Upon impact at 60 mph at a 15-deg angle the car was smoothly redirected. The car then turned back toward the barrier, began to slide sideways, and encountered soft soil that had been weakened by recent rains. The tires dug into the soil which tripped and overturned the vehicle. It is believed that a larger car would probably not have overturned under the same conditions. As discussed in subsequent sections, smaller cars have a reduced threshold of stability and conditions, such as those just described, that can trip a small car but will not trip a larger car. It is also noted that overturn did not occur when the same barrier was impacted at 60 mph at a 20-deg angle with the same model car. A post-impact trajectory similar to that in the 15-deg impact occurred, but the soil was dry and compacted.

Nontracking impacts with the G4(1S) system were not simulated. As discussed later in this chapter, under "Modifications to Selected Roadside Safety Elements to Accommodate Minicars," overturn of the nontracking minicar was virtually eliminated in the CSSB by the use of a vertically faced barrier. The G4(1S) is essentially a vertically faced barrier and very little vehicular roll or pitch motions occur during minicar impacts.

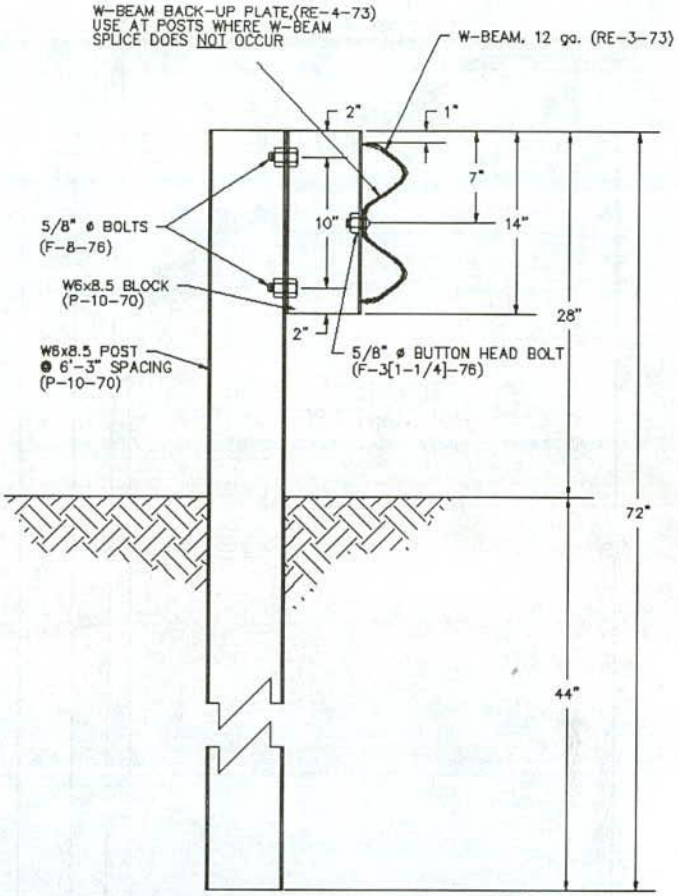

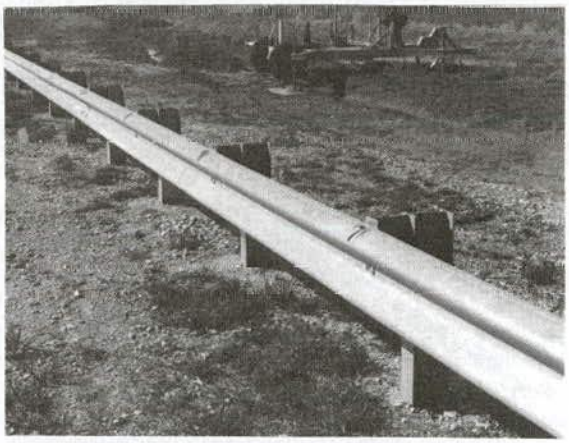

Figure 3. G4(1S) roadside barrier.

Breakaway Luminaire Supports

From discussions with FHWA and industry representatives, it was determined that cast aluminum transformer bases continue to be the most widely used breakaway device for roadside luminaire supports. It was further determined that a pole with a 40-ft to 45-ft mounting height and a 15-ft mast arm is a typical, widely used support configuration. Steel and aluminum poles are widely used, with neither having a disproportionate share of the market. The steel pole and luminaire support structure selected was as shown in Figure 4. Further details of the transformer base are given in Appendix C, test 6.

On the basis of a full-scale crash test of the system with a 1,500-lb car impacting at 20 mph, it is concluded that this and similar transformer bases will not satisfy the *NCHRP Report 230* evaluation criteria for under 1,800-lb cars. In fact, subsequent to the test reported herein, it was learned that tests of a wide variety of cast aluminum transformer bases with an 1,800-lb bogie (*12*) were unsuccessful in terms of the *NCHRP Report 230* criteria and AASHTO standards (*5*). Efforts are under way by industry to address this problem.

Analysis showed that many widely used luminaire poles that are mounted on slip bases will exhibit acceptable impact performance for under 1,800-lb cars. For example, the analysis indicates that a 35-ft steel pole with a 20-ft mast and a multidirectional slip base with a total weight of approximately 500 lb will satisfy current AASHTO criteria (*5*) for a vehicle weighing 1,250 lb.

A computer program was developed to assist in the design and analysis of breakaway sign and luminaire supports for minicar impacts. It is used to estimate the vehicular velocity change that occurs during impact with a breakaway sign or luminaire

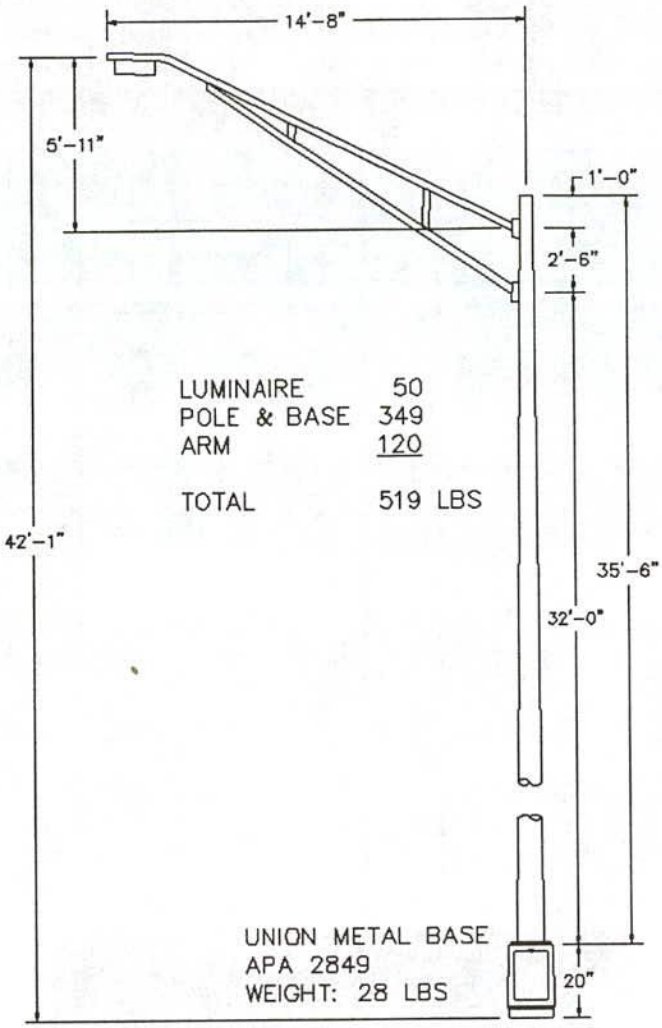

Figure 4. Luminaire support.

support. The program can be used to examine the sensitivity of impact performance to key vehicular and support parameters. Effects of structural stiffness, mass, and speed of the vehicle can be studied. Effects of mass, length, slip force, location of hinge (for a sign post), and vertical position of impact force aboveground of the support can be studied. An interesting result found by use of the program is the relatively high degree of sensitivity of impact performance to the position of the impact force on the support. This has major implications for supports located on nonlevel terrain and for impacts by the side of a vehicle. Another interesting result is the degree of sensitivity of impact performance to the activation (or lack thereof) of the hinge on a sign post, especially for a large post impacted at a high speed. Further details of the program and its applications are given in a later section of this chapter, under "Modifications to Selected Roadside Safety Elements to Accommodate Minicars," "Roadside Hardware"; and in Chapter Three, under "Specialized Analytical Procedures," "Breakaway Supports."

Breakaway Sign Supports

Based on tests of a large roadside sign system with a slip base design in which test cars weighing approximately 1,600 lb were used (*13*), it was concluded that further tests of these systems were not warranted in the present study. In the referenced study a 24-ft wide by 12-ft high sign panel supported by two 12WF45 steel posts with a standard slip base design was impacted at 20 mph and 60 mph (one of two posts hit in each test). The vehicular velocity change was approximately 10 ft/sec and 11 ft/sec for the 20 mph and 60 mph impacts, respectively. Because this is one of the largest posts in use and because the velocity changes were well below the 15-ft/sec limit (*1, 5*), it was concluded that, in general, slip-base signs will pose no serious hazard to vehicles in the 1,500-lb weight range, at least for head-on impacts. Impacts, in which the side of the vehicle strikes the support, are known to pose a much greater risk to occupants because of the relatively low lateral stiffness of most vehicles. Also, the vertical location of the resultant force on the support is thought to be higher than that exerted in a head-on impact. Since lateral stiffness is thought to be roughly proportional to the weight (or size) of the vehicle, it follows that as the weight of the design vehicle decreases, the probability of injuries in side impacts increases. To the extent possible this should be considered and breakaway designs that offer the least impact resistance should be sought. Further analysis of breakaway sign supports is given later in this chapter and in Chapter Three.

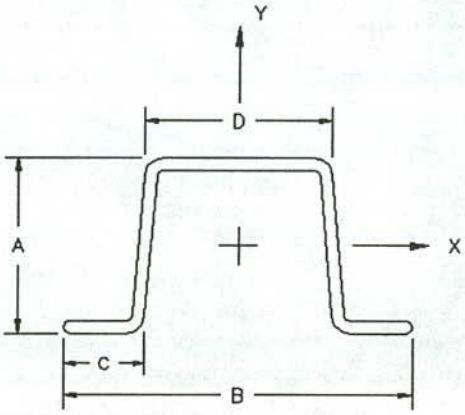

SIGN POST	A (IN)	B (IN)	C (IN)	D (IN)
4.0 lb/ft	1.750	3.50	.797	1.625

I_{XX}= .460 in^4
S_X= .511 in^3
I_{YY}=1.090 in^4
S_Y= .623 in^3

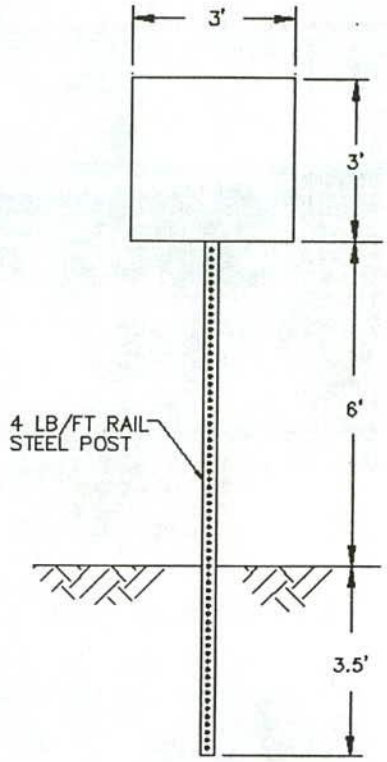

Base-Bending Sign Supports

A study at TTI (*14*) determined that the steel U-post (also called a flanged channel post) is the most widely used base-bending signpost. Sizes vary from 2 lb/ft to 4 lb/ft with the 3-lb/ft post the predominate size. In many installations the post is driven full-length into the soil. In many other installations a base U-post is first driven in the soil. Then a U-post upright is attached to the base with a relatively short, nested splice near ground level. Tests have shown that the post exhibits much better impact performance if it is made from a high carbon, relatively low ductility steel, similar to that in rail steel. Most U-posts are now produced with these properties.

A 4-lb/ft rail steel U-post was selected for evaluation in this study. The test installation was as shown in Figure 5. Note the full-length signpost was driven into the soil 3.5 ft. The sign was impacted at 60 mph with a car weighing approximately 1,500 lb and the impact point was approximately 15 in. to the right of the centerline of the car. Based on this test and supplemental computer simulations, the single 4-lb/ft steel U-post was judged to be in compliance with *NCHRP Report 230* per test 63 for cars weighing 1,500 lb or more. It must be added, however, that the system should be viewed as being only marginally acceptable for several reasons. First, the vehicle sustained considerable damage during the above-described test. Second, while the occupant impact velocity was below the 15-ft/sec limit of *NCHRP Report 230* and AASHTO (*5*), it was above the "desirable" 10-ft/sec value of AASHTO (*5*). Third, although no overturn occurred in the test or in the supplemental computer simulations, the stability of a minicar must be of concern after a noncentric impact with a signpost or other roadside features. The probability of overturn increases as the impulse on the vehicle increases because of the yawing motion that the off-center impulse produces. Fourth, a slow-speed impact test was not conducted. Previous tests of high carbon steel U-posts at

Figure 5. Small sign support details.

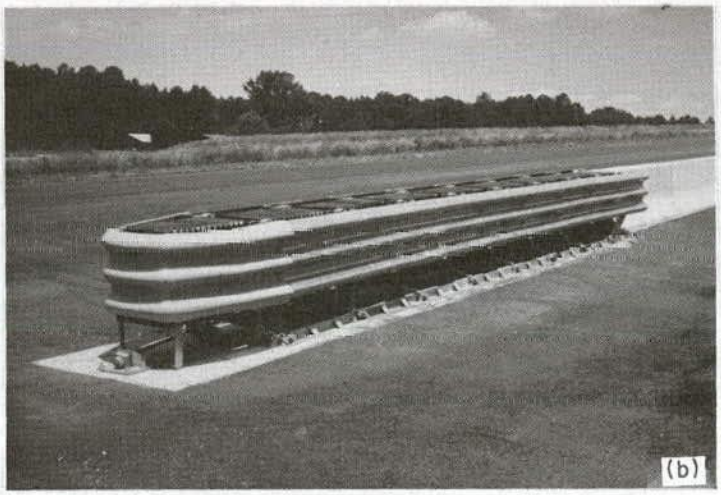

Figure 6. Widely used energy absorption devices: (a) sand-filled plastic barrels; (b) "GREAT" system

both low and high speeds indicate that the occupant impact velocity may be greater at the low-speed impact (*15*).

Further discussions of the estimated limits of performance of other small sign supports now in use are given later in this chapter under "Modifications to Selected Roadside Safety Elements to Accommodate Minicars."

Crash Cushions

It was determined through discussions with industry representatives that the sand-filled plastic barrel cushion and the GREAT system are the most widely used crash cushions. Photographs of these systems are shown in Figure 6. The sand-filled plastic barrel cushion is marketed by two different firms (*16, 17*), while the GREAT system is available from only one source (*16*).

Both systems have been tested and shown to be in compliance with the recommended evaluation criteria of *NCHRP Report 230* for an 1,800-lb vehicle. This includes test 52 for the sand-filled plastic barrel cushion and tests 44 and 45 for the GREAT system. However, neither of these systems, as presently designed and configured for 60-mph impacts, would meet the *NCHRP Report 230* evaluation criteria for under 1,800-lb cars. Nonetheless, as will be discussed later in this chapter, both systems can be designed to meet the *NCHRP Report 230* criteria for a 1,500-lb car without much difficulty.

Guardrail Terminals

The breakaway cable terminal (BCT) developed at the Southwest Research Institute (SWRI) (*18*) and the twisted and turned-down guardrail, sometimes called the "Texas twist" developed at TTI (*19*), are widely used across the United States. Neither, however, satisfies all of the *NCHRP Report 230* criteria for 1,800-lb cars. In recent studies at SWRI, the BCT was redesigned to meet the criteria for an 1,800-lb car (*20*). The new design is known as the "eccentric loader" because a device has been added to the nose of the BCT to apply an eccentric load on the guardrail during impact to enhance the buckling of the rail. The only other guardrail terminal available at the beginning of the project that met the *NCHRP Report 230* criteria for an 1,800-lb car was the SENTRE, a proprietary terminal (*16*). Its use has been limited to date.

For the foregoing reasons the eccentric loader was selected for further evaluation in this study. Details of the eccentric loader are given in Appendix C, test 7043-8, and photographs of the system are shown in Figure 7.

The eccentric loader was impacted head-on by a 1,500-lb car at 60 mph (test 45 in *NCHRP Report 230*). Based on this test it was concluded that the eccentric loader does not satisfy *NCHRP Report 230* criteria for a 1,500-lb car. Discussion of alternate guardrail terminal designs for under 1,800 lb cars is given later in this chapter.

Roadside Features

Slopes

Figure 8 shows the slope variables investigated for both fill and cut slopes. All slope analyses reported herein were made by use of the HVOSM computer program. Details of the analysis are given in Chapter Three, under "Computer Simulation Studies."

Current AASHTO policy (*24*) recommends that fill slopes be 4:1 or flatter if feasible. If the slope is steeper than 3:1, guardrail may be warranted depending on the fill height (*10*). Based on results of the present study, this policy would probably be sufficient for a minicar design vehicle. However, the propensity for overturn on an embankment is greater for a minicar than for larger cars, because surface irregularities, soft soils, etc., become more critical as the design vehicle's size decreases. More attention would have to be given to the construction and maintenance of roadside slopes. Further discussions of factors that should be considered in designing slopes for minicars are given under the section heading "Modifications to Selected

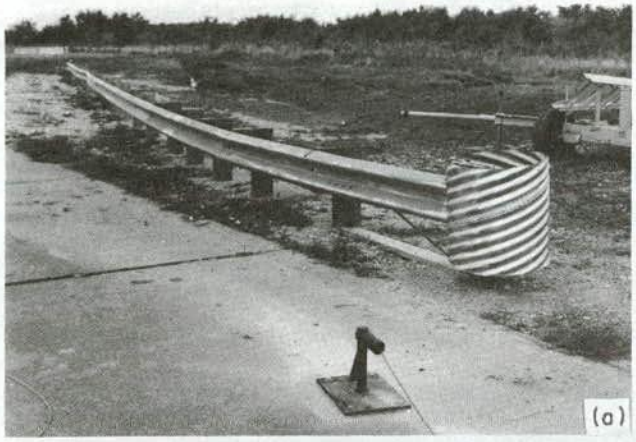

Figure 7. Eccentric loader and treatment: (a) overall view; (b) nose details.

Roadside Safety Elements to Accommodate Minicars."

The safety aspects of cut slopes similar to the geometry depicted in Figure 8 have not been studied in-depth to date. The current AASHTO policy (*24*) suggests that these slopes should normally be 3:1 or flatter, but recognizes that slopes as steep as 2:1 may be necessary. Based on results of the present study, a minicar will overturn on a 2:1 cut slope and a larger car would not. Consideration of 3:1 or flatter cut slopes would therefore be in order for a minicar design vehicle.

Ditches

Figure 9 shows the variables investigated for roadside ditches. All ditch analyses reported herein were made by use of the HVOSM computer program. Details are given in Chapter Three, under the heading "Computer Simulation Studies."

Based on current AASHTO policy (*24, 10*), foreslopes of 4:1 or flatter in combination with backslopes of 3:1 or flatter are recommended. However, foreslopes of 3:1 are acceptable where site conditions do not permit use of flatter slopes. On the basis of the results of the present study, this policy would probably be sufficient for a minicar design vehicle. It is to be noted that

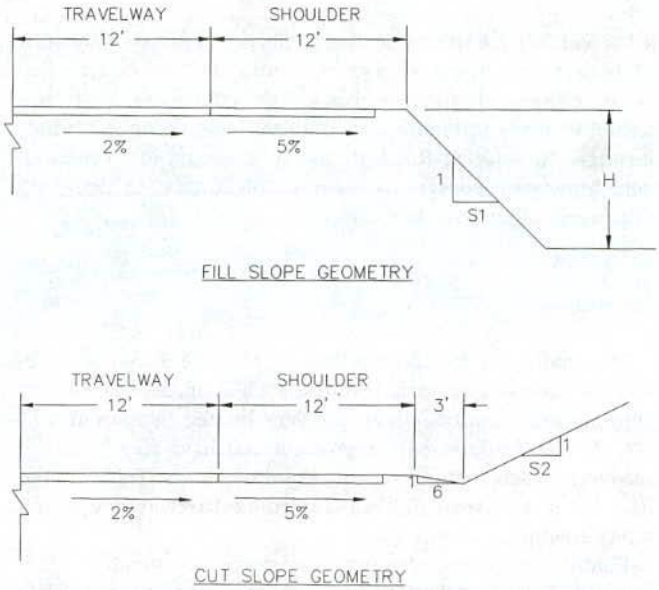

Figure 8. Fill and cut slope parameters.

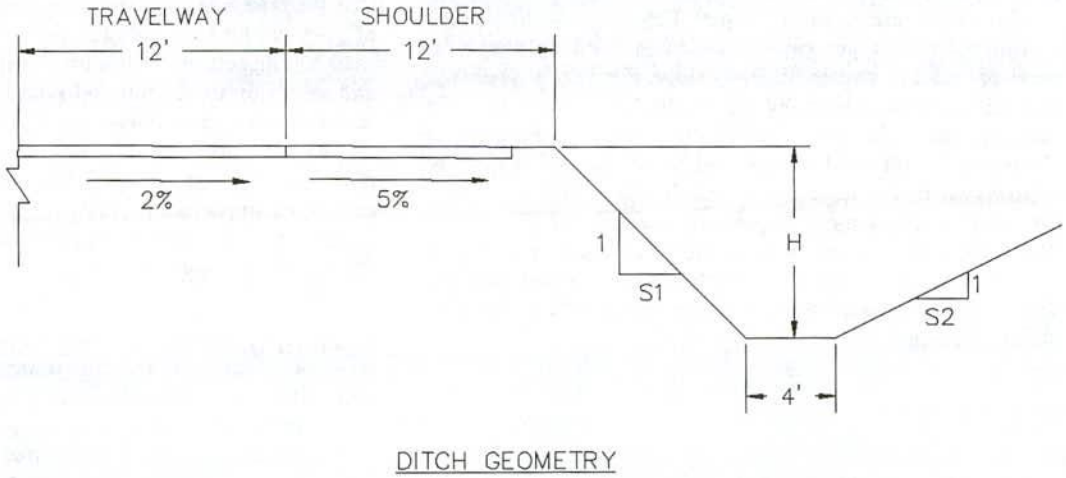

Figure 9. Ditch parameters.

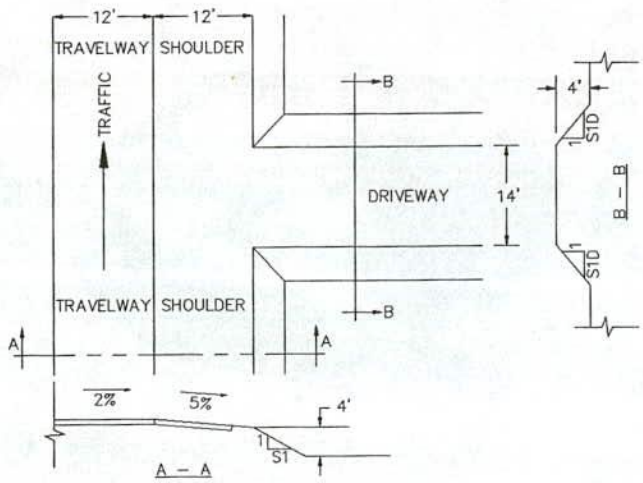

Figure 10. Driveway parameters.

a 4-ft wide ditch bottom was used in the present study. Overturn of minicars can be expected as this width approaches zero, i.e., as the cross section approaches a "V" ditch (*23*). Reference should be made to the discussion, in this chapter under "Modifications to Selected Roadside Safety Elements to Accommodate Minicars," concerning other problem areas in designing slopes and ditches for minicars.

Driveways

Nationally recognized guidelines for the safe design of driveways or similar geometric features, such as median crossovers abutting main thoroughfares, are very limited. Studies at TTI (*26, 27*) have addressed the problem and have clearly shown the hazard these features pose to errant motorists. These studies have led to standards in Texas regarding driveway design and safety treatment of culverts.

Figure 10 shows the driveway parameters investigated. Analysis included use of the HVOSM computer program to simulate vehicular encroachments and two full-scale vehicular tests with minicars. Note that no attempt was made to simulate the effects of a drainage structure or culvert and on the driveway slope. Further details are given in Chapter Three.

Although no national guidelines exist, it is believed that most states use a 6:1 or steeper driveway slope. Further, it is believed that the foreslope is typically 4:1. Studies have shown (*26, 27*) that large cars will overturn on encountering a 4:1 foreslope in combination with a 6:1 driveway slope at speeds *less* than 50 mph. As will be discussed later in this chapter, minicars overturn even more readily than do larger cars on driveways. This means that driveways as presently constructed pose a serous hazard to occupants of the current vehicle population and that the hazard will become more acute as the size of the minicar population increases.

Curbs

Although the use of curbs is discouraged on high-speed roadways, they are still used to a large extent on urban highways.

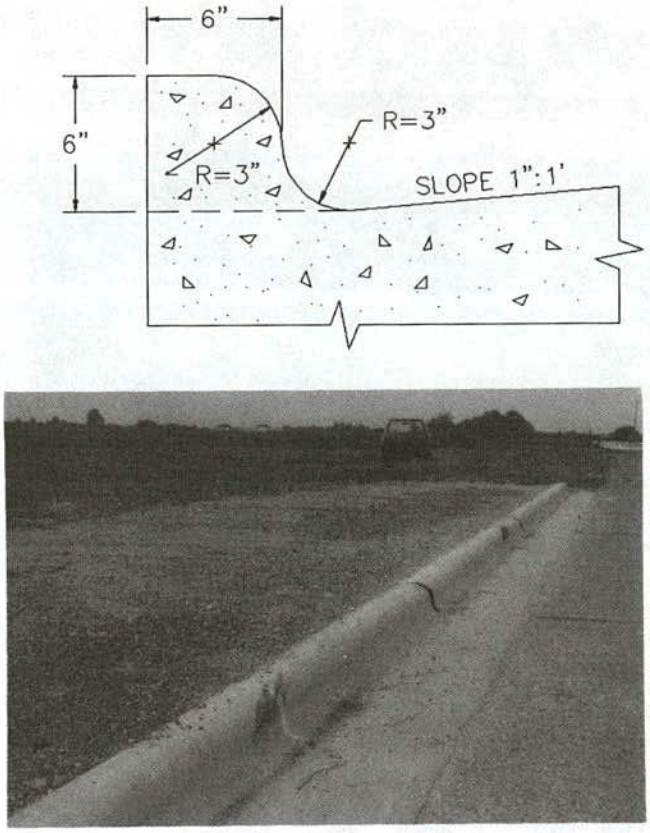

Figure 11. Curb parameters.

Shown in Figure 11 is a cross-section of the curb selected for analysis in the present study, referred to as the type "B" curb by AASHTO (*24*). It was selected because of its wide use in urban areas.

Analysis of the type B curb was made by use of the HVOSM computer program and a series of full-scale vehicular tests with minicars. Further details are given in Chapter Three, under "Full-Scale Crash Test Program" and "Computer Simulation Studies."

On the basis of the results of this analysis, it was concluded that the type B curb poses no appreciable hazard to occupants of a minicar for the conditions evaluated. Those conditions were tracking impacts with the curb at various encroachment angles and speeds up to 60 mph. Behavior of the minicar is similar to larger cars for these impact conditions. However, as discussed in Chapter Three and as documented in a recent study (*11*), minicars have a greater propensity to overturn than do larger cars when impacting a curb in a sliding or sideways motion. Suggested curb shapes to accommodate minicars are given in the following discussion.

MODIFICATIONS TO SELECTED ROADSIDE SAFETY ELEMENTS TO ACCOMMODATE MINICARS

This section summarizes potential modifications to selected roadside safety elements that may be necessary if the minicar becomes a design vehicle. These findings are based primarily

on the use of computer simulation programs previously mentioned and, to a lesser extent, on a limited full-scale crash test program with minicars. Details of the analysis procedures are given in Chapter Three.

Roadside Hardware

Rigid Longitudinal Barriers

As discussed earlier in this chapter, the CSSB (see Fig. 2) was found to be in compliance with the performance standards of *NCHRP Report 230* for minicars weighing as little as 1,250 lb. If those performance standards remain in effect, one can conclude that no changes would be necessary to the CSSB to accommodate minicars. However, there is evidence that small cars are overrepresented in overturn accidents involving the CSSB. One reason for this disparity is that in comparison to a larger car a minicar appears to have a greater propensity for overturn when striking the CSSB at impact conditions other than the test conditions of *NCHRP Report 230.* These include high angle tracking impacts and nontracking impacts in which the vehicle is sideslipping at the time of impact.

Studies of new shapes for the concrete barrier were made in an effort to mitigate the overturn problem associated with high angle or nontracking minicar impacts. Presented in Figure 12 are three designs that show promise in meeting this goal. Slopes (β) up to approximately 10 deg for the constant-slope barrier appear satisfactory. Note that the "modified CSSB" shape of Figure 12 could be a new design, or an existing CSSB could be retrofitted to achieve the shape. This concept was conceived by Ivey, et al., (*54*) at TTI. Based on a series of HVOSM computer runs, each of the shapes in Figure 12 will appreciably reduce the overturn problem. Details of these runs are given in Chapter Three.

At the time of this writing, the Texas State Department of Highways and Public Transportation was pursuing a feasibility study of the constant-slope barrier with TTI. It is anticipated that a design will be selected in the near future and that a prototype will be constructed and crash tested. In addition to the potential for improved impact performance, the height of the constant-slope barrier can be selected so that several pavement overlays can be accommodated without the necessity of raising the barrier. Note that, as opposed to the CSSB, the adding of an overlay does not alter the shape of a constant-slope barrier. For example, the barrier can be initially 42 in. high, permitting up to 10 in. of total overlay without reducing the barrier's height more than the 32 in. commonly used on the CSSB.

Use of the vertical wall or constant-slope barriers shown in Figure 12 in lieu of the CSSB would not be without some tradeoffs. Certain shallow angle impacts with the CSSB that produce no damage would cause some damage with the new shapes. However, one life saved by preventing an overturn and the associated societal cost will outweigh a very large number of minor, scrape hits. The new shapes may also require more concrete than the CSSB. To the extent possible all of the foregoing factors should be evaluated in a benefit/cost analysis if further evaluations of the new designs are planned.

Flexible Longitudinal Barriers

The G4(1S) roadside barrier, as shown in Figure 3, was found to be in compliance with the performance standards of *NCHRP Report 230* for minicars weighing as little as 1,250 lb. Based on crash tests and the analysis described in Chapter Three, it was concluded that the G4(1S) as presently designed would satisfactorily accommodate minicar impacts.

Although it was not within the scope of the study to evaluate other flexible longitudinal barriers, an attempt was made to estimate the performance of widely used barriers for minicar impacts. The analysis was based on results of the G4(1S) evaluations, a review of vehicle/barrier geometry, and recent crash tests of longitudinal barriers with an 1,800-lb car (*28*). Shown

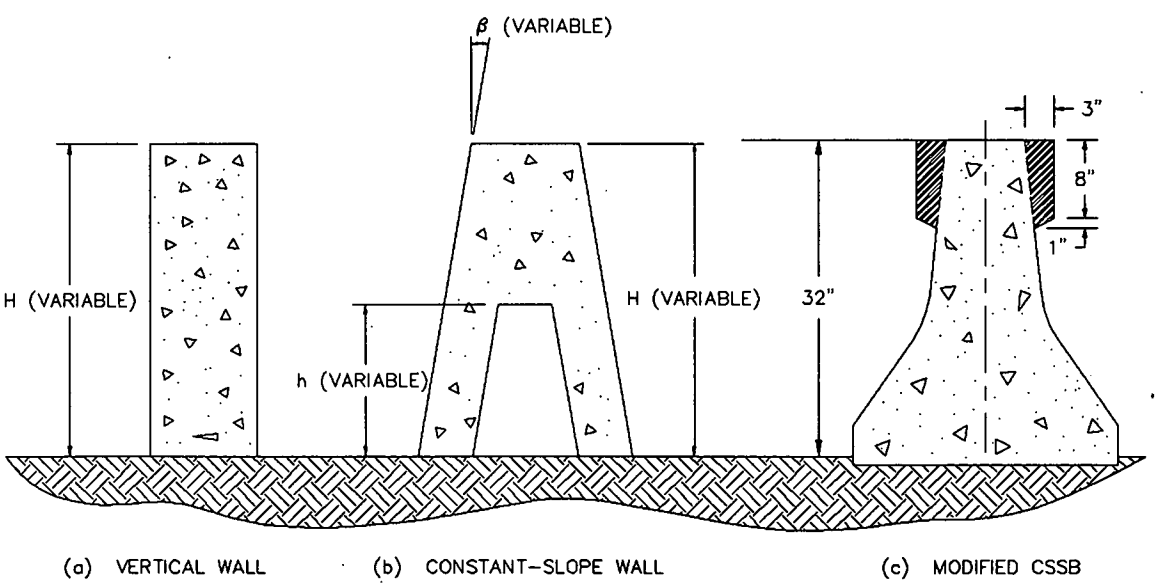

Figure 12. Potential rigid barrier shapes.

in Figures 13 through 20 are profiles of minicars in relation to selected longitudinal barriers. Barrier designations are from the AASHTO Barrier Guide (*10*). Comments about each barrier follow.

G1. Of concern in the G1 system is the potential for underriding of the cables by minicars. Note that the 1988 Honda Civic CRX-HF has a hood height approximately equal to the height of the lower cable. It is noted that tests of the G1 with the older Honda Civic, with a 30-in. hood height, were satisfactory (*28*).

G2. There are no apparent problems with the G2. Tests of this system with the older Honda Civic were satisfactory (*28*).

G3. Tests of this system with an 1,800-lb car (*28*) resulted in questionable post-impact behavior. On impact, the wheel of the vehicle wedged under the rail and the vehicle spun or yawed approximately 180-deg. Similar, and possibly more severe, behavior would probably occur with a minicar impact, especially with a vehicle like the 1988 Honda Civic.

G4(1S). No major problems are anticipated with this design for any of the minicars shown. The same conclusion would also apply to the G4(1W), G4(2W), G4(2S), and MB4S systems in the AASHTO Barrier Guide (*10*). Occupants of a minicar would experience a lateral impact velocity during recommended impact performance tests that would probably exceed the 20-ft/sec design value recommended in *NCHRP Report 230* but not the 30-ft/sec limit value cited there.

G9. No major problems are anticipated for this design for any of the minicars shown. The same conclusions would also apply to the MB9 system in the AASHTO Barrier Guide (*10*). It should be noted, however, that occupants of a minicar would experience a lateral occupant impact velocity during recommended impact performance tests that would exceed the 20-ft/sec design value recommended in *NCHRP Report 230* but not the 30-ft/sec limit value cited there.

MB2. No major problems are anticipated based on successful tests of the G2 system (*28*) with 1,800-lb cars. There is some concern, however, relative to the opening below the rail and the increased potential for underriding by the minicars.

MB3. Problems similar to those described under the G2 system occurred in tests of the MB3 system with 1,800-lb cars (*28*). The 24-in. opening below the rail may also permit underriding by some of the minicars.

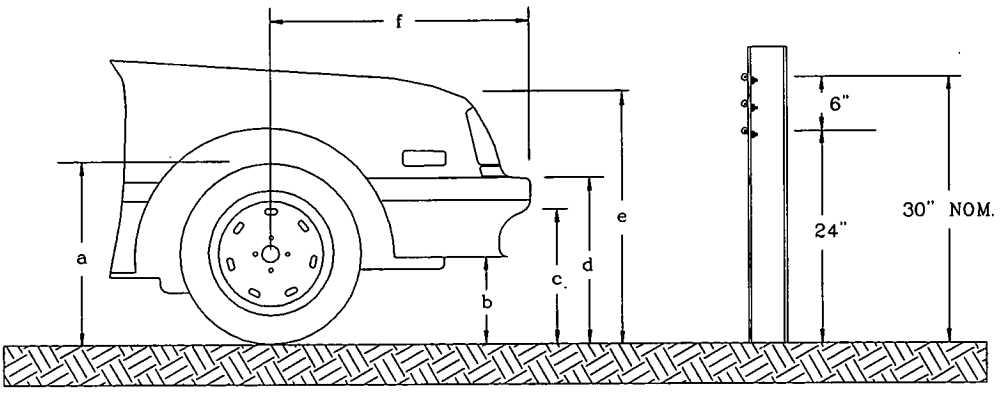

CAR	CURB WEIGHT (Lb.)	WHEEL BASE (In.)	DIMENSIONS (In.)					
			a	b	c	d	e	f
1988 Subaru Justy[1]	1675	90.0	21.0	9.5	16.0	20.5	28.5	N/A
1988 Chevrolet Sprint[1]	1600	88.4	20.5	9.3	14.0	18.8	27.0	28.5
1988 Ford Festiva[1]	1713	90.2	21.0	9.5	14.5	21.0	29.0	25.5
1988 Daihatsu Charade[1]	1775	91.3	22.0[3]	11.0[3]	15.0	20.5	28.0	29.0
1988 Honda Civic CRX-HF[1]	1819	90.6	21.0	8.0	13.8	18.8	24.8	31.0
1980 Honda Civic[1]	1800	86.0	22.0	8.5	15.6	19.6	30.8	29.3
1982 Ford Fiesta[2]	1610	89.8	20.8	9.75	14.5	18.3	30.3	25.5
1985 Fiat Uno[2]	1550	93.0	21.0	10.8	16.0	20.3	30.0	28.0
1983 Daihatsu Domino[2]	1300	84.5	19.0	12.0	15.3	19.3	29.0	21.0

[1] Sold in the U.S.A.

[2] Used as a test vehicle (not sold in the U.S.A.)

[3] Estimated

Figure 13. Profile of minicars in relation to G1 barrier.

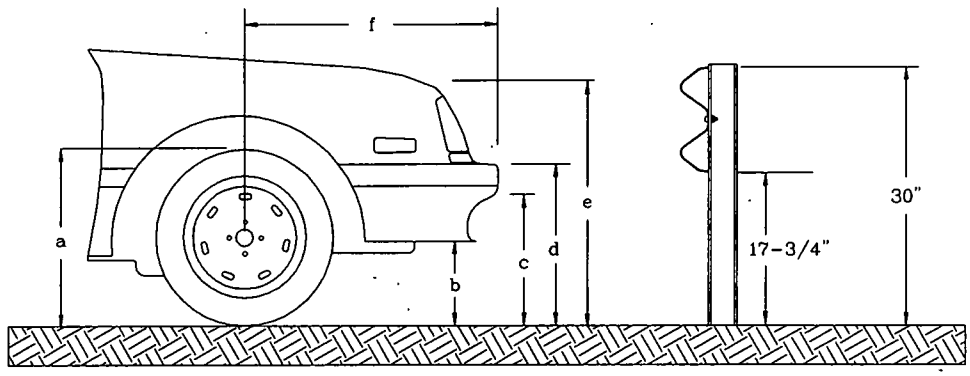

Figure 14. Profile of minicars in relation to G2 barrier. See Figure 13 for minicar dimensions.

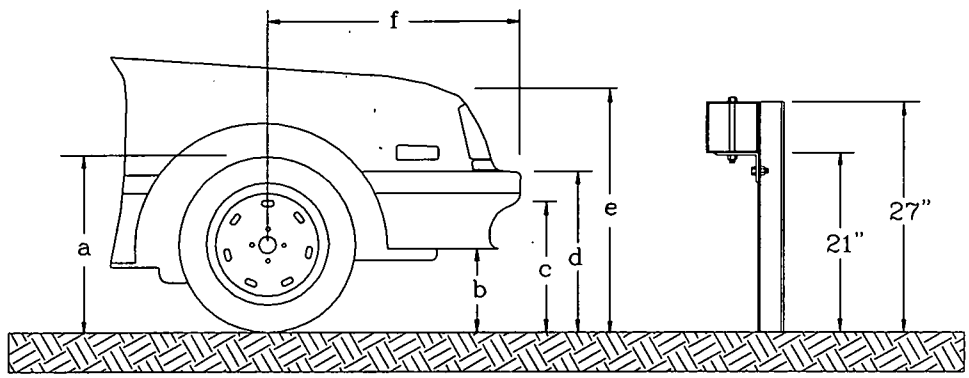

Figure 15. Profile of minicars in relation to G3 barrier. See Figure 13 for minicar dimensions.

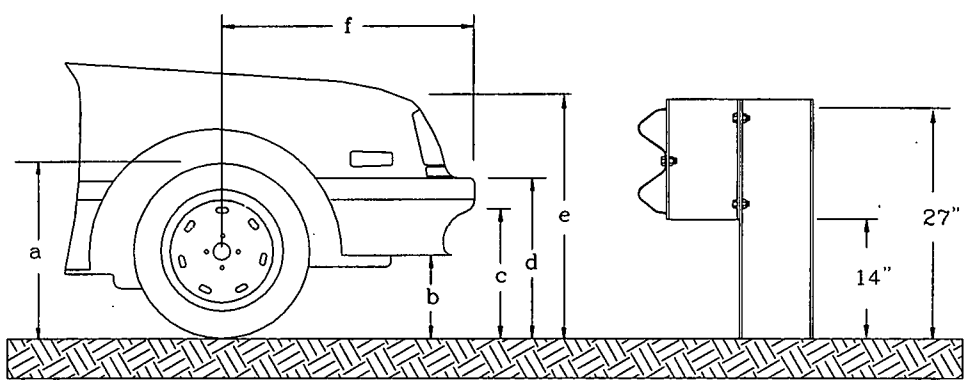

Figure 16. Profile of minicars in relation to G4(1S) barrier. See Figure 13 for minicar dimensions.

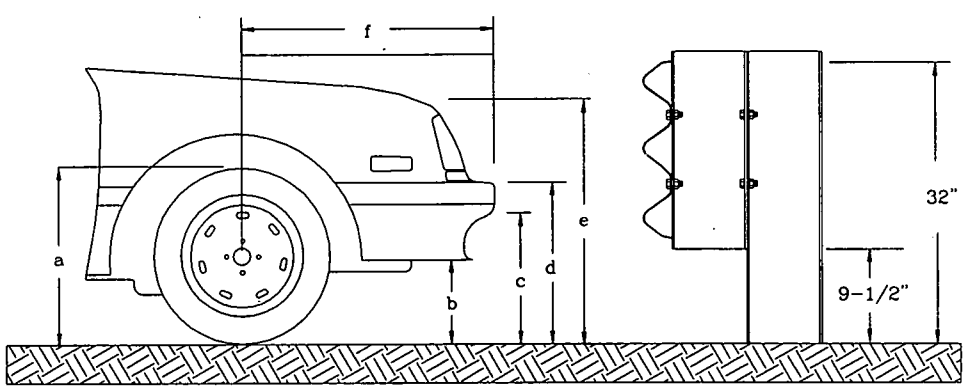

Figure 17. Profile of minicars in relation to G9 barrier. See Figure 13 for minicar dimensions.

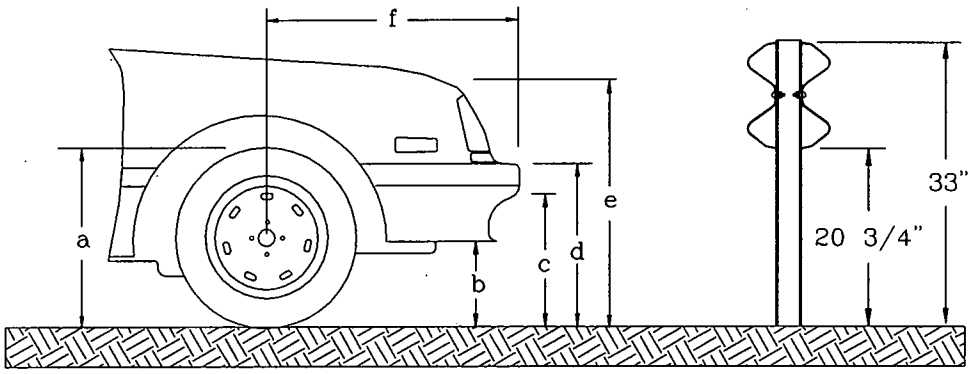

Figure 18. Profile of minicars in relation to MB2 barrier. See Figure 13 for minicar dimensions.

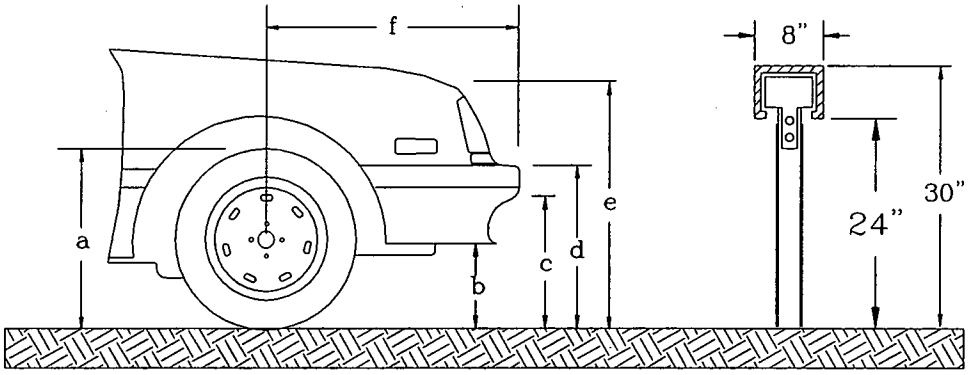

Figure 19. Profile of minicars in relation to MB3 barrier. See Figure 13 for minicar dimensions.

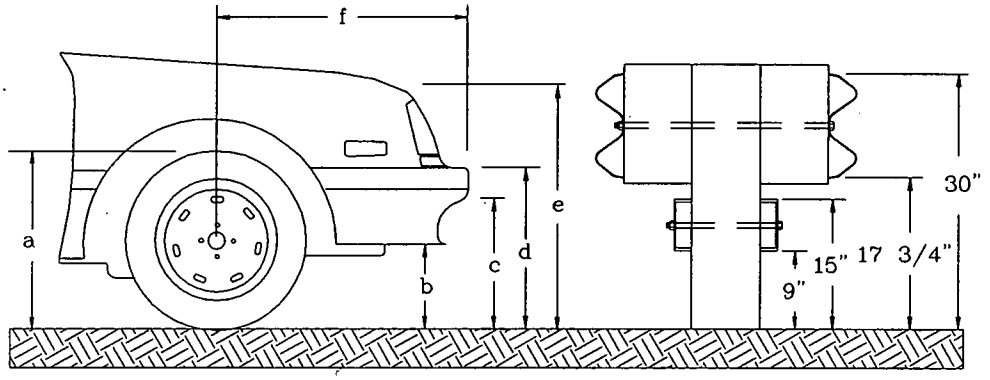

Figure 20. Profile of minicars in relation to MB4W barrier. See Figure 13 for minicar dimensions.

MB4W. No major problems are anticipated with this design for any of the minicars shown. Comments made under the "G4(1S)" discussion regarding occupant impact velocity apply to the MB4W also.

Breakaway Luminaire Supports

It is clear that modifications to most cast aluminum transformer bases for luminaire supports will be necessary to accommodate under 1,800-lb cars. In fact, results of a recent study (*12*) show that modifications will be necessary for these bases to meet current AASHTO standards that are based on an 1,800-lb car (*5*). The modifications may include features to enhance fracture, such as holes or notches, thinner sections, more brittle materials, or a combination thereof. Manufacturers of the bases are currently examining alternatives. There is concern that further weakening of the bases may compromise the structural integrity of the support. The task of accommodating an 1,800 lb-car will be difficult. Accommodating a 1,500-lb minicar within current performance standards (*1, 5*) may be beyond the state of the possible for transformer bases, at least for the near future.

Figure 21 is a California Department of Transportation Type

30 lighting standard (*39*). A multidirectional slip base is used with the installation. This installation is believed to be typical of many slip-base designs. The total weight of the steel support, above the slip plane, is approximately 490 lb. Each of the three 7/8-in. bolts is torqued to 150 ft-lb. Based on reported data (*40*), bolt torque "T" and bolt tension "N" can be approximated by $N = (K_t)(T)$ where K_t depends on the bolt diameter. For a ⅞-in. bolt, K_t is estimated to be 5.7/in. Thus, for T = 150 ft-lb = 1,800 in.-lb, N = (5.7)(1,800) = 10,260 lb.

The total tension force, N_t, is therefore approximately 30,780 lb. As discussed in Chapter Three, under "Specialized Analytical Procedures," a typical effective friction coefficient for a multidirectional slip base is approximately 0.5. Thus, the slip force is estimated to be (0.5)(30,780) = 15,390 lb. It is noted that the actual slip force can also depend on the direction of the resultant impact force and on the notch geometry of the flanges.

Further, it should be noted that significant variations in slip-base friction have been reported. Therefore, although the above procedures for linking bolt torque to slip-base force are reasonably accurate, some caution is advised when using these estimated values for specifying allowable bolt torque.

Impact performance of the support shown in Figure 21 was examined by use of the computer model described in Chapter Three, under "Specialized Analytical Procedures." As discussed in that chapter, the model predicted actual crash test results with reasonably good accuracy. The reader should note that the frontal stiffness (in. lb/in.) of the vehicles used in these parametric studies was assumed to equal the weight of each respective vehicle. Reference should be made to Chapter Three, for a discussion of frontal vehicular stiffness and its effect on vehicular velocity change.

Figures 22 and 23 are plots of the estimated vehicular velocity change, ΔV, as a function of slip-base force for four vehicular weights and for 20 mph and 60 mph impacts, respectively. The dashed line in Figures 22 and 23 is drawn at 15 ft/sec, the current limit on vehicular velocity change (*5*). Results indicate the following for the given support: (1) for the lower slip-base forces, the ΔV is appreciably greater at the higher impact speed; (2) the ΔV is more sensitive to slip base force at lower impact speeds; and (3) if the slip-base force is as computed above (approximately 15,500 lb), the support will satisfy current performance criteria (*5*) for a 1,500-lb car. The predicted velocity change for a 1,250-lb car is slightly above the 15-ft/sec ΔV limit at 60 mph (see Fig. 23).

Figure 24 is a plot of ΔV versus impact speed for four slip-base forces for the Type 30 support for a 1,500-lb car. The 5,000-lb to 20,000-lb range on slip force is believed to bracket the extremes that would occur in the field. It can be seen that ΔV increases with increasing impact speed for these conditions. However, even at the 20,000-lb slip force, the support satisfies current performance criteria (*5*) for a 1,500-lb car.

Figures 25 and 26 show estimated changes in vehicular velocity for a 45-ft steel luminaire support with dual mast arms, weighing approximately 960 lb, for impacts at 20 mph and 60 mph, respectively. This support is believed to be near the extreme in terms of weight for breakaway roadside luminaire supports. In this case there are obvious problems for high-speed impacts for vehicles weighing less than 2,000 lb. Figure 27 is a plot of ΔV versus impact speed for the same pole when impacted by a 1,500-lb car for a range of slip-base forces. It can be seen that

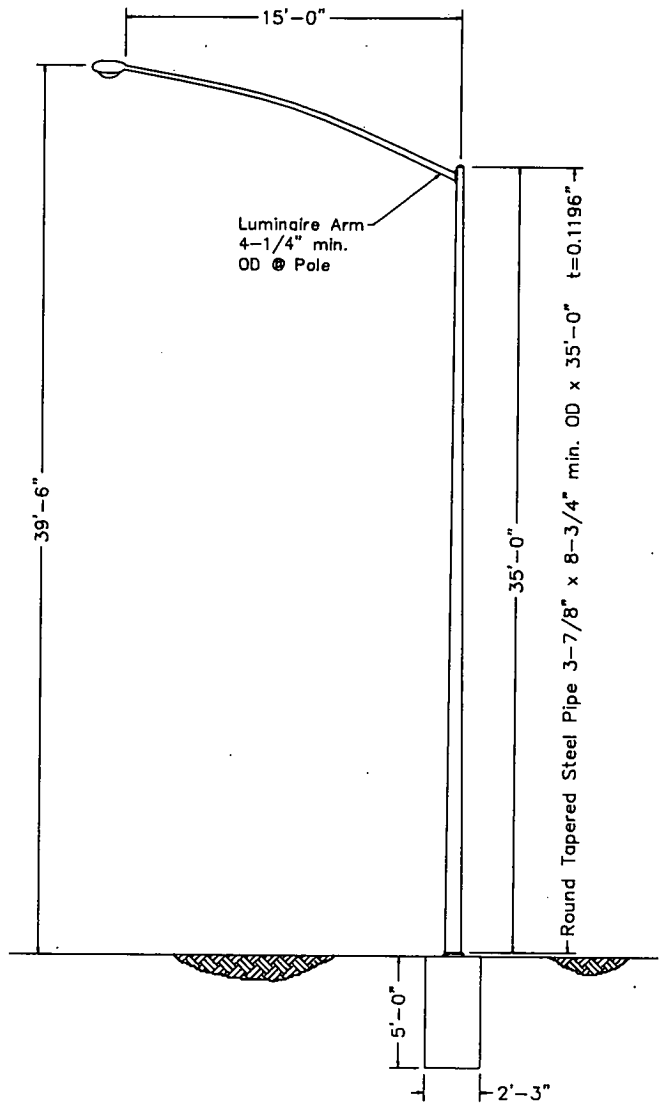

Figure 21. California type 30 luminaire support.

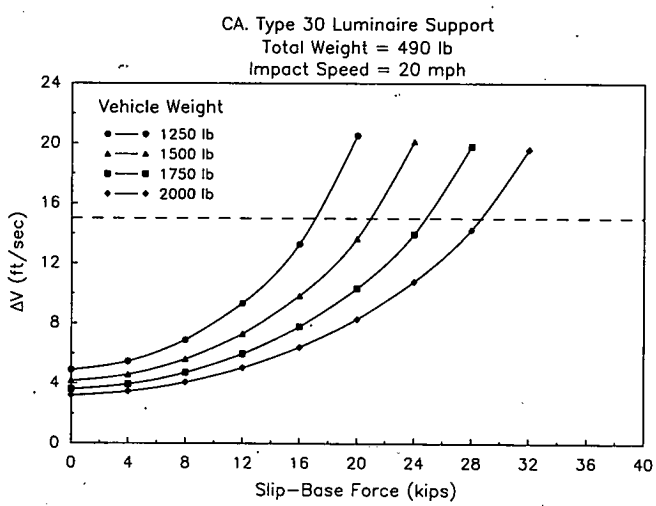

Figure 22. Change in velocity versus slip-base force.

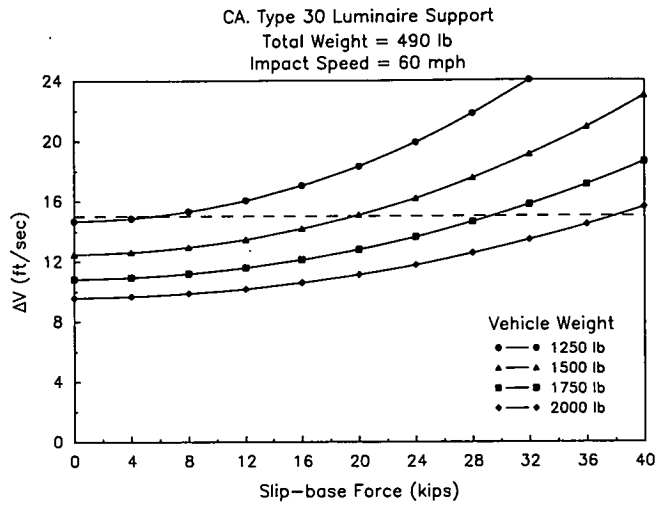

Figure 23. Change in velocity versus slip-base force.

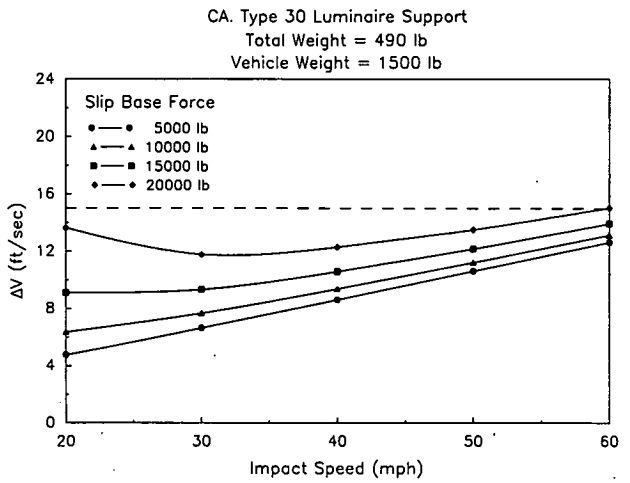

Figure 24. Change in velocity versus impact speed.

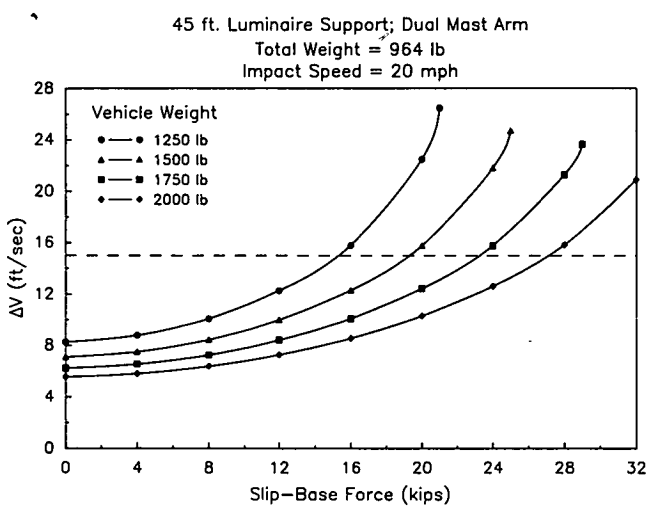

Figure 25. Change in velocity versus slip-base force.

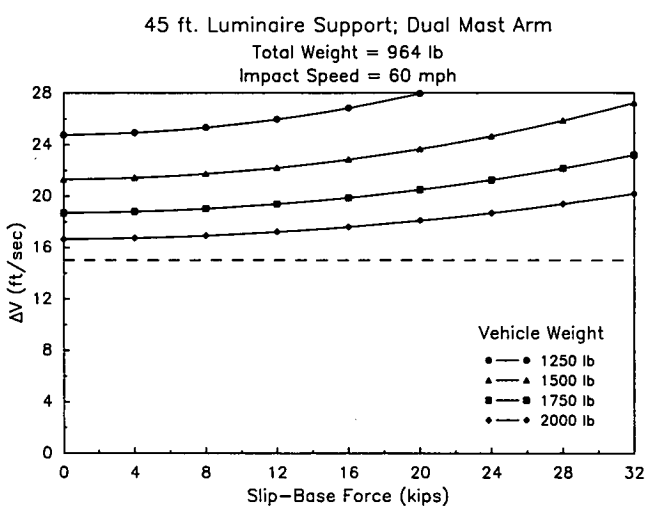

Figure 26. Change in velocity versus slip-base force.

the 15-ft/sec limit is exceeded for a slip force in excess of 20,000 lb. For a slip force less than 15,000 lb, performance is unacceptable for impact speeds in excess of about 35 mph.

If the weight of the 45-ft support were cut in half, say 500 lb, the analysis indicates satisfactory performance for a vehicle weighing 1,500 lb. It is believed that a 45-ft aluminum pole would be satisfactory.

Breakaway Sign Supports

As discussed earlier in this chapter, tests of a large sign support system with under 1,800-lb cars (*13*) were satisfactory in terms of current safety standards (*1, 5*). Further analysis of the referenced support system was made in the present study for minicars using the computer program presented in Chapter Three. Shown in Figure 28 are key sign support parameters that affect impact performance. In the reference system the parameters were as follows: S_W = 24 ft, S_D = 12 ft, S_H = 3 in.,

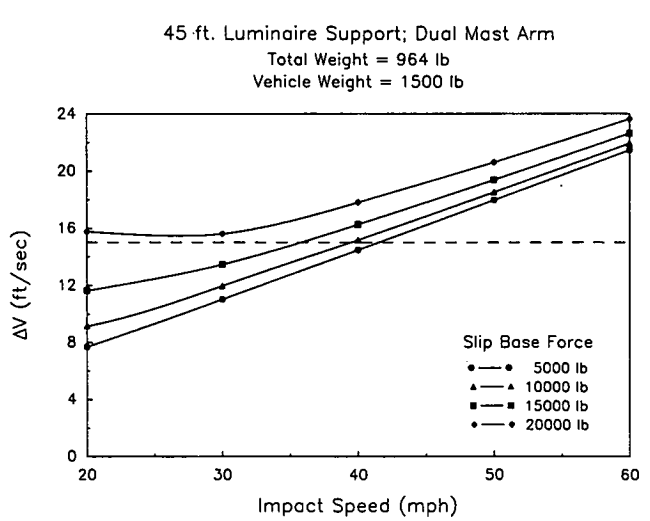

Figure 27. Change in velocity versus impact speed.

H_H = 8.25 ft, P_L = 20 ft, P_S = 15 ft, and B_H = 17.5 in.

The unit weight of each of the two supports was 45 lb/ft. Figures 29 and 30 are plots of estimated vehicular velocity change, ΔV, as related to the "effective" slip-base force for four vehicle weights at impact speeds of 20 mph and 60 mph, respectively, for the support system just described. The effective slip-base force is that necessary to activate and release the lower slip plane *and* the upper hinge mechanism. A procedure to estimate the effective force is given in this section under "Roadside Features." It depends primarily on the torque applied to the slip-base bolts and to the bolts in the hinge. Based on reported information (*13*) the effective slip-base force in the test installation was estimated to be approximately 8,000 lb.

Note that the data in Figures 29 and 30 are based on the assumption that the hinge activates and releases at both 20 mph and 60 mph. In the referenced tests (*13*) the hinge did not activate at 20 mph, whereas in the 60-mph test the hinge worked properly. Figures 31 and 32 are similar to Figures 29 and 30, except it was assumed the hinge did not activate. Note that an effective post length of 17.5 ft was used in the "no hinge" analysis although the total post length was 20 ft. This was done because the depth of the upper 5 ft of the wide-flange support is tapered down to near zero.

Figure 33 is a plot of ΔV versus signpost weight for a 1,250-lb car, for a range of effective slip-base forces, for a 60-mph impact. Parameters S_H, H_H, and B_H were as follows: S_H = 3 in., H_H = 8.25 ft, and B_H = 17.5 in. It can be seen that acceptable performance is indicated for post weights up to about 40 lb/ft for the given conditions.

Results of the analysis indicate the following, recognizing that 40-lb/ft to 45-lb/ft signposts are probably the largest in present use: (1) practically all slip-base sign supports will satisfy current safety standards for vehicles weighing as little as 1,500 lb, provided the effective slip force is not excessive and provided the hinge mechanism activates, especially for high impact speeds; (2) the ΔV is much more sensitive to the effective slip-base force at low speeds than at high speeds; (3) for large supports, such as the 45-lb/ft wide-flange post, it is essential that the hinge activate during high speed impacts; and (4) The foregoing implies that extra care will be necessary in the installation and maintenance of breakaway sign details for minicar design vehicles.

A common concern about breakaway structures is the effect of the location of the impact force relative to the slip plane on impact performance. Supports placed on side slopes, behind curbs, and so forth, can be struck at other than a "normal"

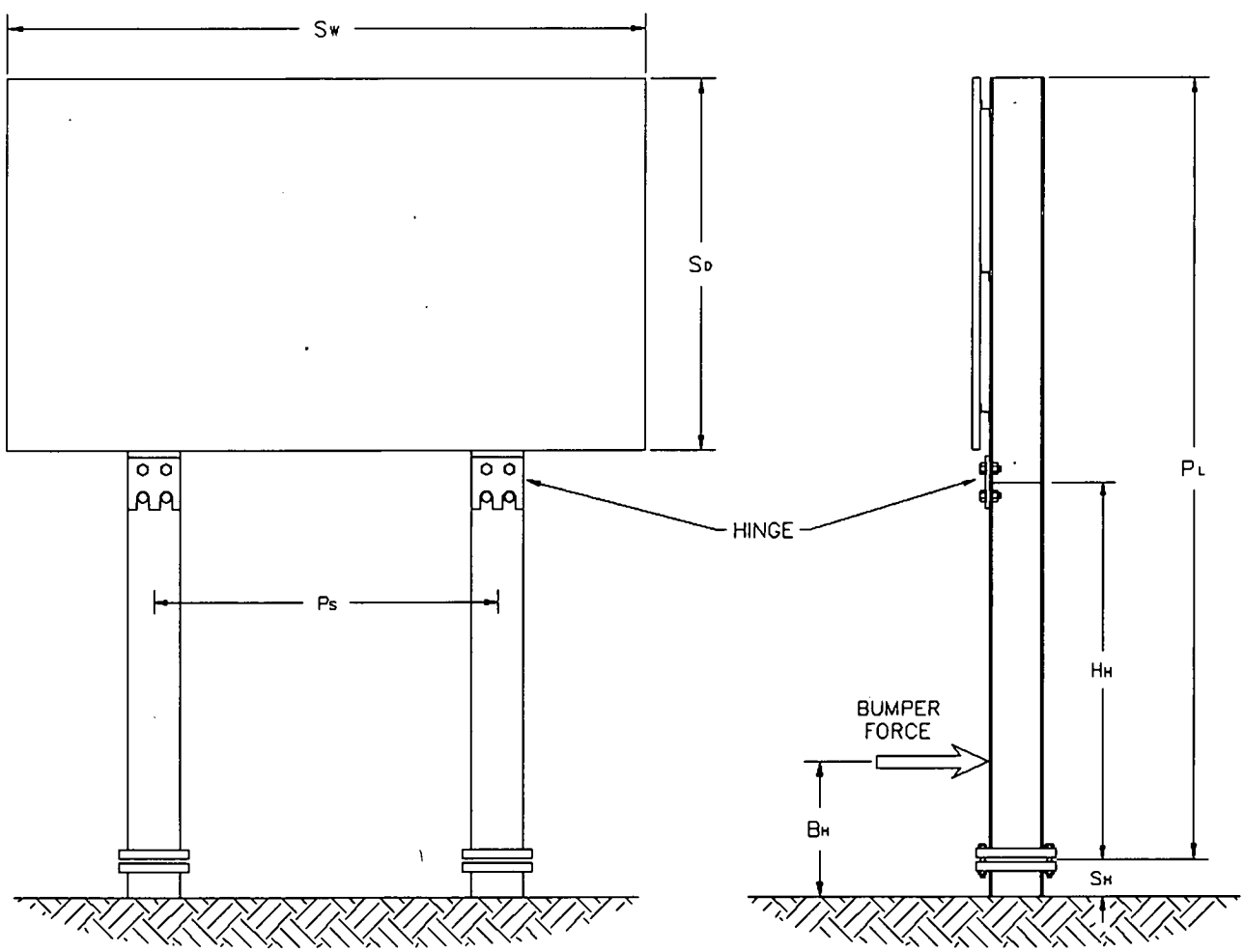

Figure 28. Breakaway sign parameters.

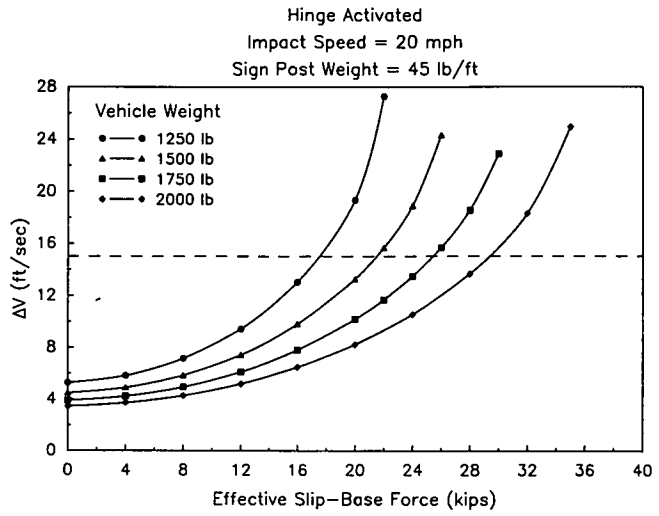

Figure 29. Change in velocity versus slip-base force.

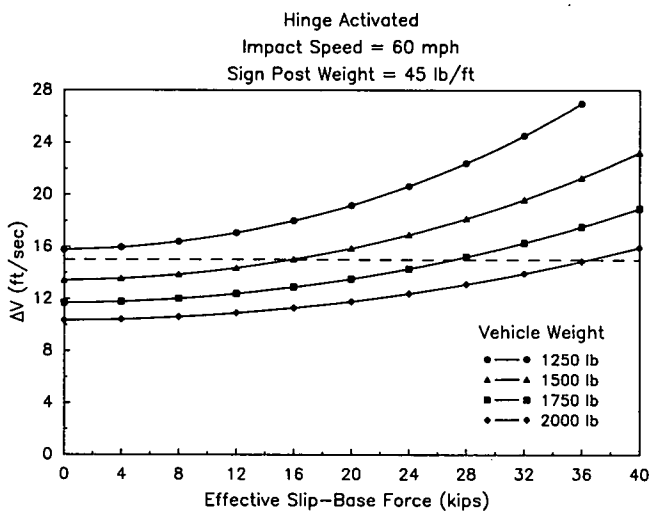

Figure 30. Change in velocity versus slip-base force.

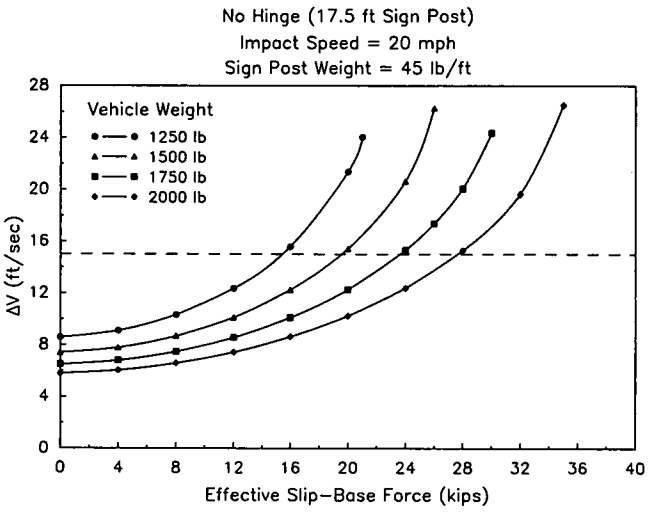

Figure 31. Change in velocity versus slip-base force.

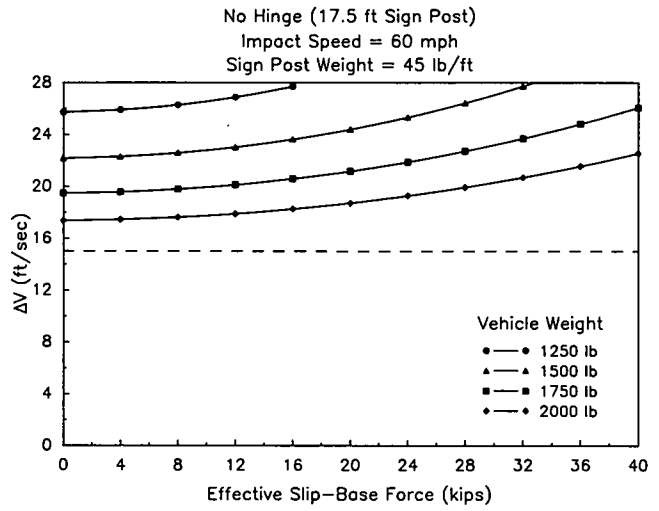

Figure 32. Change in velocity versus slip-base force.

position. The program described in Chapter Three, under "Specialized Analytical Procedures," was used to approximate the effect of this factor. The program accounts for the effect of impact force location on the transfer of momentum. It does not account for changes that may occur in the slip-base force due to the added moment on the slip plane. As such, the results should be viewed as a lowerbound on estimated changes in vehicular velocity.

Figure 34 is a plot of ΔV versus "effective" vehicular bumper height for a 60-mph impact with a 45-lb/ft signpost for a 1,500-lb car. With reference to Figure 28, the effective vehicle bumper height equals the difference in B_H and S_H. On the basis of previously described values, the effective bumper height for a 1,500-lb car is approximately 14.5 in. It can be seen that if the effective bumper height is increased from 14.5 in. to 36 in., the ΔV increases from approximately 14 ft/sec to about 24 ft/sec, a 70 percent increase.

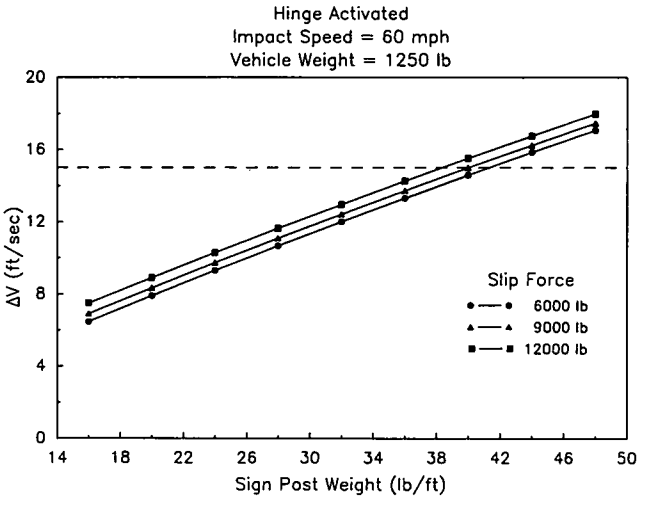

Figure 33. Change in velocity versus signpost weight.

Another key parameter in breakaway performance is the structural stiffness of the impacting vehicle. It is also very difficult to define other than by carefully controlled full-scale crash tests. A good illustration of this sensitivity can be found in a study previously cited (*13*). Four tests were conducted on the sign support previously described (the 45 lb/ft supports, etc.). Two of the tests (1147-1001 and 1147-1008) involved a 1973 Chevrolet Vega, weighing approximately 2,400 lb, impacting the post at 20 mph and 60 mph. The other two tests (1147-1009 and 1147-1010) involved a 1974 Honda Civic, weighing about 1,600 lb, also impacting the post at 20 mph and 60 mph. The average reported ΔV (from film and accelerometer data) for the vehicles were as follows:

Test Vehicle	ΔV (ft/sec) Impact Speed 20 mph	60 mph
1973 Vega	10.0	8.4
1974 Honda	9.9	9.3

One would conclude that the ΔV for the much smaller Honda should be measurably greater than that for the Vega. While there may in fact be some errors in the data, differences in the frontal stiffness of the two vehicles is believed to be a primary reason for the apparent discrepancy, especially at the low speed impacts. The frontal stiffness of a 1973 Vega and a 1981 Honda Civic (for the crush distance experienced in the tests) as measured in full-scale crash tests (*6*) were as follows:

Vehicle	Crush Stiffness (lb/in.)
1973 Vega	480–850
1981 Honda	1,600–2,300

If the stiffness of the 1974 Honda is similar to that of the 1981 Honda, the 1974 Honda is three to four times stiffer than the Vega for the crush distances that occurred in the tests. The sensitivity of the impact performance of breakaway structures to vehicular stiffness is examined further in Chapter Three, under "Specialized Analytical Procedures." It is also shown that there are major differences in the frontal stiffness of various small vehicles.

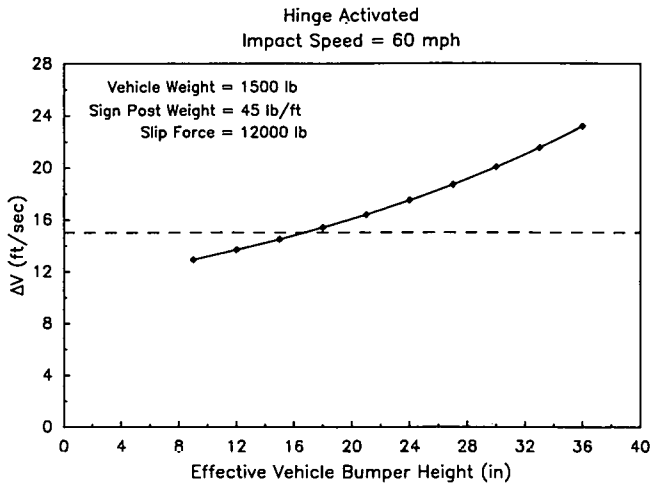

Figure 34. Change in velocity versus bumper height.

Base-Bending Sign Supports

The base-bending sign support selected for analysis in the present study was a single 4-lb/ft rail steel U-post. Properties of the post are given in Appendix C, test 7. Test and analysis of this post indicate it will be marginally acceptable for minicars weighing 1,500 lb.

Although the scope of the project did not permit an in-depth test and analysis program for other small sign support systems, estimates were made of the impact performance selected systems would exhibit for minicars. The analysis procedure used to make the estimates is given in Chapter Three, "Specialized Analytical Procedures." Results are summarized in Table 3.

Notes concerning the information in Table 3 follow:

1. Current AASHTO impact performance standards for sign and luminaire supports are stated as follows (*5*):

> Satisfactory dynamic performance is indicated when the maximum change in velocity for a standard 1,800-pound (816.5 kg) vehicle, or its equivalent, striking a breakaway support at speeds

Table 3. Estimate of performance of selected small sign supports for minicars.

SIGN SUPPORT SYSTEM	IMPACT SPEED (MPH)	ESTIMATED VEHICULAR VELOCITY CHANGE (FT/SEC) 1,500 LB VEHICLE	1,250 LB VEHICLE
A. 3 lb/ft High Strength (80 KSI) Steel U-Post with Ground Splice (Three-Post Installation)	21.7	18.5	28.6
	61.6	12.0	14.7
B. 5 in. I.D. Standard Steel Pipe with Multidirectional Slipbase (Single-Post Installation)	45.5	7.2	8.8
C. 4 in. x 6 in. (Nominal Dimensions) Southern Pine Wood Post, Unweakened (Single-Post Installation)	20.7	12.4	16.2
D. 2 1/2 in. x 2 1/2 in., 10 Gauge, Square Perforated Steel Tube and Stub (Single-Post Installation)	20.4	13.3	17.6
	61.4	12.3	15.0
E. 2 3/8 in. O.D., 13 Gauge Steel Tube with "Poz-Loc Anchor" (Two-Post System)	20.6	21.1	30.2

from 20 mph to 60 mph (29.33 fps to 88 fps) (32 kmph to 97 kmph) does not exceed 15 fps (4.57 mps) [the authors note that under Federal Highway Administration Regulation (Part 625, 23 CFR) 16 fps is acceptable], but preferably does not exceed 10 fps (3.05 mps) or less.

All breakaway supports in multiple support sign structures shall be considered as acting together to cause a change in impact vehicle velocity unless each support is designed to independently release from the sign panel, the sign panel has sufficient torsional strength to ensure this release, and the clear distance between supports is eight feet (2.44 m) [the authors note that the 1988 AASHTO *Interim Specifications for Bridges* changed the "eight feet" to "seven feet"] or greater.

To avoid vehicle undercarriage snagging, any substantial remains of a breakaway support, when it is broken away, should not project more than four inches (0.102 m) above a 60-inch (1.524 m) chord aligned radially to the centerline of the highway and connecting any point, within the length of the chord, on the ground surface on one side of the support to a point on the ground surface on the other side.

2. Systems A, D, and E have been crash tested according to current AASHTO specifications (*5*) and are in compliance with those specifications. Although systems B and C have only been crash tested with larger cars (weighing 2,250 lb or more), there is little doubt that they will meet the current AASHTO specifications, and that is the reason they are included in Table 3.

3. System A is a new design developed for the Arizona Department of Transportation by TTI (*29*). It is similar to a steel U-post ground splice system developed several years ago (*30*) and now in wide use across the United States. Based on the given estimates, a three-post system, in which the outer posts are within an 8-ft spacing, would not satisfy AASHTO criteria for the two minicar weights shown. Based on the analysis procedure of Chapter Three, "Specialized Analytical Procedures," a system with one or two posts within an 8-ft spacing would be acceptable for the 1,500-lb car and the 1,250-lb car.

4. Tests of single signposts with slip-base designs with larger cars clearly demonstrate the low impact resistance of these designs. As shown in Table 3, the estimated velocity change of a relatively large support in System B is well below the 15-ft/sec limit, even for a 1,250-lb car. Some increase in the vehicular velocity change values can be expected for a 20-mph impact, but they are expected to be below the 15-ft/sec limit for both minicars.

5. It appears that a single 4 in. by 6 in. unweakened wood post (System C) and a single 2½ in. by 2½ in., 10-gauge perforated steel tube (System D) would be acceptable for a 1,500-lb car. The estimated vehicular velocity change for a 1,250-lb car would exceed the 15-ft/sec limit by 1.2 ft/sec and 2.6 ft/sec for Systems C and D, respectively.

6. System E would be unacceptable for the two-post installation in which the supports were within 8 ft of each other. For a single-post installation or for an installation in which the posts are spaced 8 ft or more, acceptable performance is indicated for both the 1,500-lb car and the 1,250-lb car.

HVOSM computer runs were also made to study the post-impact behavior of small cars following impact with a small sign support. Depending on the magnitude of the impulse imparted to the vehicle and its location relative to the vehicle's centerline, sideslipping and possibly overturn can occur after an off-center impact. Details of these runs are given in Chapter Three, under "Computer Simulation Studies."

It should be noted that virtually all crash testing of small sign supports has involved installations placed in very stiff soils. Recent tests have shown that the performance of small sign support systems can be significantly degraded when installed in softer soils. Additional research is needed to better identify soft soil effects.

Crash Cushions

The two crash cushions selected for analysis in the present study included the sand-filled plastic barrels and the GREAT system. As mentioned earlier in this chapter, under "Performance of Selected Roadside Safety Elements for Minicars," neither of these cushions, as presently designed for high-speed roadways, would comply with *NCHRP Report 230* evaluation criteria for minicars.

Figure 35 shows a configuration of sand-filled plastic barrels designed to meet *NCHRP Report 230* criteria for vehicles in the 1,800-lb to 4,500-lb weight range. Also shown in Figure 35 is a configuration designed to meet *NCHRP Report 230* criteria for vehicles in the 1,350-lb to 4,500-lb weight range. It can be seen that the modification consists of simply adding a 200-lb module to the front of the cushion—a very inexpensive modification. The modified design does, however, require an additional 3 ft of space to accommodate the added module. Analysis of the system is given in Chapter Three. It is estimated that in a 60-mph head-on impact, the occupants of a vehicle whose gross weight is 1,350 lb would impact the interior of the vehicle at a velocity slightly less than 30 ft/sec, just below the preferred 30-ft/sec limit of *NCHRP Report 230*. The stopping distance would be approximately 21 ft, and the average vehicular deceleration would be approximately 5.7 G's. It is noted that the sand-filled plastic barrels can also be easily configured for lower design speeds.

Table 4 gives an estimate of the impact performance of the GREAT system and other commonly used crash cushions for a 1,500 lb vehicle. Also given in Table 4 is an estimate of the performance that could be achieved if "reasonable" modifications were made to accommodate a 1,500-lb car. As indicated, all current systems would probably produce an occupant impact velocity in excess of 40 ft/sec. Further, as indicated, some of the systems could be modified at a reasonable cost to achieve a "less than 40 ft/sec" occupant impact velocity, while others could not be modified without significant cost increases. According to *NCHRP Report 230*, it is essential that the occupant impact velocity be less than 40 ft/sec and it is recommended that it not exceed 30 ft/sec. It is noted that the systems listed in Table 4 were developed and are marketed by Energy Absorption Systems, Inc. (*16*).

Guardrail Terminals

Analysis of the 60-mph eccentric loader test with a 1,500-lb Fiat Uno (see Appendix C, test 7043-8) revealed some interesting results. First, the occupant impact velocity criteria of *NCHRP Report 230* was satisfied, i.e., the measured value of 27.4 ft/sec (calculated from accelerometer data) was less than the recommended limit of 30 ft/sec. Comparison of test 7043-8 with the same test of the eccentric loader involving a 1,821-lb Honda Civic (see test RBCT-13 of Ref. 20) shows the occupant impact velocity of the Fiat Uno was actually less than that of the Honda Civic (29.1 ft/sec calculated from acceler-

ometer data). This seems to violate basic principles of mechanics since the weight of the Fiat (1,530 lb) was 16 percent less than the Honda. However, further analysis led to the second interesting observation. As can be seen in Figure 36 (a), the Fiat sustained considerable damage during test 7043-8. In fact, the engine was torn from its mounts and there was deformation of, and intrusions into, the passenger compartment. Details of the passenger compartment damage are given in Appendix C. The relatively low occupant impact velocity was attributed to the large vehicular deformations, i.e., the vehicle absorbed a large amount of energy.

A review of the longitudinal vehicular acceleration during test 7043-8 shows the vehicle was subjected to a high impulse upon initial contact. This is a result of three events that take place over a very short time duration. They are, not necessarily in order of occurrence, an acceleration of the mass in the nose of the eccentric loader (about 110 lb), fracture of the first wooden post, and buckling of the W-beam.

The Honda Civic shown in Figure 36 (b) impacted an experimental end treatment similar to the original BCT design (*38*). It was tested in accordance with test 45 of *NCHRP Report 230*. Although the Honda sustained considerably less damage than the Fiat, the occupant impact velocity computed during the Honda test was in excess of 34 ft/sec. In other words, while the Honda was subjected to a considerably larger impulse, it actually sustained less damage than the Fiat. It is apparent that the frontal stiffness of the Fiat is significantly less than that of the Honda. Therefore, while the "softer" front end of the Fiat produced a theoretically acceptable occupant impact velocity, it unfortunately also permitted the integrity of the passenger compartment to be violated.

A visual review of the frontal structure of selected 1988 model under 1,800-lb cars suggests that the frontal stiffness of these

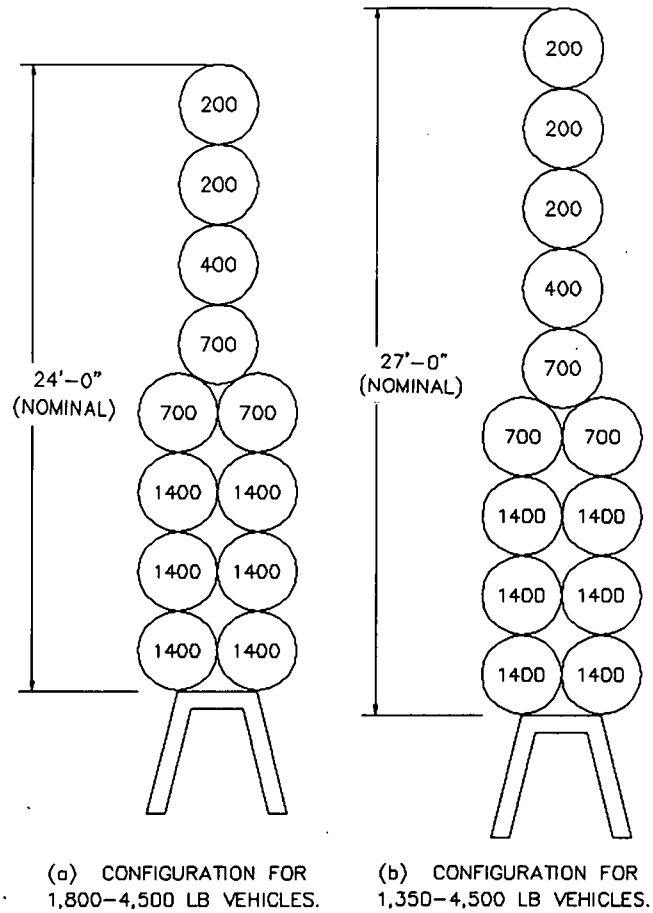

Figure 35. Sand-filled plastic barrel crash cushion.

Table 4. Estimated performance[1] of crash cushions when impacted[2] by a 1,500-lb car.

	Current Design		Modified Design	
	Occupant Impact Velocity (ft/sec)	Ridedown Acceleration g's	Occupant Impact Velocity (ft/sec)	Ridedown Acceleration g's
CRASH CUSHION TYPE				
G-R-E-A-T/G-R-E-A-T cz Systems (Hex-Foam Cartridge)	40-45	<20	<40[3]	<20
G-R-E-A-T/G-R-E-A-T cz Systems (Hi-Dri Cartridges)	45-50	>25	NA[4]	NA
Hex-Foam Sandwich System	40-45	<20	<40[3]	<20
Hi-Dri Sandwich System	45-50	>25	NA[4]	NA
Hi-Dro Sandwich System	50-55	>25	NA[4]	NA

[1] Estimated based on actual crash cushion performance with larger vehicles and theoretical performance of the 1,500 vehicle indicated.
[2] NCHRP 230 Test Number 52 (60 mph, 0 deg, centered) but with a 1,500 lb vehicle.
[3] The modifications would include unit extension (3-5 ft), weight reduction of some hardware elements and adjustment of the energy absorbing elements (replacement cartridges). These modifications would result in a unit price increase of less than 30% and could be made available in retrofit packages for existing installations.
[4] These systems cannot be reasonably modified due to excessive hardware and energy absorbing element weight and reduced ability to modify crush characteristics. Modifications would require excessive unit extension (>6 ft), retrofit packages would not be practical and price increases would be greater than 50%.

NOTE: Data in this table were provided by Energy Absorption Systems, Inc. (16).

Figure 36. Photographs of cars after end treatment tests: (a) Fiat Uno after test 7043-8; (b) Honda Civic after special BCT test.

cars is similar to that of the Fiat. Most of the cars have an integral or reinforced shell body in lieu of the heretofore conventional frame and sheet metal construction. The new body styles are efficient in terms of minimizing weight and reducing operating costs. However, softer vehicular structure will generally degrade the performance of "lumped impulse" safety features such as the eccentric loader and breakaway structures.

Photographs of the front and rear undercarriage structure of the four cars tested in the present study are shown in Figure 37. A 1979 Honda Civic undercarriage is also shown for com-

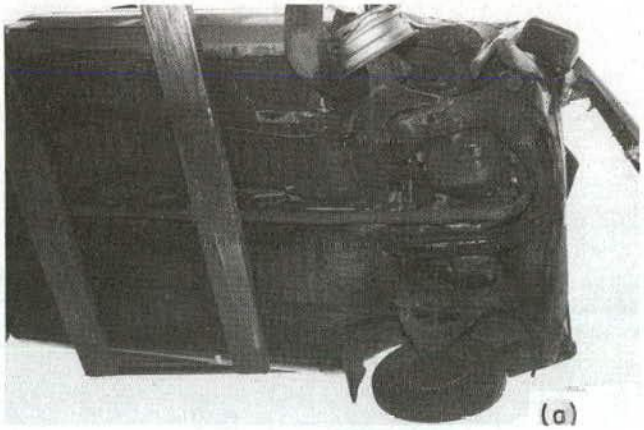

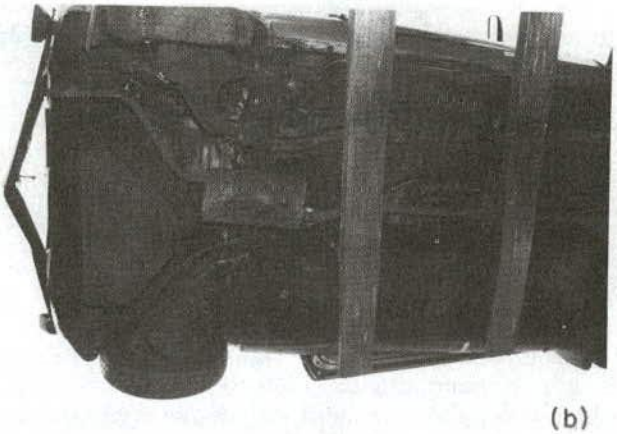

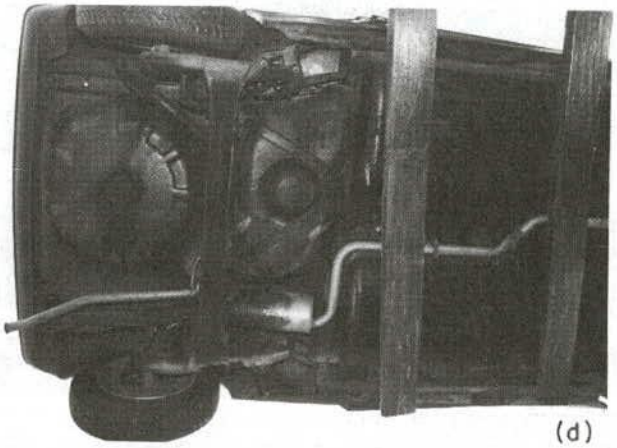

Figure 37. Undercarriage of vehicles: (a) 1983 Daihatsu Domino, front; (b) 1983 Daihatsu Domino, rear; (c) 1985 Fiat Uno, front; (d) 1985 Fiat Uno, rear; (e) 1982 Ford Fiesta, front; (f) 1982 Ford Fiesta, rear; (g) 1985 Chevrolet Sprint, front; (h) 1985 Chevrolet Sprint, rear; (i) 1979 Honda Civic, front; (j) 1979 Honda Civic, rear.

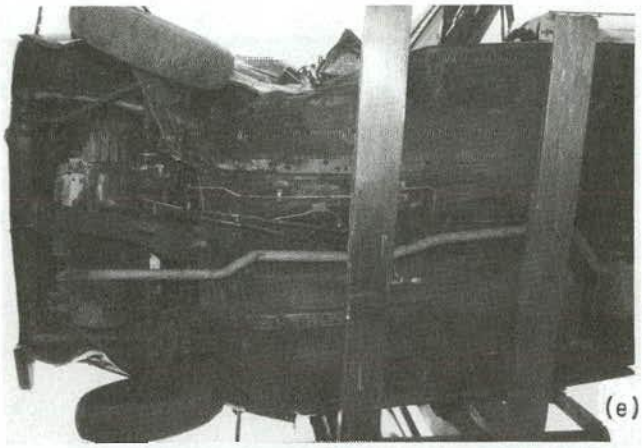

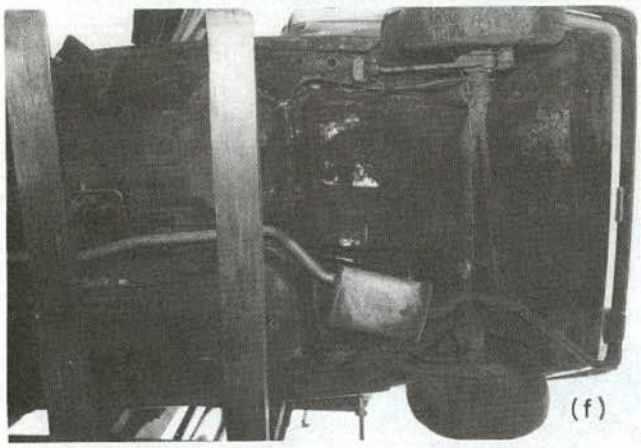

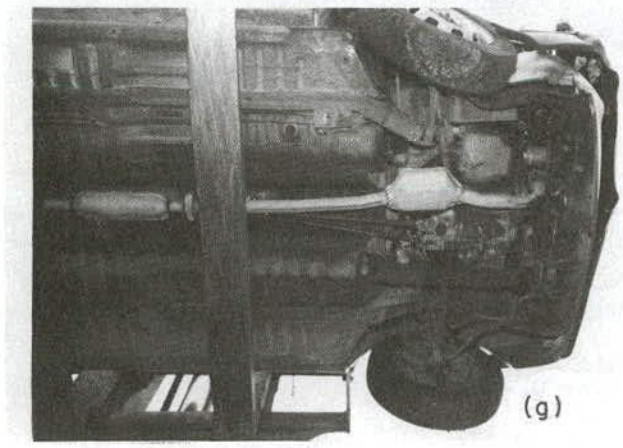

Figure 37. Continued

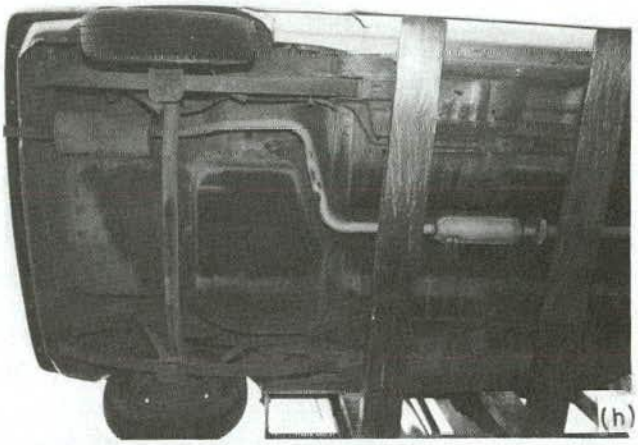

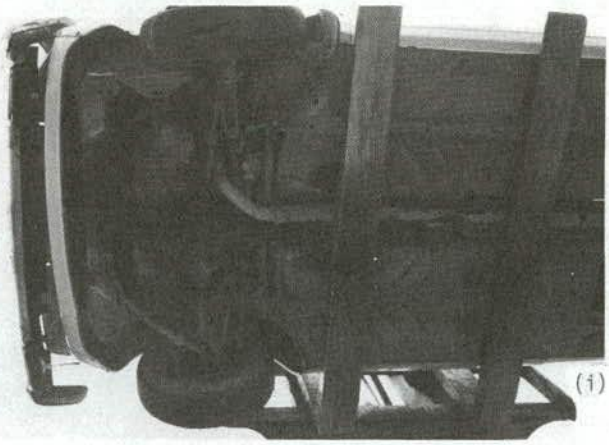

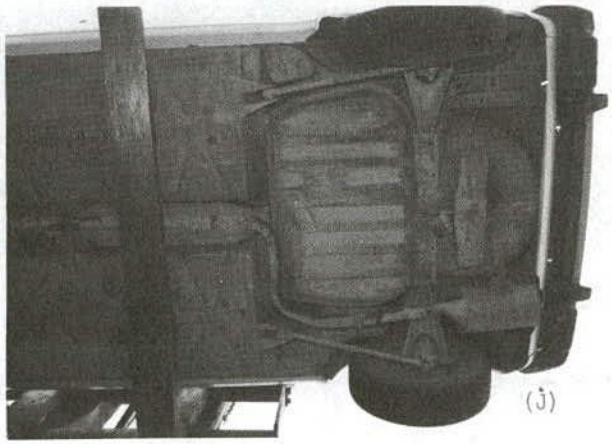

Figure 37. Continued

parative purposes. The photographs were made after the test program was completed and, hence, there are varying degrees of damage to the vehicles. Note that the two transverse members appearing in each photograph are fork-lift supports used to elevate the cars for the photographs.

Improvement in the eccentric loader impact performance can be made by reducing the mass of the structural elements in the nose or by further reductions in the buckling strength of the W-beam. Use of aluminum structural members in lieu of steel members in the nose could possibly reduce the mass by 50 percent to 60 percent. Further weakening of the W-beam for axial compressive loads may also be feasible. A "split rail" concept recently investigated at TTI (*38*) could probably be used to further weaken the rail. As shown in Figure 38, the W-beam is cut along its length. The length and number of the cuts can be varied to achieve a specified dynamic buckling load. With

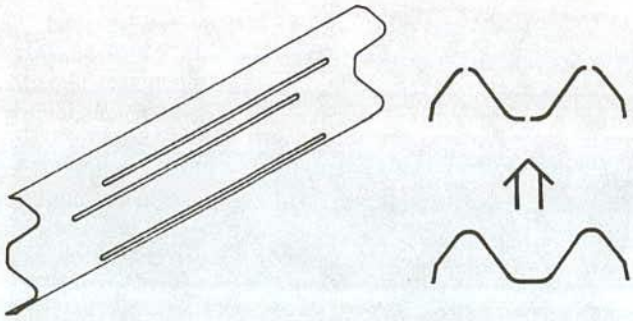

Figure 38. Split rail concept for end treatment.

three cuts as shown in Figure 38, the W-beam is essentially reduced to four flat plates over the length of the cut. The combined buckling load of the four "slender" columns is much less than the unweakened W-beam. The concept was, in fact, used to modify the original BCT design, the details of which are given in Ref. 38. The modified design was subject to the four performance tests of *NCHRP Report 230* that include two tests with an 1,800-lb car and found to be in compliance with the evaluation criteria.

Unfortunately, it is very difficult to analytically quantify the improved impact performance that may be achieved by using the split rail concept with the eccentric loader design. The researchers were unable to analytically model the complex dynamic response of the eccentric loader design, and it was not within the scope of the project to conduct additional crash tests.

Another very promising design developed at TTI and presented in Ref. 38 is the "Guardrail Extruder Terminal" (GET). The concept is illustrated in Figures 39 and 40 and photographs of the GET are shown in Figure 41. For impacts on the nose of the terminal, the guardrail is flattened and extruded out and in front of the advancing vehicle. Energy is dissipated in a controlled and predictable manner. Side hits downstream from the terminal are redirected because the terminal also acts as an anchor to develop the necessary tension in the W-beam. The system was shown to be in full compliance with *NCHRP Report 230* criteria as judged by the results of four crash tests, including two tests with an 1,800-lb car.

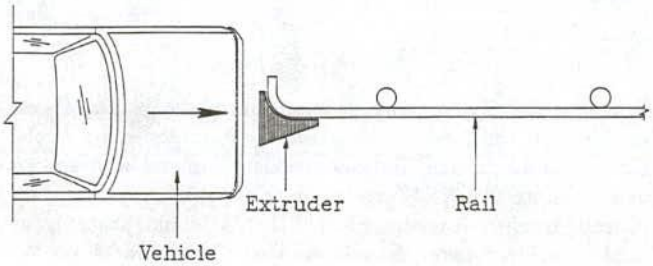

Figure 39. Guardrail extruder terminal.

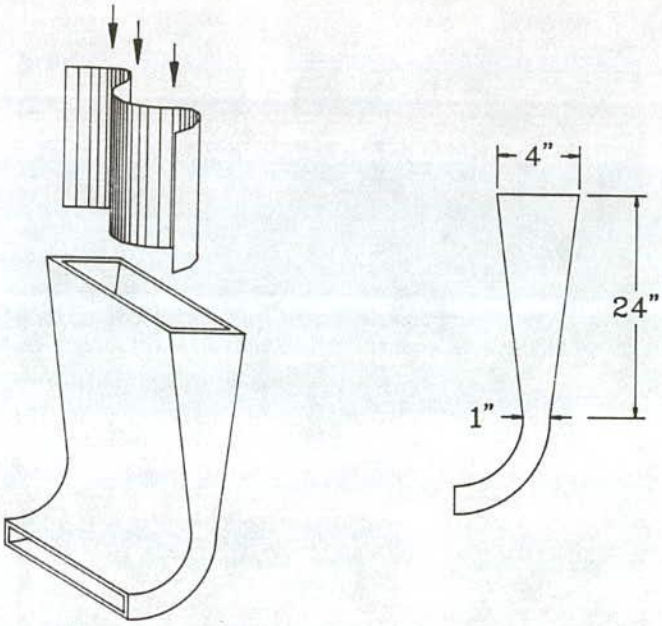

Figure 40. Guardrail extruder terminal details.

Figure 41. Photographs of guardrail extruder terminal.

It was shown in Ref. 38 that the impact performance of the GET can be described analytically with reasonably good accuracy. Therefore, using the analytic model, an investigation of the impact performance of the GET for under 1,800-lb cars was made. An estimate of the occupant impact velocity for a range of under 1,800-lb cars, for a 60 mph head-on impact with the GET, is shown in Figure 42. It is noted that, according to *NCHRP Report 230,* 40 ft/sec is the limit for the longitudinal occupant impact velocity, but 30 ft/sec or less is recommended. As noted in Figure 42, the results are based on the current extruder design which weighs 340 lb and dissipates approximately 13,000 ft-lb of energy per foot of rail extruded. Some weight could be trimmed from the current design, but as shown in Figure 43, it would not appreciably reduce the occupant impact velocity. An estimate of the occupant impact velocity as related to vehicular impact speed is shown in Figure 44. It can be seen that the higher vehicular impact speeds are more severe, and it can also be seen that the severity of the lighter vehicle is more sensitive to impact speed.

It should be noted that in the model used in evaluating the GET, it is assumed that the vehicle dissipates no energy in crushing. This obviously is not true, but the assumption is made in the interest of not understating the occupant impact velocity. The actual occupant impact velocity will decrease with increasing vehicular crush. However, as was demonstrated in the test of the eccentric loader with a 1,500-lb car (see test 7043-8, Appendix C), there is a limit to the extent of crush that can be tolerated, beyond which the structural integrity of the passenger compartment is violated, regardless of the theoretically computed occupant impact velocity. It is difficult to estimate how much the GET would crush the front of a 1,500-lb car. Based on a comparison of the longitudinal deceleration versus time data for test 7043-8 and a similar test with the GET using an 1,800-lb car (test MB-6 of Ref. 38), it can be seen that the initial impulse produced by both devices is roughly equal. However, the eccentric loader is a "gating" system that allows a vehicle to penetrate behind the barrier. These systems tend to be more lumpy and have periods of high decelerations separated by periods of very low deceleration. Further, the eccentric loader requires a flared end and performs better with increasing flare distances. Conversely, the GET is designed to be installed on a tangent section of barrier and is an attenuating system that brings impacting vehicles to a controlled stop. Therefore, the GET exhibits a more uniform deceleration after the initial impulse. Thus, the two terminals have been developed for different applications and cannot be directly compared.

Although both systems have been successfully crash tested according to *NCHRP Report 230,* their field performance has not been adequately investigated. As discussed above, if these systems prove to perform well during in-service evaluations, additional development will be required to improve their performance for minicars.

The SENTRE and TREND are two commercially available end treatments (*16*). As presently sold, neither system would satisfy *NCHRP Report 230* criteria for a 1,500-lb car. However, industry representatives have estimated that both could be modified to accommodate a 1,500-lb car with moderate changes in detail and cost.

Roadside Features

Slopes

Computer simulation studies conducted in the present study, details of which are given in Chapter Three, "Computer Sim-

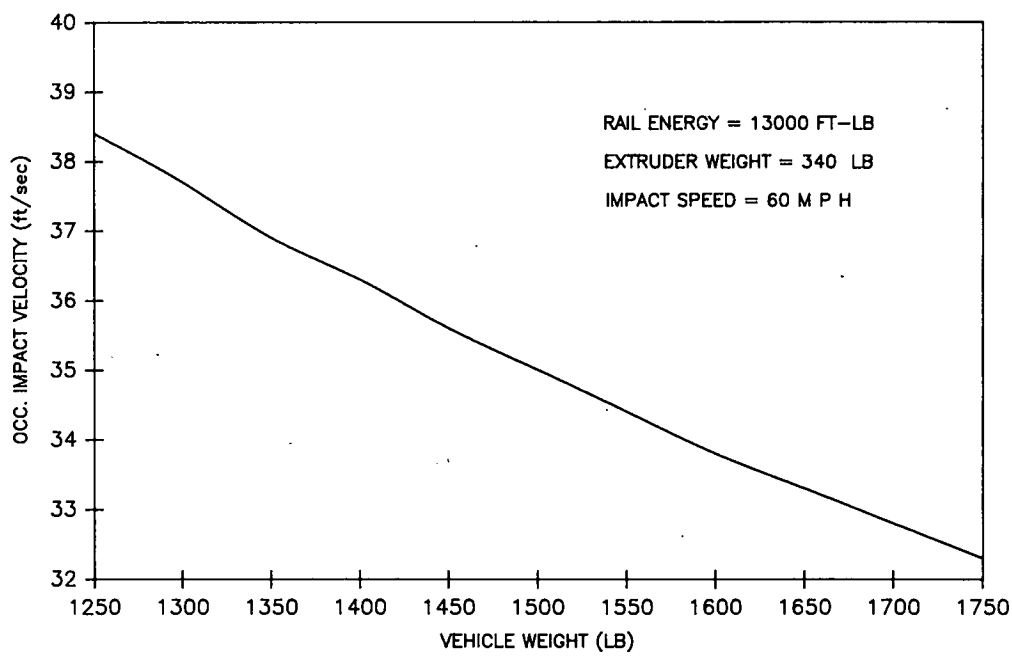

Figure 42. Estimated performance of GET for under 1,800-lb cars.

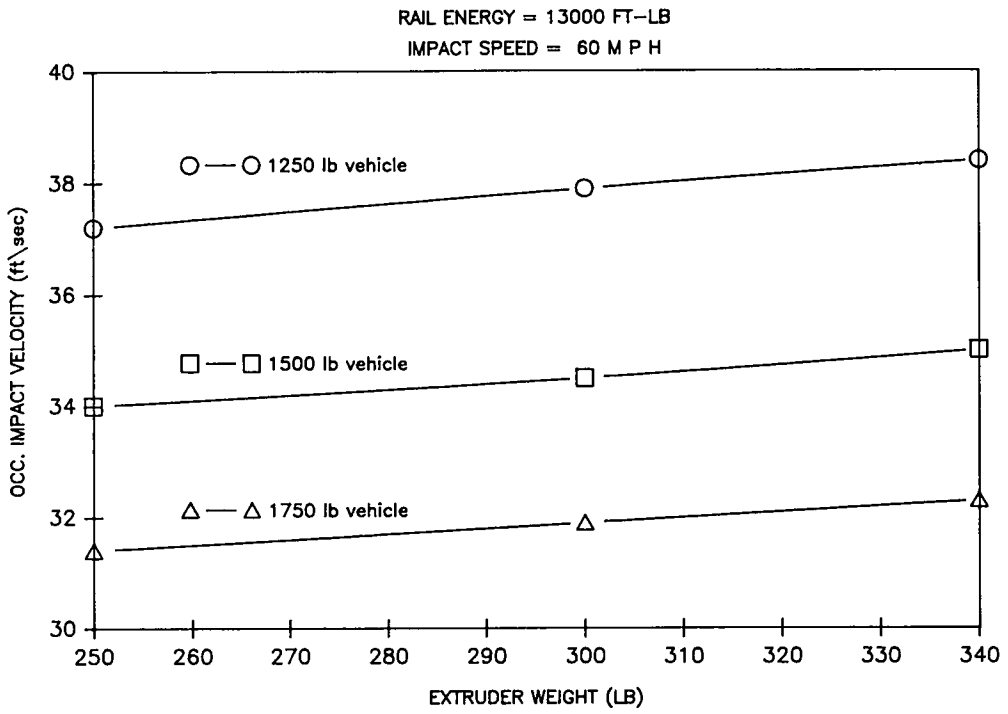

Figure 43. Occupant impact velocity versus extruder weight.

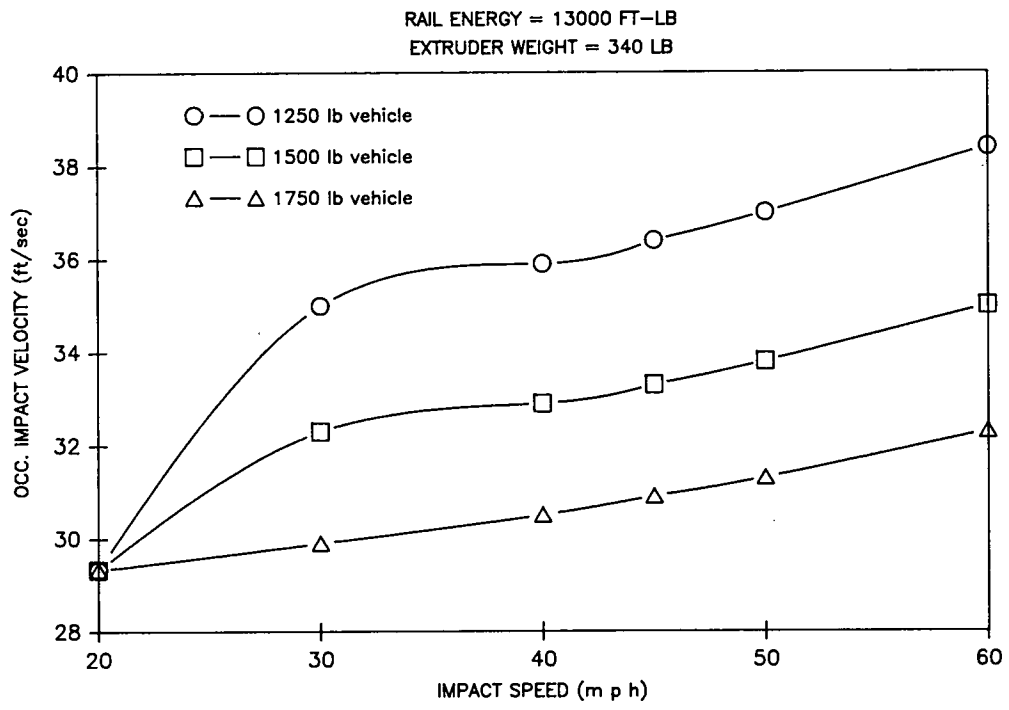

Figure 44. Occupant impact velocity versus impact speed for GET.

ulation Studies," and other studies involving full-scale tests and computer simulations of small vehicles (*7, 11, 23*) found that minicars can negotiate slopes as steep as 3:1 at approximately 60 mph without overturning for certain conditions. If the slope is dry and well compacted (this implies a friction coefficient of approximately 0.5) and free of irregularities, such as small boulders or large rocks, washouts, or other features that could trip the vehicle, overturn is not predicted for either tracking or nontracking encroachments on foreslopes for fill sections as steep as 3:1 and fill heights up to 20 ft.

The above findings notwithstanding, evidence is mounting from accident studies that the rate of overturn for all vehicle sizes on slopes increases significantly for slopes steeper than 4:1 (*11, 31*). Further, the same studies found that overturn rates on 3:1 and 2:1 slopes were approximately equal. There is also evidence (*11*) that smaller vehicles tend to overturn at a greater rate than do larger vehicles on a given slope.

It is apparent that many roadside slopes are not well compacted and free of irregularities. Under wet conditions, tires can rut and form a tripping mechanism. Further, as shown in Chapter Three, "Specialized Analytical Procedures," and in the literature (*11*), a slope irregularity that would not trip a larger car can trip a minicar.

This leads to a very difficult question that to date has largely not been addressed: What is a reasonable set of conditions for which roadside slopes should be designed for safety? Should they be designed for certain types and sizes of irregularities, friction values, or soil conditions? It should be noted that under certain conditions a vehicle will overturn on a flat surface.

On the basis of the foregoing discussion, it is clear that as the design vehicle gets smaller, roadside slope design and maintenance will become more critical. At a minimum, if the present AASHTO standards (*24*) are maintained, more effort will be needed in the construction and maintenance of roadside slopes to avoid the problem that irregularities and soil conditions pose to minicars. More in-depth accident studies and benefit/cost analyses will be needed to further assess the problem and possible solutions. Studies will also be needed to define the typical slope conditions for design and analysis purposes.

For cut slopes, the geometry of which is shown in Figure 8, it was found that minicars will overturn on 2:1 or steeper slopes for 60-mph encroachments. Simulation of larger cars for the same conditions did not result in overturn. This implies that the current AASHTO policy (*24*) that permits cut slopes as steep as 2:1 may need to be changed if the minicar becomes a design vehicle.

Ditches

Reference is made to Figure 9 for the specific ditch geometry examined in the present study. Simulations indicate that a minicar as small as 1,250 lb can negotiate this ditch geometry for a foreslope as steep as 3:1 in combination with a backslope as steep as 3:1 for certain conditions. If the slopes and ditch bottom are well compacted and free of irregularities or features that could trip the vehicle, overturn is not predicted for either tracking or nontracking encroachments at 60 mph.

However, reference is made to the discussion in the preceding section on "Slopes" regarding overturn propensity of cars on slopes and the effect slope irregularities have on minicar stability. Observations given in the "Slope" section with regard to potential changes in slope design to accommodate minicars are applicable to ditch sections also.

Driveways

Reference is made to Figure 10 for the driveway geometry examined in the present study. No attempt was made to simulate the effects of drainage structures or culvert ends on the driveways. Simulation runs, supported to a limited extent by two full-scale vehicular tests, indicate that a minicar has approximately an equal propensity for overturn on a given driveway configuration as does a large car. In previous studies (*26, 27*) of larger cars it was concluded that a foreslope of 8:1 or flatter, in combination with a driveway slope of 10:1 or flatter, was needed to prevent overturn for 60-mph tracking encroachments. Based on the present study a foreslope of 6:1 or flatter, in combination with a driveway slope of 10:1 or flatter, would be needed to prevent overturn of a minicar encroaching at 60 mph. The values were determined for the minicar approaching the driveway in a tracking mode. Overturn propensity is increased significantly if the car is sliding sideways into the driveway, especially if a drainage structure is in the vehicle's path.

It is recognized that flattening driveway slopes is costly due to added fill and longer culverts. Safety treatments of culvert ends are also needed to maintain the safety benefits of the flatter slopes. Benefit/cost studies will be needed to assess these and other factors. A recent study of TTI indicates it is cost beneficial to provide safety treatments to driveway culvert ends within the "clear zone" for all but very low-volume roadways (*25*).

Curbs

Reference is made to Figure 11 for the curb geometry selected for study. It is an AASHTO type "B" mountable curb (*24*). A series of full-scale vehicular tests with a minicar and a series of computer simulations with minicars show that for tracking impacts, this curb can be easily and safely mounted at encroachment angles up to 15 deg and speeds up to 60 mph.

Unfortunately, in many run-off-the-road accidents the vehicle is yawing or sliding sideways. As discussed in Chapter Three, "Specialized Analytical Procedures," and as shown in a recent study (*11*), a surface discontinuity or irregularity such as a steep-faced curb can trip and cause a sliding vehicle to overturn at relatively low speeds. For a given curb configuration the propensity for overturn increases as the vehicle size decreases.

To minimize the probability of a minicar overturning when sliding into a curb, the slope of the curb face should be as flat as possible, preferably 30 deg or less (*11*). AASHTO curb types C, E, and G (*24*), shown in Figure 45, satisfy the criterion. Studies have indicated that an initial face of up to approximately 2 in. can be used on these designs without degrading the impact performance (*11*).

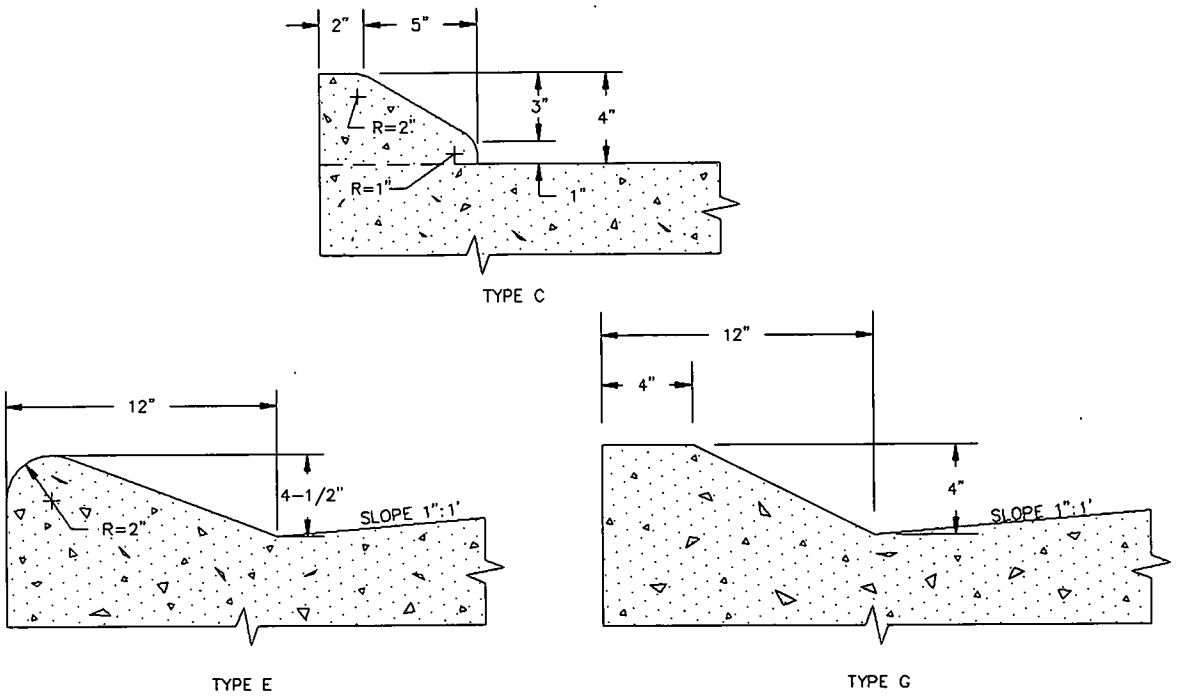

Figure 45. Preferred AASHTO highway curbs.

CHAPTER THREE

ANALYSIS PROCEDURES AND RESULTS

Several analysis techniques were used in pursuit of the project tasks. Heavy emphasis was placed on the calibration and use of computer programs designed to simulate complex vehicle-roadway interaction problems. A full-scale crash test program was conducted to (1) gain valuable insight on the performance of selected, widely used roadside safety elements when impacted by minicars and (2) to provide a data base from which the aforementioned computer programs could be calibrated for minicars. For certain types of roadside safety features, specialized analysis techniques were developed and used. This chapter describes the evaluation procedures and results obtained therefrom.

SELECTION AND CALIBRATION OF COMPUTER PROGRAMS

Candidate computer programs considered for use in the project included GUARD (*2*), HVOSM (*3*), BARRIER VII (*8*), and CRUNCH (*9*). A critique of these programs and their use in the design and analysis of roadside safety elements can be found in the literature (*32*) and will not be repeated here. Basically, GUARD is a three-dimensional program developed to study the impact of a vehicle with longitudinal barriers. Its original use was to study the effects of a vehicle's bumper design on the impact performance of guardrails. HVOSM is a three-dimensional program developed to study a range of vehicle-roadway problems including the handling response of a vehicle on and off the travelway and impacts with longitudinal barriers. BARRIER VII is a two-dimensional program developed to study in-plane vehicular response to impacts with flexible, longitudinal barriers. CRUNCH is an extension of GUARD to include simulation of articulated vehicles. Following is a discussion of the programs selected for simulation of roadside safety elements and the procedures used in their calibration.

Roadside Hardware

Rigid Longitudinal Barriers

Computer programs HVOSM and GUARD were considered for simulation of impacts with the rigid concrete safety-shaped barrier (CSSB). Both have three-dimensional response capabilities, a necessity to study the potential for vehicular overturn following impact with the CSSB. Both also have limitations with

regard to simulation of the CSSB. Neither program can accurately simulate the tire scrubbing forces that occur during CSSB impacts. The suspension model used in GUARD is quite limited in relation to that used in HVOSM. In HVOSM the vehicle's tires can interact with the sloped face of the CSSB, but the vehicle's sheet metal can only interact with a vertical wall.

Previous studies of CSSB impacts with HVOSM have met with reasonably good success (*33, 34*). The version of HVOSM used in these studies was one modified by TTI to include "hardpoints" within the vehicle's structure (*33*). This version was also used in the first phase of the present study in initial calibration efforts for minicars (*4*). Tests of an 1,800-lb car from a previous study (*35*) were simulated and the results compared well with test results. In all of these studies, however, special calibration techniques have had to be used because of inherent limitations of HVOSM. As perceived by the TTI researchers, a major limitation involved the vertical wall assumption. A key variable in previous calibration efforts was the lateral location of the vertical wall.

It was decided that, as part of the present project, an effort would be made to modify the RD2 version of HVOSM (*3*) to permit the vehicle's structure to interact with the sloped faces of the CSSB or with barriers of other shapes. In making these modifications, errors were also found and corrected in various subroutines. A discussion of the modifications and corrections is given in Appendix D.

An attempt was also made to incorporate recent changes to the HVOSM tire model to improve simulation of scrubbing forces during shallow angle contacts with curbs and edge drops on shoulders (*23, 36*). Upon receipt of a revised version of HVOSM, the researchers attempted to simulate a small car impact with the CSSB. It was, then, learned that the barrier impact routines had been removed in the revised version. An attempt was made to install these routines, but after considerable effort, it was concluded that this could not be done within the scope of the project. It is noted that, with the proper placement of hardpoints and proper selection of hardpoint stiffness values, the lateral forces on a tire or rim can be approximated in a manner similar to that in Refs. 23 and 36. As described subsequently, this was done in calibration of HVOSM for CSSB impacts. A description of the calibration of HVOSM for CSSB impacts is given in Appendix E.

It must be understood that even with the foregoing modifications and approximations, limitations still remain with regard to the simulation of impacts with a rigid barrier and, in particular, impacts with the tire and suspension models and with data to describe their characteristics. During impact, the leading tire and associated suspension system typically is subjected to extremely high loads and loading rates, resulting in large displacements and usually structural failure in the form of bent rims and a wheel jammed up and back from its normal position. Very little data are available on tire and suspension system damping properties for high loading rates. The models simply are not designed to simulate structural failures. These limitations notwithstanding, the HVOSM program is a useful tool, when properly calibrated, in the analysis of barrier and vehicle parameters as they affect impact performance.

Flexible Longitudinal Barriers

Vehicle underride, wheel snag, and overturn are potential problems associated with small car impacts with flexible barrier systems. Of all candidate simulation programs, the GUARD program is best suited for predicting these types of responses. Note that GUARD does not simulate wheel snag, but its occurrence can be inferred from the wheel's position in relation to the barrier's posts. The HVOSM is very limited in terms of flexible barrier simulation due to the gross nature in which the barrier is modeled. GUARD was therefore chosen to simulate minicar response to impact with a flexible barrier.

GUARD was calibrated and used by TTI researchers in a study (*7*) that preceded the present project. In the referenced study GUARD was used to simulate tests of small cars (1,800 lb) impacting the G4(1S) barrier at encroachment speed of 60 mph and at encroachment angles of 15 deg and 20 deg. GUARD was found to be capable of accurately predicting the degree of wheel snag for mini-size vehicles. It also gave reasonably good correlation with tests for most other measures of simulation accuracy, such as overall vehicle motion, maximum barrier deflection, and maximum vehicle crush. However, it was found to overestimate vehicular acceleration for most impacts.

In the initial phase of the present project, GUARD was subjected to further calibration efforts for the tests of Ref. 7. Vehicle structural stiffness was the primary parameter that was adjusted to improve the simulation. The program was recalibrated using the two full-scale G4(1S) crash tests conducted in the present study. A description of the calibration of GUARD for simulating G4(1S) barrier impacts is given in Appendix E.

Breakaway Supports

A key factor in evaluating the impact performance of a breakaway sign or luminaire support is the change in the velocity of the impacting vehicle during contact with the support. Upon reviewing existing computer programs capable of estimating vehicular velocity change, it was concluded that a new program should be written. The program should properly account for the key vehicular and support parameters. It should be user friendly and operational on a personal computer. It should have applications as a research tool or as an aid in the design and analysis of breakaway structures by practicing engineers. A program to satisfy these criteria was written and calibrated. It is described later in this chapter under "Specialized Analytical Procedures."

Another factor of concern is the stability and behavior of a vehicle following impact with a breakaway structure. It has been shown that violent overturns can occur if the impact causes the vehicle to yaw or spin out, common after off-center impacts with sign or luminaire supports. The problem is thought to become more acute as the size of the impacting vehicle decreases. Some success has been realized in simulating this occurrence by use of a modified version of the HVOSM program (*37*). The referenced program was calibrated and used in the present study to examine the post-impact behavior of minicars. Details are given under "Computer Simulation Studies" and in Appendix E.

Another factor of concern, primarily in breakaway luminaire supports, is the trajectory of the support in relation to the impacting vehicle. It has been demonstrated in many crash tests that the support often falls on some part of the vehicle following low speed impacts. Fortunately, the roof structure on most cars is of sufficient strength to prevent major intrusion into the passenger compartment. Analysis of this factor was not undertaken in the present study.

Base-Binding Sign Supports

There is no computer program capable of simulating the impact behavior of a vehicle in collision with a base-bending sign support. The dynamic response of the post-soil system is highly nonlinear with failure modes that are extremely difficult to define and model.

In the absence of this capability the HVOSM program was used to study vehicular behavior for an impulse as determined from the crash test of a base bending sign support (see Appendix C, "Full-Scale Crash Tests"). A version of HVOSM, as revised at TTI (*37*) to allow input of an arbitrary impulse, was used in this phase of the project. Factors such as occupant impact velocity and the post-impact trajectory of the vehicle were determined. Calibration of HVOSM for sign impacts is given in Appendix E. Details of parametric studies are discussed in this chapter under "Computer Simulation Studies."

Crash Cushions

Most crash cushions now in use across the United States were developed and are marketed by private industry. Special materials, design procedures, and analysis tools have evolved during the development process. The characteristics of these materials and the analysis tools are not generally made available to the public. Reliance must, therefore, be made on the manufacturers to estimate changes that would be necessary to accommodate minicars. As indicated earlier in this report, such information was provided.

The principles by which the impact performance of a sand-filled plastic barrel crash cushion can be estimated are well known. Analysis of this system is given in this chapter under "Specialized Analytical Procedures."

Guardrail Terminals

There is no comprehensive computer program capable of simulating the impact performance of the eccentric loader guardrail terminal selected for study in the present project. Attempts to mathematically model the dynamic buckling behavior of an eccentrically loaded W-beam in an earlier TTI study were not successful (*41*). An attempt was made, however, to study the behavior of the vehicle following an off-center, head-on impact with the eccentric loader. The HVOSM program was used for this purpose. Calibration of the program and results of these simulations are given in Appendix E and in this chapter under "Computer Simulation Studies."

Roadside Features

Roadside geometric features selected for evaluation were as follows: slopes—fill and cut; ditches, driveways, and curbs.

Each of these features was evaluated via the HVOSM program. Use of HVOSM for simulating these features has been made by TTI (*7, 21, 26, 27, 42*) and others (*11, 23, 43*). In these studies, HVOSM has been shown to compare reasonably well with full-scale vehicular tests of the respective features. The primary purpose of the simulations in the present study was to examine the stability of under 1,800-lb cars as they traversed the above features.

The TTI version of HVOSM (*44*) and the RD2 version (*3*) were considered for simulating encroachments on roadside geometric features. A desirable feature of the TTI version not present in the RD2 version is the ability of specified vehicular contact points (other than the tires) to interact with the terrain. This feature is important for bumper or sheet metal contact with the terrain. A feature in the RD2 version not present in the TTI version is the ability to simulate four-wheel independent suspension, a characteristic of certain minicars. Runs were made with both versions on selected fill slopes to evaluate the effects of a solid rear axle versus independent rear suspension. Only minor differences were observed in the results where no vehicle contact points interacted with the terrain. It was therefore decided that the TTI version would be used because vehicle/terrain interaction is often an important factor in vehicular response.

While the HVOSM program has compared reasonably well with full-scale tests of the above roadside geometric features, further comparisons were made in the present study. As described in Appendix E, HVOSM was calibrated with minicar tests of a driveway configuration and tests of an AASHTO type B curb. Use of HVOSM in parametric studies of roadside safety features is discussed under "Computer Simulation Studies."

FULL-SCALE CRASH TEST PROGRAM

A series of full-scale crash tests were conducted to evaluate the performance of widely used roadside safety elements when impacted by under 1,800-lb cars. The tests also provided a valuable data base from which computer programs could be calibrated for under 1,800-lb cars. Seven different roadside features were examined in the test program. They were: (1) concrete safety-shaped barrier (CSSB); (2) strong-post, W-beam guardrail on steel posts; (3) luminaire support mounted on a frangible transformer base; (4) base-bending small sign support; (5) "eccentric-loader" end treatment for W-beam guardrail; (6) AASHTO type "B" curb, 6 in. high; and (7) side slope, driveway slope combination.

As applicable, *NCHRP Report 230* (*1*) guidelines were followed in the conduct and evaluation of the tests. Each test was intended to represent an "occupant risk" test specified in *NCHRP Report 230*. It is noted that *NCHRP Report 230* does not address the evaluation of roadside safety features such as ditches, driveways, curbs, and the like. In the absence of guidelines the procedure followed in the present study was to conduct a series of tests in order of increasing severity until the test vehicle was not restorable for further tests. Test series 7043-9 (curb) and 7043-10 (driveway geometry) were conducted in this manner. This procedure was followed primarily with a view toward the development of a data base for calibration of the HVOSM program.

Each safety element listed above was tested with a vehicle weighing approximately 1,500 lb. Fiat Unos were used in these tests. In addition the CSSB was tested with three other cars, namely, a 1,250-lb Daihatsu Domino, a 1,550-lb Chevrolet Sprint, and a 1,610-lb Ford Fiesta. The CSSB received more attention in the crash test program because of its wide use and because of major concern for the stability of small cars following impact with the CSSB. Further details of the cars and their properties are given in Chapter Two under "Selection of Minicars and Measurements of Their Properties," Appendix B, Appendix C, and in the Phase I report (*4*).

A summary of the tests and results therefrom is given in Table 5. Comprehensive details of each test are given in Appendix C. In relation to *NCHRP Report 230* evaluation criteria, the following test results are noted.

CSSB. Tests 7043-1 and 7043-4 were in full compliance. Tests 7043-2 and 7043-12 were marginally acceptable because the lateral occupancy impact velocities exceeded the recommended 20-ft/sec value but were below the 30-ft/sec limit. It is noted that tests of a G4(2W) barrier (a flexible barrier) with an-1,800-lb car for the same impact conditions also produced marginal occupant impact velocities (*28*). Test 7043-3 was marginally acceptable because the lateral ridedown acceleration exceeded the 15 g recommended design value but was less than the 20-g limit.

G4(1S). Both tests (7043-5 and 7043-11) were marginally acceptable because the lateral occupant impact velocity slightly exceeded the recommended 20-ft/sec design value. Also, in test 7043-11 the lateral ridedown acceleration exceeded the recommended 15-g design value. As just noted, tests of a G4(2W) barrier with an 1,800-lb car for the same impact conditions also produced marginal occupant impact velocities (*28*). Some wheel snag occurred in the 20-deg test, but it did not adversely affect the performance.

Luminaire Support. Test 7043-6 was not in compliance because the base did not break away and longitudinal occupant impact velocity exceeded 15-ft/sec limit.

Base-Bending Sign Support. Test 7043-7 was in compliance, but the vehicle sustained considerable damage.

Eccentric Loader Guardrail Terminal. Although the occupant impact velocity criteria were satisfied, the ridedown accelerations were excessive. Further, in the judgment of the research team the "intrusion" criteria of *NCHRP Report 230* were not satisfied. The intrusions and penetrations of the passenger compartment observed in test 7043-8 (see Appendix C, "Full-Scale Crash Tests," for description of damage) would have exposed the occupants to a high risk of serious injuries. It should be noted that an assessment of the intrusion criteria necessarily requires a subjective evaluation. It is anticipated that NCHRP Project 22-7, to update *NCHRP Report 230,* will address the need for more objective intrusion criteria.

AASHTO Type "B" Curb. NCHRP Report 230 does not address the impact performance of curbs. However, based on all available measures, all five tests were satisfactory.

Driveway Slope. NCHRP Report 230 does not address the impact performance of roadside geometric features. However, test 7043-10A can be judged to be marginally acceptable because the longitudinal ridedown acceleration exceeded the recommended 15-g design value, and test 7043-10B can be judged to be not acceptable because the longitudinal ridedown acceleration exceeded the 20-g limit.

COMPUTER SIMULATION STUDIES

A major portion of this project was devoted to the calibration and application of computer programs for simulating under 1,800-lb car interactions with roadside safety elements. In excess of 1,000 HVOSM computer runs and over 150 GUARD runs were made in the process. Numerous runs were also made with a specialized computer program written to evaluate the impact performance of breakaway sign and luminaire supports. The selection of computer programs and their calibration were discussed earlier in this chapter under "Selection and Calibration of Computer Programs." Described in this section is the application of the programs to evaluate limits of performance of current designs and to evaluate potential modifications to current designs to accommodate under 1,800-lb cars.

Because of the large number of simulation runs made and the extremely voluminous output therefrom, it was not feasible to include details of each run in this report. Rather, an attempt is made to summarize the significant findings. Detailed output from each run described in this section, as well as each final calibration run (see Appendix E), was stored on floppy disks. An individual interested in the stored data should contact one of the authors at TTI to arrange for copying the data. The data are stored on approximately 250 floppy disks.

Roadside Hardware

Rigid Longitudinal Barriers

A modified version of HVOSM developed in the present study (see Appendix D) was used to simulate rigid barrier impacts. A major effort was devoted to the modification and application of HVOSM to study the impact performance of the CSSB for a variety of conditions. Simulations were also made of impacts with potentially new rigid barrier designs.

In the initial phases of the study the simulations focused on the impact performance of the CSSB based on *NCHRP Report 230* performance criteria, as called for in the problem statement and tasks. Those criteria involve tracking impacts at 60 mph and impact angles of 15, 20, and 25 deg. Runs were therefore made for these conditions for the four under 1,800-lb cars selected for the project, i.e., a Daihatsu Domino, a Fiat Uno, a Chevrolet Sprint, and a Ford Fiesta.

In accordance with *NCHRP Report 230* guidelines the results of the runs were evaluated in terms of occupant risk factors, namely, vehicular stability and occupant impact velocity. To meet the referenced criteria the vehicle must remain upright and the occupant impact velocities must satisfy the following:

Occupant Impact Direction	Recommended (ft/sec)	Limit (ft/sec)
Longitudinal	30	40
Lateral	20	30

According to *NCHRP Report 230,* an occupant whose impact velocity is at the "limit" can be expected to experience "severe but not life threatening" injuries. The limit values can be divided by "appropriate acceptance factors, *F,* to establish less severe design values" according to *NCHRP Report 230.* Suggested values are 1.33 for the longitudinal direction and 1.5 for the lateral direction, as reflected in the foregoing recommended values.

Reference should be made to *NCHRP Report 230* for the procedure used in computing the occupant impact velocity. In summary, the procedure, referred to as "Method I" herein, is as follows:

1. Using longitudinal and lateral vehicular accelerations (as determined with respect to a moving vehicular coordinate system at the center of mass of the vehicle) versus time data, determine (by double integration) the times at which the movement of an

Table 5. Crash test summary.

		IMPACT CONDITIONS			TEST RESULTS									
					VEHICLE DATA					OCCUPANT RISK VALUES				
										IMPACT VEL. (ft/sec)		RIDEDOWN ACCEL.(g's)		
TEST ARTICLE	TEST NO.	VEHICLE WT (lb)[a]	SPEED (mph)	IMPACT ANGLE (deg)	EXIT SPEED (mph)	EXIT ANGLE (deg)	TIME OF EXIT (sec)	MAX. PITCH ANGLE (deg)	MAX. ROLL ANGLE (deg)	LONG.	LAT.	LONG.	LAT.	COMMENTS
A. Concrete Safety Shaped Barrier (See Figure 6)	7043-1	1,560	58.4	15.0	49.8	1.8	0.265	10.6	-7.2	11.2	18.4	0.9	8.2	Smooth redirection.
	7043-2	1,560	59.9	21.9	46.8	1.5	0.260	15.8	9.2	18.4	25.0	-1.6	7.5	Smooth redirection.
	7043-3	1,280	60.0	16.0	53.2	1.8	0.211	16.6	11.2	12.1	14.9	-1.8	17.7	Smooth redirection.
	7043-4	1,610	61.6	16.0	52.0	2.9	0.274	-9.2	-12.9	12.1	19.3	1.8	6.0	Smooth redirection.
	7043-12	1,530	61.6	20.1	54.7	7.4	0.208	7.5	-30.3	12.4	21.1	0.8	9.0	Smooth redirection.
B. G4(1S) Roadside Barrier (See Figure 7)	7043-5	1,550	61.2	15.6	47.3	7.6	0.282	6.8	-7.0	9.9	21.6	0.7	12.2	Smooth redirection. Vehicle overturned after sideslipping in soil downstream from barrier.
	7043-11	1,553	61.8	20.6	47.1	6.8	0.335	11.4	2.9	15.2	20.6	-4.6	17.1	Smooth Redirection. Minor wheel contact with a guardrail post.
C. Luminaire Support with Transformer Base (See Figure 8)	7043-6	1,520	20.0	0	0	N/A	N/A	1.2	-3.8	26.9	2.5	-2.4	1.7	Support did not break away.
D. Base-Bending Sign Support (See Figure 9)	7043-7	1,530	59.8	0	50.4	N/A	0.111	0.8	-6.8	12.9	4.6	-1.4	-0.3	Considerable vehicle damage. However, vehicle remained stable and did not spin out.
E. "Eccentric Loader" Guardrail End Terminal (See Figure C-75, Appendix C)	7043-8	1,530	60.4	0	24.7	N/A	0.310	3.2	-4.9	27.4	None	-23.2	-18.7	Did not pass NCHRP 230 Criteria due to deformation of and intrusions into passenger compartment and ridedown accelerations were excessive.
F. AASHTO Type "B" Curb (See Figure 15)	7043-9A	1,550	33.0	5.0	N/A	N/A	N/A	-3.5	6.9	None	None	-0.8	-3.1	Left-side tires mounted curb. No damge to vehicle.
	7043-9B	1,550	45.6	5.0	N/A	N/A	N/A	-2.4	7.2	None	5.1	-1.9	1.0	Left-side tires mounted curb. Slight dent in left-front rim.
	7043-9C	1,550	30.0	15.0	N/A	N/A	N/A	-3.0	6.2	None	None	-2.0	5.0	Vehicle traversed curb. Dent in left-front rim.
	7043-9D	1,550	46.8	15.0	N/A	N/A	N/A	-1.8	6.6	None	2.8	-2.7	-0.6	Vehicle traversed curb. Left front tire aired out. Left-side rims and right-front rim dented.
	7043-9E	1,550	63.0	15.0	N/A	N/A	N/A	-2.0	7.2	None	5.4	-3.0	3.2	Vehicle traversed curb. Front tires aired out. Left-side rims and right front rim dented. Some damage to left front suspension system.
G. Driveway Slope Tests (See Figure C-121, Appendix C)	7043-10A	1,550	40.6	15.0	N/A	N/A	N/A	-15.1	-9.8	8.4	7.4	-18.1	4.3	Vehicle airborne for 30 ft. Vehicle remained upright and stable. Damage to left front suspension system due to traversal of culvert end section.
	7043-10B	1,550	51.6	15.0	N/A	N/A	N/A	15.2	-9.8	5.1	3.3	-23.0	7.7	Vehicle airborne for 53 ft. Vehicle remained upright and stable. Damage to front undercarriage and front suspension system.

[a] Does not include weight of dummy.

"occupant" (as represented by an unconstrained lump mass) equals 1.0 ft in the lateral direction and 2.0 ft in the longitudinal direction. These distances are the assumed flail spaces for an unconstrained occupant.

2. Using vehicular accelerations versus time data, determine the change in the vehicle's longitudinal and lateral velocities at the respective times determined in step 1. These changes equal the occupant impact velocities in the respective directions.

The above procedure is routinely used to evaluate crash tests at TTI through computer analysis of digitized crash test data. A special computer program was written to apply the procedure to evaluate HVOSM output. The program is described in Appendix G.

It is recognized that the *NCHRP Report 230* procedure for computing occupant risk is a first-order approximation to the complex problem of the kinematics of an unconstrained "occupant." Nonetheless, it incorporates inconsistencies and inappropriate assumptions. An improved method for estimating occupant impact velocities was developed and it is referred to as "Method II" herein. Its inclusion in the present study is for comparative purposes and not as a replacement for the *NCHRP Report 230* procedure. Future studies should, however, give strong consideration to the improved procedure. Improvements are as follows:

1. *More exact flail space geometry.* The improved procedure more accurately defines the actual flail space geometry of the passenger compartment, whereas the current procedure assumes a 1.0-ft lateral flail space and a 2.0-ft longitudinal flail space, regardless of the direction of the occupant's movement. For example, if a car leaves the road to the right and strikes a guardrail, an unconstrained driver can flail laterally across the entire front seat, a distance in excess of 3 ft.

2. *More exact tracking of occupant movement.* In the improved procedure occupant movement is tracked to determine the sequence in which surfaces are impacted and velocity components are adjusted accordingly. For example, if the occupancy strikes the side of the car first, the lateral component of velocity goes to zero. The occupant then moves parallel to the side of the car until striking the instrument panel, or possibly striking the side of the car again (for certain types of vehicular movement). In the *NCHRP Report 230* procedure, lateral and longitudinal movements are assumed to be independent of each other.

3. *Properly accounts for angular movement of vehicle.* The impact velocity of an occupant with a surface in the passenger compartment depends on the relative velocity between the vehicle and occupant. In addition to translational motion (as assumed in the *NCHRP Report 230* procedure), there is often very rapid angular motion, especially in longitudinal barrier impacts. The velocity of a given point on a passenger compartment surface depends on this angular motion, and this is included in the improved model, whereas it is neglected in the *NCHRP Report 230* procedure. Yaw rates of 150 deg/sec are common for 60-mph/15-deg impacts with the CSSB. Yaw rates of this magnitude can increase the relative velocity by 6 ft/sec or more.

A description of the improved procedure is given in Appendix G.

Simulation results to evaluate the response of under 1,800-lb cars for tracking impacts with the CSSB, per *NCHRP Report 230* recommended test conditions, are given in Table 6. Note that five of the runs were calibrated with actual crash tests (see Appendix E, "Rigid Longitudinal Barriers," under "Calibration of Computer Programs").

For purposes of analysis and characterization of vehicular stability, five terms are used. They are defined, somewhat arbitrarily, as follows: (1) stable—vehicle is smoothly redirected; (2) sideslip—with reference to Figure 46, the vehicle is sideslipping when $\mathrm{TAN}^{-1}(|V|/u) > 20$ deg; (3) spinout—with reference to Figure 46, the vehicle spins out when $u \leq 0$; (4) marginal—response is marginal when roll and/or pitch angle exceeds 40 deg but vehicle does not overturn (see Figure 47 for definition of angular rotation); and (5) overturn—when angular rotation in the roll and/or pitch direction is 90 deg or more, the vehicle has overturned. From Table 6 it can be seen that with one exception, stable performance is predicted for all vehicles for the given impact conditions.

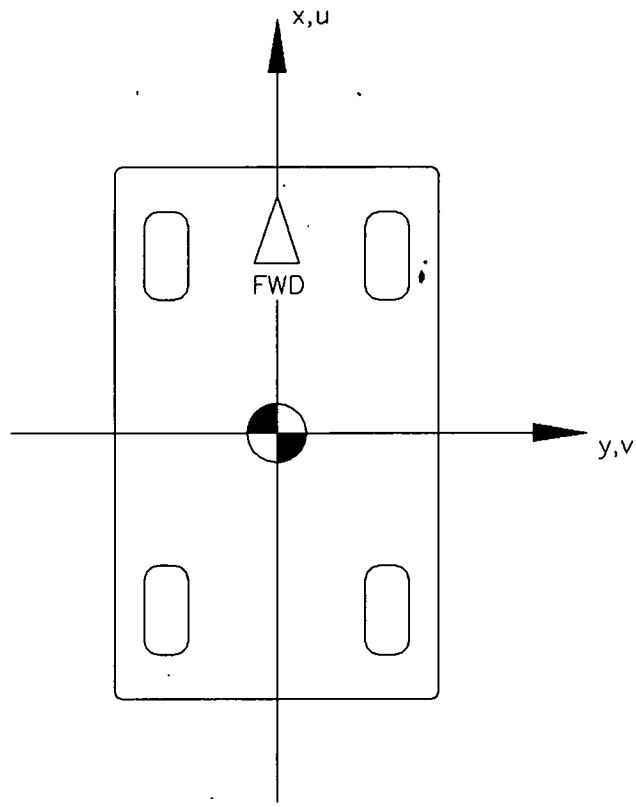

u = COMPONENT OF VEHICLE VELOCITY IN X DIRECTION.

v = COMPONENT OF VEHICLE VELOCITY IN Y DIRECTION.

$$\text{SIDESLIP ANGLE} = \mathrm{TAN}^{-1}\frac{|v|}{u}$$

Figure 46. Vehicle velocity components.

Table 6. Simulation of CSSB tracking impacts.

		IMPACT CONDITIONS		EXIT CONDITIONS		VEHICLE PARALLEL TO BARRIERS					
VEHICLE	TOTAL INERTIAL WEIGHT (lb)	SPEED (mph)	ANGLE (deg)	SPEED (mph)	ANGLE (deg)	TIME (sec)	DISTANCE TRAVELED (ft)	MAX. ROLL (deg)[a]	MAX. PITCH (deg)[b]	MAX. HEIGHT OF CLIMB (ft)	STABILITY RATING
Fiat Uno[c]	1,560	58.4	15.0	53.8	-3.70	0.263	21.12	-9.80 5.42	5.07 -4.57	1.23	Stable
Fiat Uno[d]	1,560	59.9	21.9	51.7	-3.47	0.272	21.05	-11.86 18.29	5.09 -4.36	1.44	Stable
Fiat Uno	1,560	60.0	25.0	49.5	-5.17	0.275	20.60	-12.9 26.09	5.02 -2.11	1.48	Stable
Daihatsu Domino[e]	1,280	60.0	16.0	54.7	-2.21	0.417	33.91	-14.96 8.04	5.91 -3.04	0.63	Stable
Daihatsu Domino	1,280	60.0	20.0	52.5	-1.06	0.308	24.22	-7.73 28.47	6.53 -2.14	1.57	Stable
Daihatsu Domino	1,280	60.0	25.0	49.5	-3.70	0.207	15.53	-9.47 41.72	7.34 -1.16	1.30	Marginal
Ford Fiesta[f]	1,610	61.6	16.0	56.2	-0.17	0.663	55.21	-14.79 6.18	11.31 -5.13	1.63	Stable
Ford Fiesta	1,610	60.0	20.0	51.6	0.0	0.803	62.45	-15.68 11.96	11.85 -5.16	1.8	Stable
Ford Fiesta	1,610	60.0	25.0	49.4	-0.01	0.776	57.29	-17.66 9.60	11.27 -4.65	1.89	Stable
Chevy Sprint	1,530	60.0	15.0	55.2	-0.76	0.243	20.11	-16.15 9.08	6.38 -5.89	1.15	Stable
Chevy Sprint[g]	1,530	61.6	20.1	53.5	-2.09	0.227	18.49	-17.26 6.77	7.88 -6.64	1.48	Stable
Chevy Sprint	1,530	60.0	25.0	49.1	-0.82	0.413	30.81	-21.24 8.24	9.63 -7.34	1.60	Stable

[a] For Roll angles: (+) - Rolling into the barrier; (-) - Rolling away from the barrier
[b] For Pitch angles: (+) - Pitching up: (-) - Pitching down
[c] Simulation of test 7043-1
[d] Simulation of test 7043-2
[e] Simulation of test 7043-3
[f] Simulation of test 7043-4
[g] Simulation of test 7043-12

Table 7 gives the estimated occupant impact velocities for the runs of Table 6. Note that values given under the column "From Test Method I" were determined from crash test data in accordance with *NCHRP Report 230* procedures. They are given in Table 7 for comparative purposes. Values given under the column "From Simulation Method I" were determined from HVOSM output in accordance with *NCHRP Report 230* procedures. Values given under the column "From Simulation Method II" were determined from HVOSM output in accordance with the improved procedure previously discussed, and detailed in Appendix G.

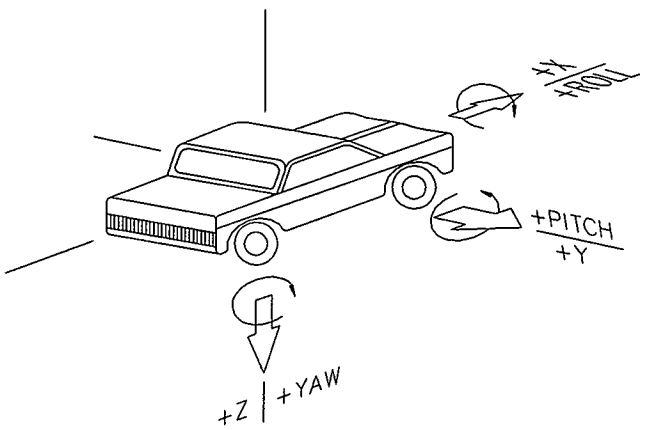

Figure 47. Positive sign convention for vehicle.

Two items are noted with regard to the data in Table 7. First, although measurable differences exist between the Method I test and simulation longitudinal occupant impact velocities in certain tests, the overall correlation between test and simulation occupant impact velocities is considered good. The lateral occupant impact velocities from the simulations with Method I are within ±12 percent of the test values. This is significant for two reasons: (1) vehicle/barrier impacts involve very complex mechanisms that are difficult to simulate within the limitations of existing computer programs, and (2) the lateral occupant impact velocity is generally more critical than the longitudinal velocity for impact with longitudinal barriers.

The second item is that the occupant impact velocities as determined by Method II are significantly different from the comparable Method I values, especially for the lateral values. In every case the Method II values are greater than the Method I values. Reference should be made to preceding paragraphs for a discussion of the differences in the two methods of analysis. The primary reason for the large differences in the values of Table 7 for the two methods is the differences in the flail space distance. In Method I, the distance is arbitrarily set at 1.0 ft; while in Method II, it depends on the direction the occupant is moving. For a longitudinal barrier impact in which the right side of the vehicle strikes the barrier, the unconstrained driver can flail across the front seat and impact the right door, a distance in excess of 3 ft. Because all simulated impacts were right-side impacts, the large flail space distance governs in Method II.

Recent studies have found that the small car is overrepresented in overturn accidents, including those involving the CSSB (*11*). Because the five crash tests of minicars conducted in the present study and the simulation runs of Tables 6 and 7 gave no indication of unstable performance, efforts were directed toward the study of impact conditions different from those just described. It is known that vehicles impact barriers at various angle/speed combinations in a tracking condition. Further, analysis of accident data (*23*) indicates that a large percentage of vehicles strike barriers in a nontracking condition. A series of HVOSM runs were therefore made to estimate vehicle performance for these "atypical" conditions. The purpose of these runs was to examine the stability question. An analysis of occupant impact velocities was not made.

Figure 48 shows the impact parameters included in the study of rigid barriers. Note that θ is the angle formed by the resultant translational velocity vector of the vehicle and the longitudinal axis of the barrier. ψ is the angle formed by the longitudinal axis of the vehicle and the longitudinal axis of the barrier, and $\dot{\psi}$ is the angular velocity or yaw rate of the vehicle as it strikes the barrier. A clockwise direction for $\dot{\psi}$ was arbitrarily selected because this is believed to be more critical in terms of overturn potential than a counterclockwise direction. Obviously, some nontracking accidents occur with the vehicle spinning clockwise, and some occur with the vehicle spinning counterclockwise. It is not known which, if either, direction is predominant for barrier impacts. A value of 15 deg/sec was used for $\dot{\psi}$. It is known that yaw rates of 20 to 30 deg/sec can be achieved in an emergency steer maneuver. The rate can be much higher if the vehicle strikes another vehicle or object prior to impacting the barrier. For tracking impacts, note that $\psi = \theta$ and $\dot{\psi} = 0$.

Table 8 gives the results of a series of HVOSM runs for high

Table 7. Occupant impact velocities for the simulations of impacts with CSSB.

	Impact Conditions		Occupant Impact Velocity (ft/sec)					
			Longitudinal			Lateral		
			From Test	From Simulation		From Test	From Simulation	
Vehicle	Speed	Angle	Method I	Method I	Method II	Method I	Method I	Method II
Fiat Uno[a]	58.4	15.0	11.2	7.7	3.9	18.4	16.9	22.8
Fiat Uno[b]	59.9	21.9	18.4	14.8	8.9	25.0	23.6	33.2
Fiat-Uno	60.0	25.0	N/A	17.7	11.8	N/A	24.7	37.4
Daihatsu Domino[c]	60.0	16.0	12.1	6.8	5.4	14.9	16.6	24.0
Daihatsu Domino	60.0	20.0	N/A	12.2	8.5	N/A	19.9	29.6
Daihatsu Domino	60.0	25.0	N/A	17.6	14.0	N/A	25.0	34.6
Ford Fiesta[d]	61.6	16.0	12.1	9.4	6.1	19.3	17.3	26.1
Ford Fiesta	60.0	20.0	N/A	12.3	9.2	N/A	19.9	29.9
Ford Fiesta	60.0	25.0	N/A	17.9	13.1	N/A	25.4	36.3
Chev. Sprint	60.0	15.0	N/A	7.5	3.3	N/A	17.2	24.5
Chev. Sprint[e]	61.6	20.1	12.4	12.2	7.7	21.1	20.7	32.5
Chev. Sprint	60.0	25.0	N/A	16.9	11.2	N/A	23.5	37.

[a] Simulation of test 1
[b] Simulation of test 2
[c] Simulation of test 3
[d] Simulation of test 4
[e] Simulation of test 11

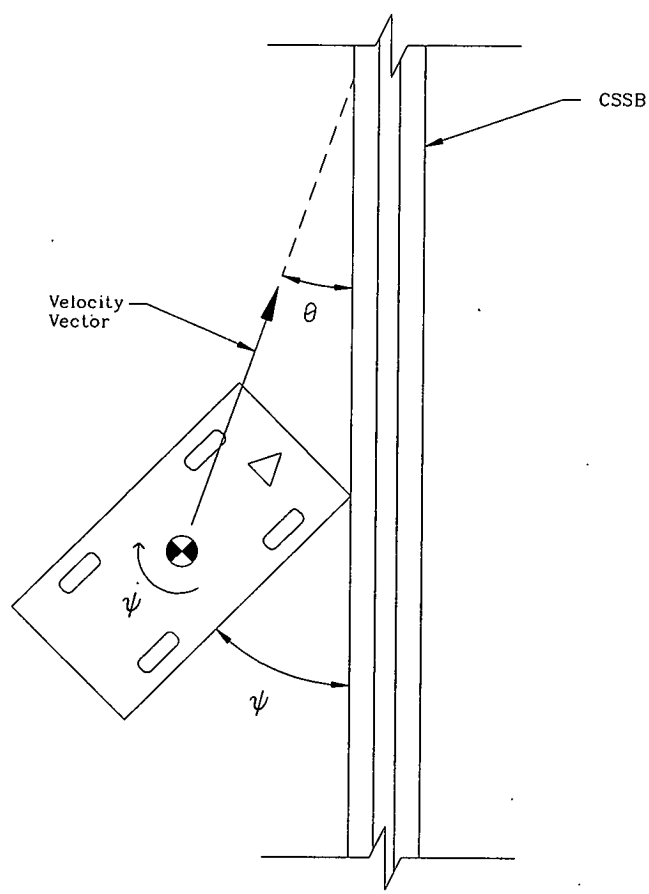

Figure 48. Impact parameters.

speed/angle, tracking impacts with the CSSB for a variety of cars. The Ford Fiesta was not included in these and subsequent computer studies of the CSSB because its performance was found to be similar to the Chevrolet Sprint. The Honda Civic weighed approximately 1,800 lb and the Plymouth Fury weighed approximately 4,500 lb. It can be seen that the small cars exhibited a significantly greater overturn propensity for these conditions than did the large car. It is also apparent that the probability of injury would be high for the larger speed/angle combinations, regardless of the vehicle's stability or size.

Table 8. Stability study for high speed/angle tracking impacts with CSSB. See Figure 48 for definition of angle θ.

(a) Fiat Uno-45

Angle θ (Deg) \ Speed (mph)	30	45	60
35	Stable	Stable	Stable
45	Stable	Marginal	Overturn
60	Overturn	Overturn	Overturn

(b) Daihatsu-Domino

Angle θ (Deg) \ Speed (mph)	30	45	60
35	Stable	Stable	Stable
45	Spinout	Spinout	Marginal
60	Overturn	Overturn	Overturn

(c) Chevrolet Sprint

Angle θ (Deg) \ Speed (mph)	30	45	60
35	Stable	Stable	Stable
45	Sideslip	Marginal	Overturn
60	Overturn	Overturn	Overturn

Table 8. Continued

(d) Honda Civic

Angle θ (Deg) \ Speed (mph)	30	45	60
35	Spinout	Stable	Stable
45	Marginal	Overturn	Overturn
60	Overturn	Overturn	Overturn

(e) Plymouth Fury

Angle θ (Deg) \ Speed (mph)	30	45	60
35	Stable	Stable	Stable
45	Sideslip	Sideslip	Sideslip
60	Sideslip	Sideslip	Sideslip
75	Spinout	Spinout	Spinout

Figure 49 is a plot of the yaw, pitch, and roll angles of the 45-mph/45-deg Chevrolet Sprint run from Table 8. In analyzing the nature of the angular response, it must be remembered that the angles are measured with respect to axes fixed at impact. Further, the angles are assumed to be zero at the time of impact. In this case the longitudinal axis of the vehicle was oriented 45 deg to the longitudinal axis of the barrier at impact. An increasing negative yaw angle means that the car rotated toward the barrier after impact.

Table 9 gives the results of HVOSM runs of nontracking impacts with the CSSB for a variety of cars. Note that the results given in Table 9 refer to the post-impact behavior. By definition, the vehicle is sideslipping at impact for each run. Again, these results clearly indicate a much greater overturn problem for the small cars at these conditions than for the large car. Yaw, pitch, and roll angles with respect to time of a selected Chevrolet Sprint run are shown in Figure 50.

Figure 12 of Chapter Two shows three potential, new rigid barrier designs that were examined. As discussed below, these shapes greatly reduce the small car overturn problem. Other possible benefits of the shapes were discussed in Chapter Two, section heading "Modifications to Selected Roadside Safety Elements to Accommodate Minicars," under "Roadside Hardware."

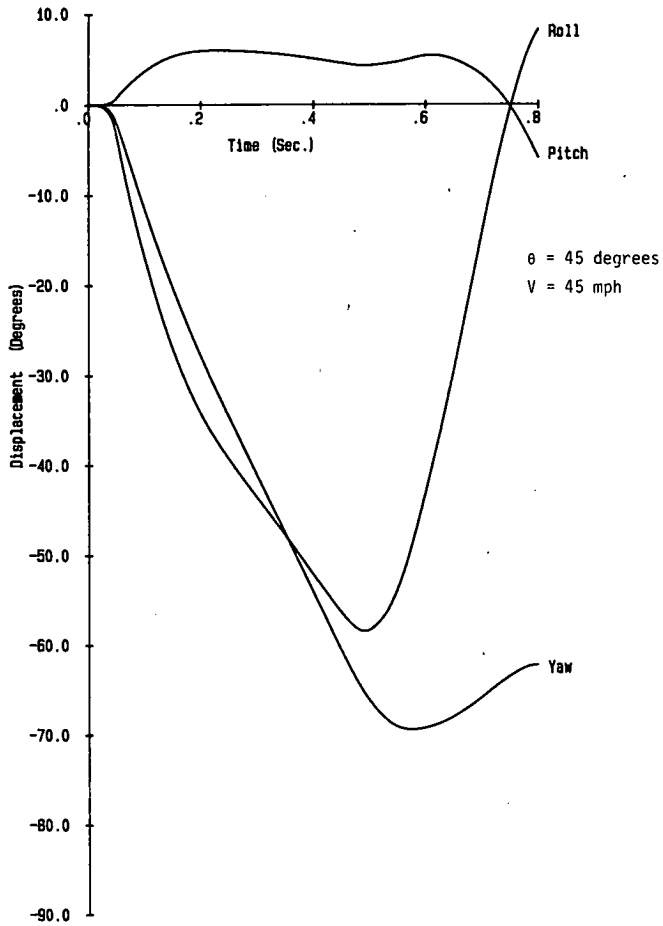

Figure 49. Roll, pitch, and yaw angles for high angle tracking impact with CSSB by Chevrolet Sprint.

Table 10 gives the results of HVOSM runs of nontracking impacts with the Chevrolet Sprint with the constant-slope barrier. No tracking runs were made because the nontracking impacts were assumed to be more critical in terms of overturn. With reference to Figure 12, H was set at 32 in. Note that the β equal to zero case represents a vertical wall. A scaled drawing of the sloped wall in comparison with the CSSB is shown in Figure 51. A comparison of the results of Table 10 with comparable results of Table 9 shows that a distinct reduction of the overturn problem is achieved with the new designs. Yaw, pitch, and roll angles with time of a selected run of the β = 8.9-deg case are shown in Figure 52. Figure 53 shows the same data for the β = 0-deg case. Data in Figures 52 and 53 can be compared with data for the CSSB in Figure 50.

Tables 11 and 12 give results of HVOSM runs of high speed/angle impacts and nontracking impacts with the modified CSSB design (see Figure 12). A Chevrolet Sprint was simulated in these runs. Comparison of Table 11 with part (c) of Table 8 shows that the modified CSSB design does reduce the overturn problem for most of the impact conditions expected to occur in the field. Even though overturn is still indicated for 45-mph/60-deg impact condition for the modified CSSB, the probability of serious injuries or fatalities for these conditions would be high regardless of the vehicle's post-impact stability. A comparison of Table 12 with part (c) of Table 9 also shows that

Table 9. Stability study for nontracking impacts with CSSB. See Figure 48 for definition of angles θ and ψ. Also note: $\dot{\psi}$ = + 15 deg/sec in each run.

(a) Fiat Uno-45

Speed (mph) / Angle θ (Deg) / Angle ψ (Deg)	30		45		60	
	15	25	15	25	15	25
45	Overturn	Overturn	Overturn	Overturn	Overturn	Overturn
60	Overturn	Overturn	Overturn	Overturn	Overturn	Overturn
75	Overturn	Marginal	Overturn	Overturn	Overturn	Overturn

(b) Daihatsu-Domino

Speed (mph) / Angle θ (Deg) / Angle ψ (Deg)	30		45		60	
	15	25	15	25	15	25
45	Overturn	Overturn	Overturn	Overturn	Overturn	Overturn
60	Overturn	Overturn	Overturn	Overturn	Overturn	Overturn
75	Overturn	Overturn	Overturn	Overturn	Overturn	Overturn

(c) Chevrolet Sprint

Speed (mph) / Angle θ (Deg) / Angle ψ (Deg)	30		45		60	
	15	25	15	25	15	25
45	Overturn	Overturn	Overturn	Overturn	Overturn	Overturn
60	Spinout	Overturn	Overturn	Overturn	Overturn	Overturn
75	Spinout	Spinout	Spinout	Spinout	Spinout	Marginal

(d) Honda Civic

Speed (mph) / Angle θ (Deg) / Angle ψ (Deg)	30		45		60	
	15	25	15	25	15	25
45	Overturn	Overturn	Overturn	Overturn	Overturn	Overturn
60	Overturn	Overturn	Overturn	Overturn	Overturn	Overturn
75	Overturn	Marginal	Overturn	Overturn	Overturn	Overturn

(e) Plymouth Fury

Speed (mph) / Angle θ (Deg) / Angle ψ (Deg)	30		45		60	
	15	25	15	25	15	25
45	Stable	Stable	Stable	Stable	Stable	Stable
60	Sideslip	Sideslip	Sideslip	Sideslip	Sideslip	Overturn
75	Spinout	Spinout	Spinout	Spinout	Spinout	Spinout

Table 10. Stability study for nontracking impacts with constant slope barrier. See Figure 48 for definition of angles θ and ψ. Also note: $\dot{\psi}$ = + 15 deg/sec in each run.

(a) Constant Sloped Barrier, β = 8.9 degrees

Speed (mph) / Angle θ (Deg) / Angle ψ (Deg)	30		45		60	
	15	25	15	25	15	25
45	Stable	Stable	Stable	Stable	Stable	Stable
60	Spinout	Spinout	Spinout	Spinout	Spinout	Overturn
75	Spinout	Spinout	Spinout	Spinout	Spinout	Spinout

(b) Vertical Wall, β = 0.0 degree

Speed (mph) / Angle θ (Deg) / Angle ψ (Deg)	30		45		60	
	15	25	15	25	15	25
45	Stable	Stable	Stable	Stable	Stable	Stable
60	Stable	Stable	Stable	Stable	Spinout	Spinout
75	Spinout	Spinout	Spinout	Spinout	Spinout	Spinout

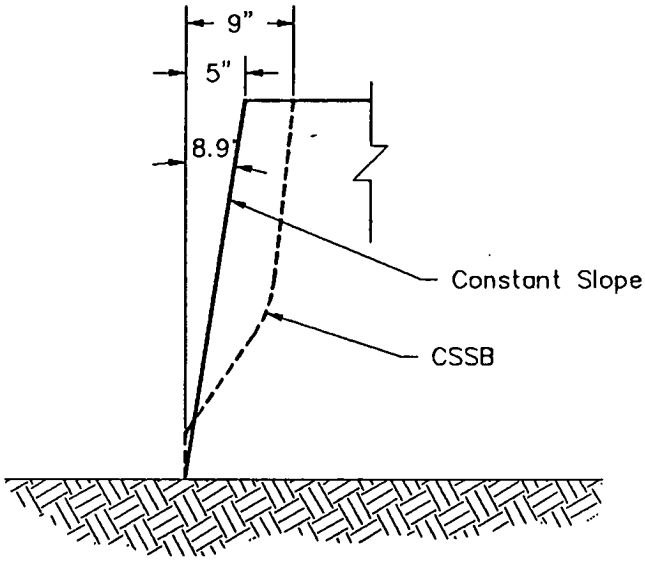

Figure 51. Constant sloped barrier and CSSB profiles.

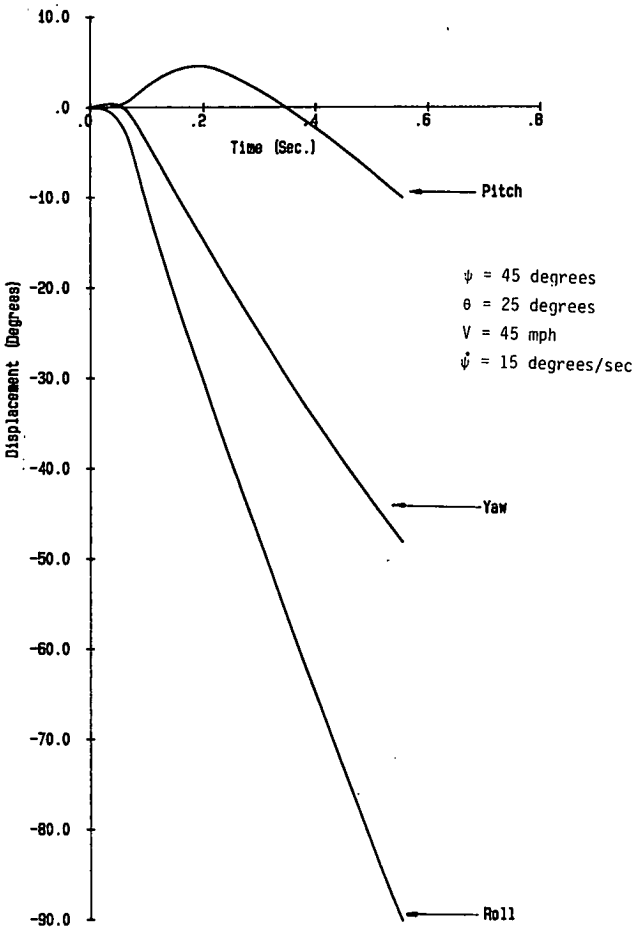

Figure 50. Roll, pitch, and yaw angles for nontracking impact with CSSB by Chevrolet Sprint.

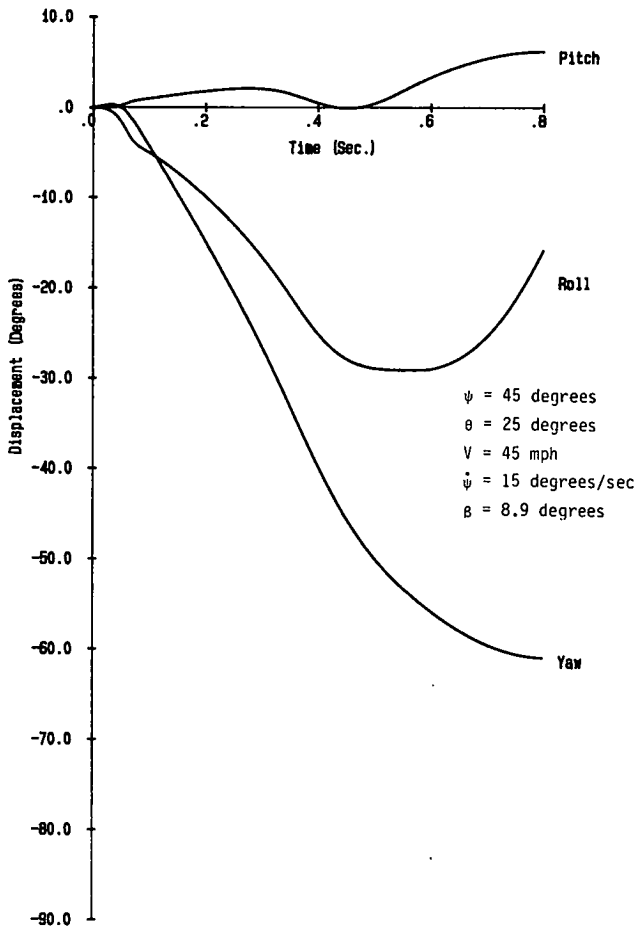

Figure 52. Roll, pitch, and yaw angles for nontracking impact with constant slope barrier by Chevrolet Sprint.

Table 11. Stability study for high speed/angle tracking impacts of Chevrolet Sprint with Modified CSSB. See Figure 48 for definition of angle θ.

Angle θ (Deg) \ Speed (mph)	30	45	60
35	Stable	Stable	Stable
45	Stable	Stable	Stable
60	Spinout	Overturn	Overturn

Table 12. Stability study for nontracking impacts of Chevrolet Sprint with modified CSSB. See Figure 48 for definition of angles θ and ψ. Also note: $\dot{\psi}$ = + 15 deg/sec in each run.

Angle ψ (Deg) \ Angle θ (Deg) \ Speed (mph)	30		45		60	
	15	25	15	25	15	25
45	Stable	Stable	Stable	Stable	Stable	Stable
60	Spinout	Spinout	Spinout	Spinout	Overturn	Overturn
75	Spinout	Spinout	Spinout	Spinout	Spinout	Spinout

the modified CSSB significantly reduced the overturn problem for nontracking impacts.

Figures 54 and 55 show the angular response of the Chevrolet Sprint on impacting the modified CSSB in a high angle tracking condition and a nontracking condition, respectively. Impact conditions are as indicated on the figures. A comparison of Figure 54 with Figure 48 and a comparison of Figure 55 with Figure 50 shows the degree to which the modified CSSB reduces the roll response.

Flexible Longitudinal Barriers

Reference should be made to Appendix E, under "Flexible Longitudinal Barriers," for a discussion of the calibration of the GUARD program for simulation of G4(1S) barrier impacts. On completion of the calibration, the program was used to examine the impact performance of a range of minicars for tracking impacts of 15 deg and 20 deg at an impact speed of 60 mph. The purpose of these simulations was to determine occupant risk values and to estimate the degree of wheel snag that may occur.

Table 13 summarizes results of the GUARD study of minicar impacts with the G4(1S) barrier. The Ford Fiesta performance was very similar to the Chevrolet Sprint and it was therefore not included in the analysis.

As shown, the GUARD program predicts that the G4(1S) barrier will perform satisfactorily for minicar impact speeds up to 60 mph and angles up to 15 degrees. As the impact angle

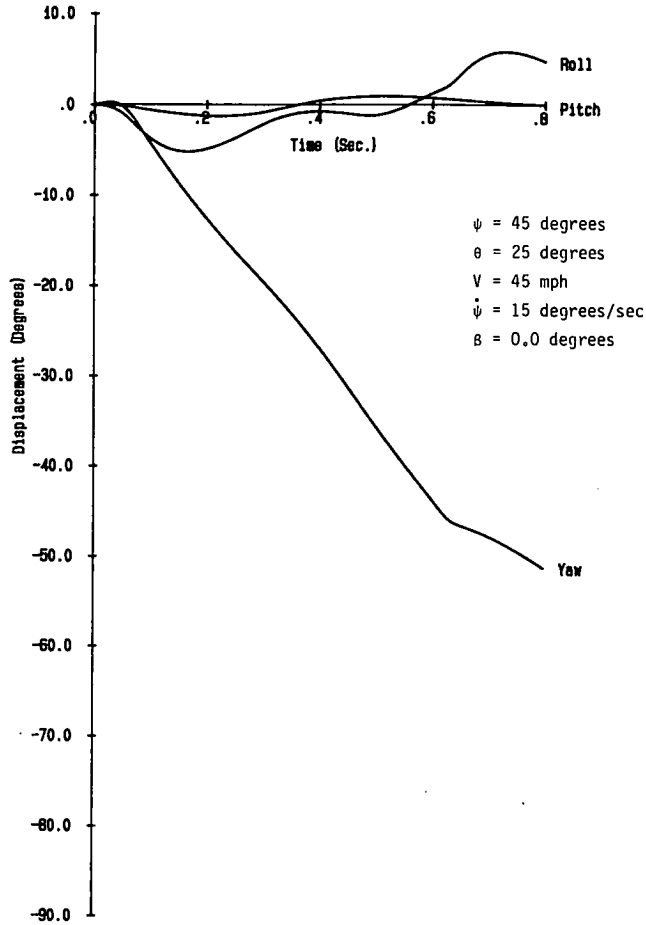

Figure 53. Roll, pitch, and yaw angles for nontracking impact with vertical barrier by Chevrolet Sprint.

increases to 20 degrees, some wheel snagging can be expected. It should be noted that wheel snagging is not necessarily a catastrophic or unacceptable event. Many small car tests involving relatively severe wheel snags indicate that occupant severity levels are generally within acceptable limits. Further, wheel snag does not usually destabilize impacting vehicles and, as a result, seldom leads to rollover. In fact, in many cases the damaged front wheel causes the vehicle to be steered back toward the barrier after impact, preventing a return of the vehicle to the travelway.

The predicted occupant impact velocities in the longitudinal direction are all below the preferred 30-ft/sec value. With one exception, the predicted occupant impact velocities in the lateral direction are all between the preferred 20-ft/sec value and the 30-ft/sec limit. Similar results were found in tests of an 1,800-lb car impacting the G4(2W) guardrail system (*28*).

On the basis of the tests and simulations reported herein, it was concluded that the G4(1S) barrier will satisfy the evaluation criteria of *NCHRP Report 230* for minicars. However, if wheel snag proves to be a problem, it can be eliminated by increasing the depth of the blockout from 60 to 10 in. For a G4(1S) system, replacing the W 6×9 blockout with a W 10×12 blockout would increase material requirements by approximately 0.5 lb

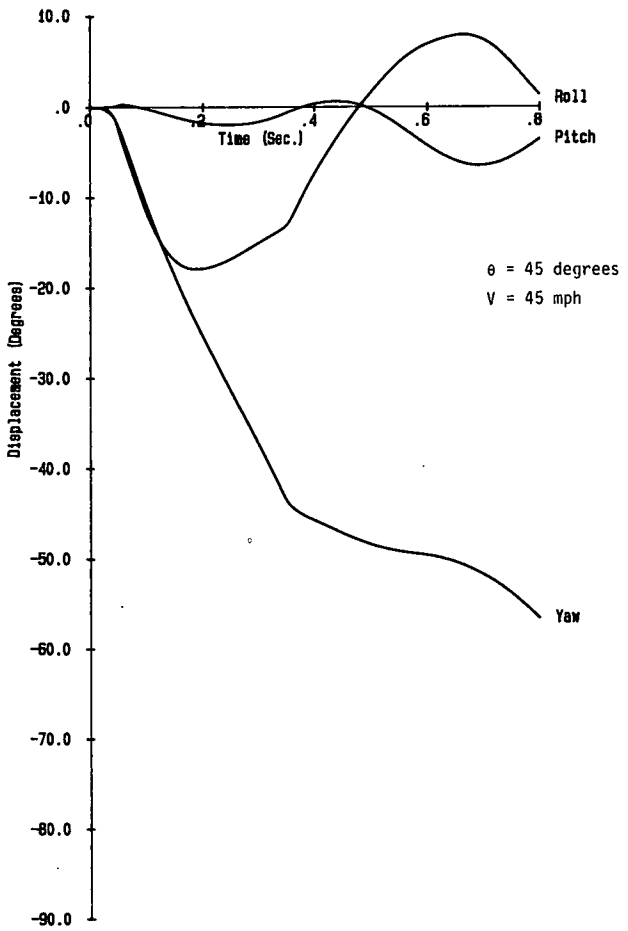

Figure 54. Roll, pitch, and yaw angles for high angle tracking impact with modified CSSB by Chevrolet Sprint.

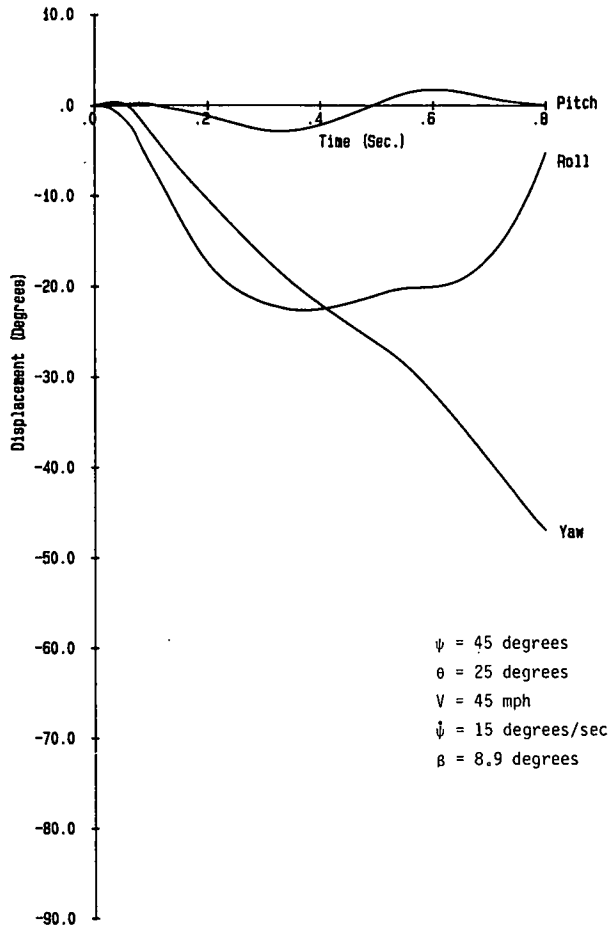

Figure 55. Roll, pitch, and yaw angles for nontracking impact with modified CSSB by Chevrolet Sprint.

Table 13. Simulation study of minicar impacts with G4(1S) barrier. Note: Occupant impact velocity values computed per Method I discussion in Chapter Three, under "Computer Simulation Studies," "Rigid Longitudinal Barriers."

Parameter	Daihatsu		Fiat[b]		Sprint	
Impact Angle (deg)	15.0	20.0	15.6	20.6	15.0	20.0
Impact Speed (mph)	60.0	60.0	61.2	61.8	60.0	60.0
Exit Angle (deg)	6.8	8.0	6.8	4.9	5.5	7.1
Exit Speed (mph)	51.9	48.8	50.9	47.7	52.0	48.1
Occupant Impact Vel.[c] (ft/sec)						
Longitudinal	20.1	16.1	12.1	19.2	22.3	16.8
Lateral	22.2	25.1	23.9	24.5	19.9	23.3
Max. 50 ms. Acceleration (g's)						
Longitudinal	3.2	5.3	3.7	5.0	2.7	4.8
Lateral	9.2	11.5	9.5	10.1	8.2	11.6
Wheel Snag (Y/N)	[a]	Y	N	Y	N	Y
Max. Roll Angle (deg)	1.0	0.2	0.6	1.1	1.7	1.9
Max. Pitch Angle (deg)	0.1	0.2	1.2	2.5	0.1	1.0

[a] Marginal wheel snagging.
[b] These are simulations of the two tests of the G4(1S) system with the Fiat. See Section E-2, Appendix E, for a discussion of the GUARD calibration for these tests.
[c] Values computed per Method I.

of steel per foot of guardrail. Construction costs would likewise increase by about 25 cents per foot or approximately 2 percent over that of the present G4(1S) system assuming a present cost of $12.50 per foot.

Nontracking impacts with the G4(1S) system were not simulated. As discussed earlier, under "Rigid Longitudinal Barriers," overturn of the nontracking minicar was virtually eliminated in the CSSB by the use of a vertically faced barrier. The G4(1S) is essentially a vertically faced barrier and very little vehicular roll or pitch motions occur during minicar impacts.

A special high angle impact condition was simulated and results are summarized in Table 14 for three minicars. As expected, high occupant impact velocities are predicted. However, it is predicted that the barrier will contain and redirect the cars without overturn or spinout.

Breakaway Supports

A computer program was written and calibrated for simulating the impact performance of vehicular impacts with breakaway sign and luminaire supports. The program and its application is presented in Chapter Three, "Specialized Analytical Procedures." The program was used to study the im-

portance of key vehicle/breakaway support parameters and to better define limits of performance.

Base-Bending Sign Supports

Computer analysis of base-bending sign supports involved the use of HVOSM to study vehicular response due to an experimentally determined impulse. The impulse, or force-time data, was estimated from acceleration-time data measured during the test of a 4-lb/ft steel U-post (see Appendix C, test 8). Calibration of HVOSM for this purpose is described in Appendix E. Note that the vehicle used in the test and subsequent calibration of HVOSM was a Fiat Uno. The force-time data and the location of the impulse selected during the calibration are also given in Appendix E. This analysis obviously assumed that the impulse is independent of the mass and stiffness characteristics of the vehicle. For the vehicles simulated, this assumption is believed to be reasonably valid since the range of mass and stiffness properties of these vehicles is not believed to be significantly large.

Shown in Figures 56, 57, and 58 are the angular displacements with time of the Daihatsu Domino, Chevrolet Sprint, and Ford Fiesta for the aforementioned impulses. Note that these impulses

Table 14. Guard simulation of high angle impacts with G4(1S) barrier. Note: Occupant impact velocity values computed per Method I discussion in Chapter Three, under "Computer Simulation Studies," "Rigid Longitudinal Barriers."

Parameter	Daihatsu	Fiat	Sprint
Impact Angle (deg)	45.0	45.0	45.0
Impact Speed (mph)	45.0	45.0	45.0
Exit Angle (deg)	15.4	9.8	13.9
Exit Speed (mph)	20.7	23.0	20.2
Occupant Impact Vel.[a] (ft/sec)			
Longitudinal	39.0	42.4	41.2
Lateral	26.1	29.1	26.1
Max. 50 ms. Acceleration (g's)			
Longitudinal	13.0	15.3	14.3
Lateral	12.4	15.6	13.7
Wheel Snag (Y/N)	Y	Y	Y
Max. Roll Angle (deg)	4.8	7.3	3.2
Max. Pitch Angle (deg)	1.3	7.2	2.1

[a] Values computed per Method I...

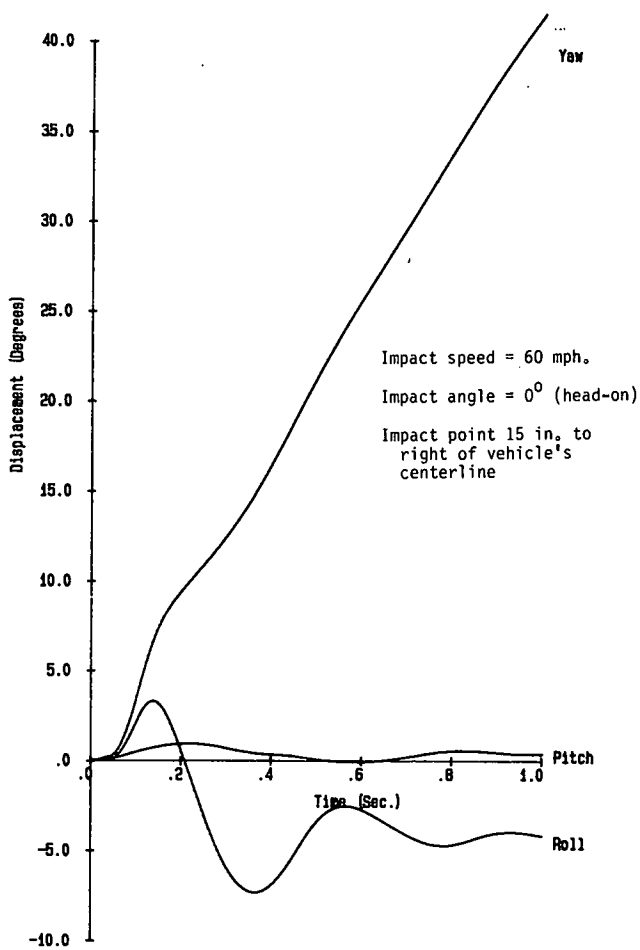

Figure 56. Roll, pitch, and yaw angles versus time, Daihatsu Domino, small sign impact.

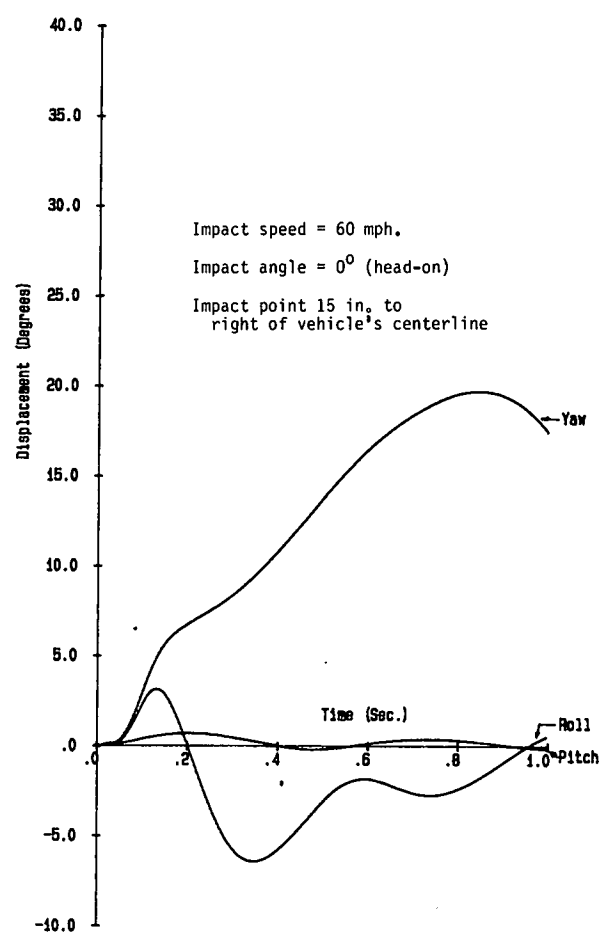

Figure 57. Roll, pitch, and yaw angles versus time, Chevrolet Sprint, small sign support.

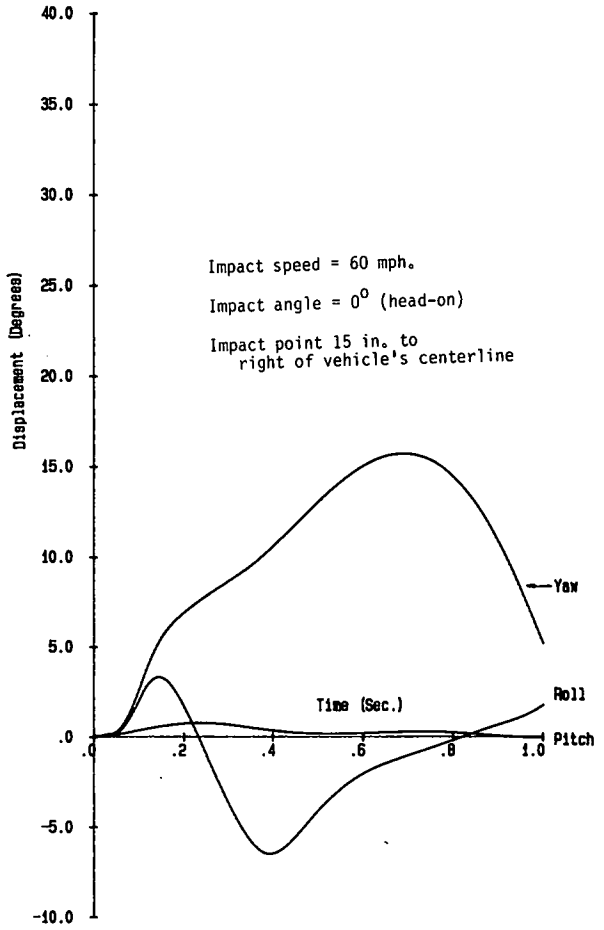

Figure 58. Roll, pitch, and yaw angles versus time, Ford Fiesta, small sign support.

Table 15. Occupant impact velocities for the small sign support impacts.

			Occupant Impact Velocity (ft/sec)					
			Longitudinal			Lateral		
Signpost	Vehicle	Impact Speed	From Test Method I	From Simulation Method I	From Simulation Method II	From Test Method I	From Simulation Method I	From Simulation Method II
Single-Support Sign Installation (4 lb/ft Steel U-Post)	Fiat Uno	59.8	12.9[a]	9.3	9.2	4.6[a]	4.4	5.8
	Dihatsu Domino	60.0	N/A	10.7	10.8	N/A	5.5	6.7
	Ford Fiesta	60.0	N/A	8.7	8.9	N/A	5.1	5.9
	Chevrolet Sprint	60.0	N/A	9.1	9.2	N/A	5.3	6.1

[a] Values from test 7043-7 results.

were applied approximately 15 in. to the right of the vehicle's centerline on the front bumper. Reference should be made to Appendix E for the response of the Fiat Uno. It can be seen that for the assumed impulses, the Daihatsu would spin out but all vehicles are predicted to remain upright subsequent to impact. The yaw angles of the Sprint and the Fiesta are seen to peak in the positive direction, then begin a return to zero. This is due to the self-correcting steer input (caused by pneumatic trail of tire) present in a free-wheeling (steer degree of freedom) front wheel. These corrections will occur so long as the sideslip angle does not exceed approximately 20 deg. In each run the recovery area was assumed to be flat and without surface irregularities or soft soil that could trip the vehicle.

Table 15 gives predicted occupant impact velocities for impact with the sign support for the four cars indicated. Reference should be made to "Computer Simulation Studies" in this chapter under "Roadside Hardware" and to Appendix G for a discussion of the two methods used to compute the occupant impact velocities. On the basis of the results given in Table 15, the 4 lb/ft U-post sign will perform satisfactorily at high impact speeds for all the cars analyzed.

A more simplified analysis was made of a variety of other small sign supports. Details of the analysis procedure are given under "Specialized Analytical Procedures," "Small Sign Supports."

Analysis was also made, using the HVOSM, of a range of generalized impulse values to better understand the manner in which small cars respond to "impulse-type" impacts including sign supports, luminaire supports, and breakaway end treatments. Figure 59 shows the parameters used in the analysis. Note that in each of the four cases, the force, F_I, was assumed to act over 0.1 sec. The impulses were applied to the Chevrolet Sprint. It was assumed to have a velocity of 60 mph at the time of the impulse, and it was assumed to be free-wheeling (no steer impact) after the impulse. Results of these runs are summarized in Table 16. For the given conditions and an impulse of 500 lb-

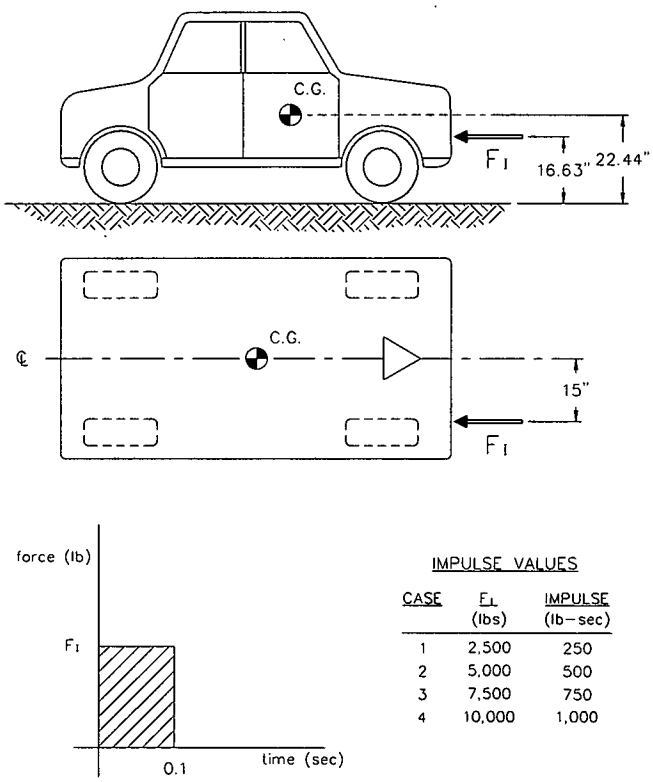

Figure 59. Generalized impulse parameters.

Table 16. Simulation results of a Chevrolet Sprint subjected to a generalized impulse.

Impulse (lb-sec)	Force (lb)	Speed (mph)	Maximum Roll (deg)	Maximum Pitch (deg)	Yaw After 2 sec (deg)	Occupant Impact Velocities (ft/sec) Longitudinal Method I	Longitudinal Method II	Lateral Method I	Lateral Method II
250	2,500	60	3.18 -4.13	-0.39 0.31	13.11	5.82	6.1	5.28	9.1
500	5,000	60	2.29 -5.86	-1.04 0.76	71.92	10.0	10.4	5.7	6.9
750	7,500	60	3.88 -7.11	-1.70 1.24	127.51	16.1	16.1	6.0	7.7
1,000	10,000	60	5.48 -7.73	-2.57 2.04	173.48	20.0	21.7	6.0	8.4

sec, spinout of the vehicle is predicted even though the occupant impact velocities are below recommended limits. Although no overturns are predicted, if the spinning vehicle encounters terrain irregularities, the probability of overturn will increase.

Crash Cushions

Analysis of widely used and commercially available energy absorbing crash cushions and end treatments was made by outside sources and supplied to the researchers. Results of these analyses are given under "Specialized Analytical Procedures," "Crash Cushions." Analysis of a sand-filled plastic drum system is also given in that section.

Guardrail Terminals

Computer analysis of a guardrail terminal involved the use of HVOSM to study vehicular response due to an experimentally determined impulse. The impulse, or force-time data, was estimated from acceleration-time data measured during the test of an eccentric loader (Appendix C, "Full-Scale Crash Tests," test 9). Calibration of HVOSM for this purpose is described in Appendix E, "Eccentric Loader BCT." The vehicle used in the test and subsequent calibration of HVOSM was a Fiat Uno. The force-time data and the location of the impulse selected during the calibration are also given in Appendix E. This analysis assumed that the impulse is independent of the mass and stiffness characteristics of the vehicle. For the vehicles simulated, this assumption is believed to be reasonably valid since the range of mass and stiffness properties of these vehicles is not believed to be significantly large.

Shown in Figures 60, 61, and 62 are the angular displacements with time of the Daihatsu Domino, Chevrolet Sprint, and Ford Fiesta for the aforementioned impulses. Note that these impulses were applied approximately 15 in. to the right of the vehicle's centerline on the front bumper. Reference should be made to Appendix E for the response of the Fiat Uno. It can be seen that for the assumed impulses, all of the vehicles would spin out, but all vehicles are predicted to remain upright subsequent to impact. In each run, the recovery area was assumed to be flat and without surface irregularities or soft soil that could trip the vehicle, conditions that are probably the exception rather than the rule in practice.

Table 17 gives predicted occupant impact velocities for impact with the eccentric loader for the four cars indicated. Reference

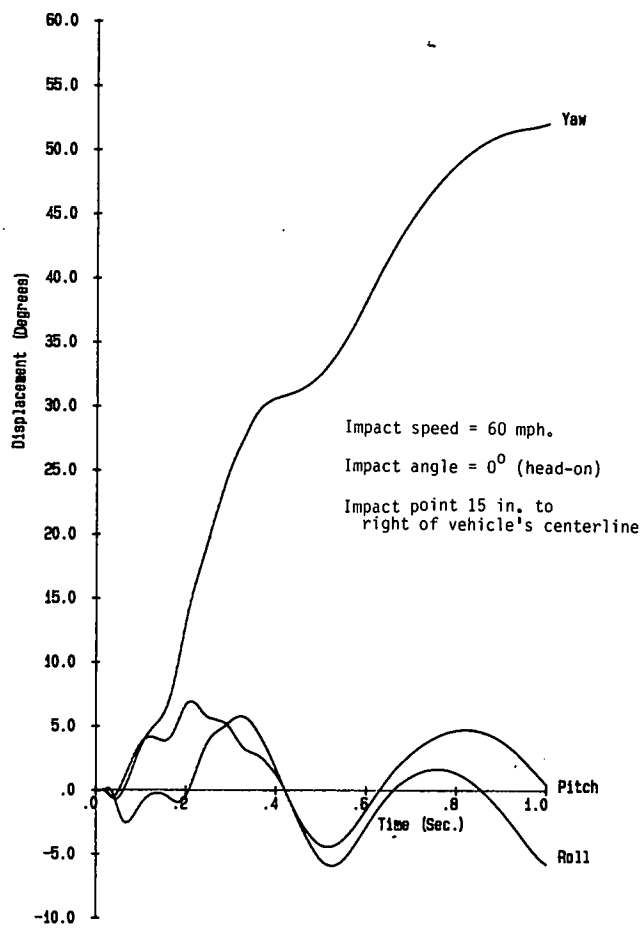

Figure 60. Roll, pitch, and yaw angles versus time, Daihatsu Domino, eccentric loader.

should be made to "Computer Simulation Studies" in this chapter under "Roadside Hardware," and to Appendix G for a discussion of the two methods used to compute the occupant impact velocities. Based on the results given in Table 17, the eccentric loader would be satisfactory for all the cars analyzed. However, the above simulation results must be viewed in light of the results of the full-scale test of the eccentric loader by a Fiat Uno, as reported in Appendix E. In that test, although the occupant impact velocity was below the recommended limit, the ridedown accelerations were excessive, the Uno sustained

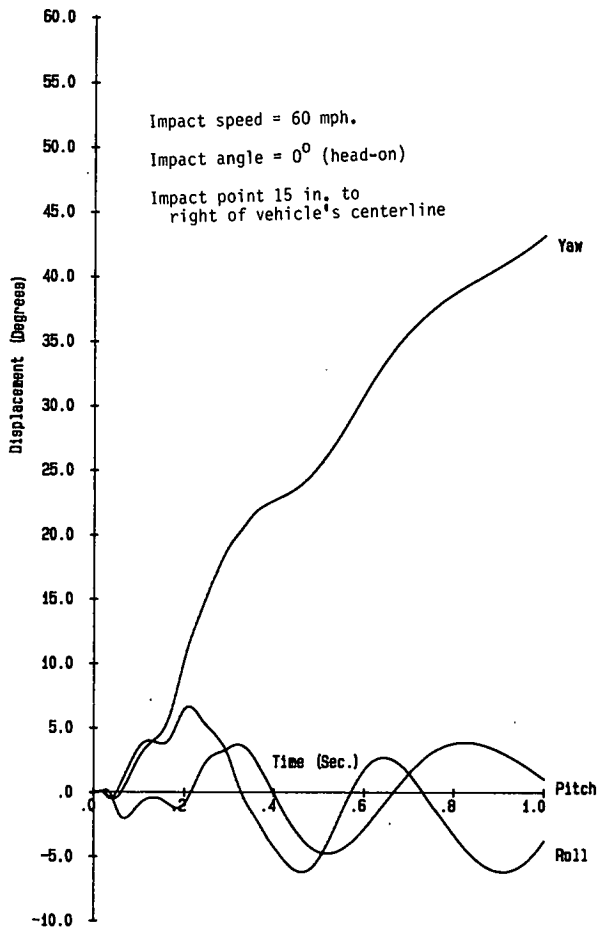

Figure 61. Roll, pitch, and yaw angles versus time, Chevrolet Sprint, eccentric loader.

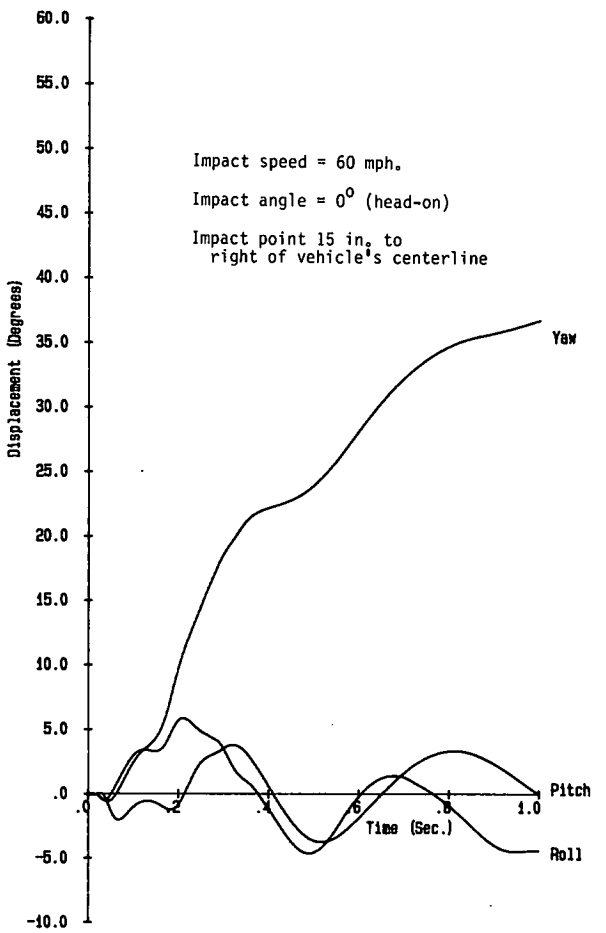

Figure 62. Roll, pitch, and yaw angles versus time, Ford Fiesta, eccentric loader.

Table 17. Occupant impact velocities for the eccentric loader simulation.

			Occupant Impact Velocity (ft/sec)					
			Longitudinal			Lateral		
		Impact	From Test	From Simulation		From Test	From Simulation	
Appurtenance	Vehicle	Speed	Method I	Method I	Method II	Method I	Method I	Method II
Eccentric Loader Terminal	Fiat Uno	60.4	27.4[a]	26.6	26.6	No Impact	7.1	9.6
	Dihatsu Domino	60.0	N/A	28.5	28.0	N/A	3.4	11.2
	Ford Fiesta	60.0	N/A	26.2	26.2	N/A	3.4	9.1
	Chevrolet Sprint	60.0	N/A	26.6	26.5	N/A	3.7	9.5

[a] Value from test 7043-8 results.

severe frontal damage, and there were deformations of, and intrusions into, the passenger compartment. As a consequence, the results were judged to be not in compliance with the *NCHRP Report 230* criteria. It is not known if the other small cars examined in the above HVOSM study would undergo similar deformations. In viewing the undercarriage (see Figure 37) and overall structural design of the under 1,800-lb cars one could conclude that similar behavior would occur due to similar structural designs. However, the dynamic crush properties of a vehicle are extremely difficult to quantify other than by experimental methods.

Roadside Features

Slopes

Shown in Figure 8, of Chapter Two, are the variables investigated for roadside fill and cut slopes. For reasons previously discussed, all slope analyses reported herein were made with the TTI version of HVOSM computer program (*44*).

In most of the computer runs the car was directed off the travelway in a tracking condition at a 15-deg encroachment angle. At a specified time the vehicle was given a steer input to simulate the response of a driver in a panic situation, trying to return to the road. This is illustrated in Figure 63. Note that the steer input began 1 sec after the vehicle left the travelway, an approximate perception-reaction time for many drivers. The initial speed of the vehicle was 60 mph in each case, and the vehicle was assumed to be in a coast mode (no traction or braking) upon leaving the travelway. The embankment was

assumed to be composed of a dry, well-stabilized soil with a tire-soil sliding friction coefficient of 0.5.

Fill slopes of 6:1, 4:1, and 3:1 in combination with fill heights of 5 ft, 10 ft, and 20 ft were investigated. Results of the HVOSM runs are summarized in Tables 18 through 21 for the respective small cars. Terms used under the "Remarks" column are defined as follows: (1) stable—vehicle continues to track throughout the traversal without sideslip or spinout; (2) sideslip—with reference to Figure 46, the vehicle sideslips when $TAN^{-1}(|u|/V) > 20$ deg; (3) spinout—with reference to Figure 46, the vehicle spins out when $u \leq 0$; (4) marginal—response is marginal when roll and/or pitch angle exceeds 40 deg, but vehicle does not overturn; angular rotations are defined in Figure 47; (5) overturn—when angular rotation in the roll and/or pitch direction is 90 deg or more, the vehicle has overturned.

It can be seen that overturn is not predicted in any of the

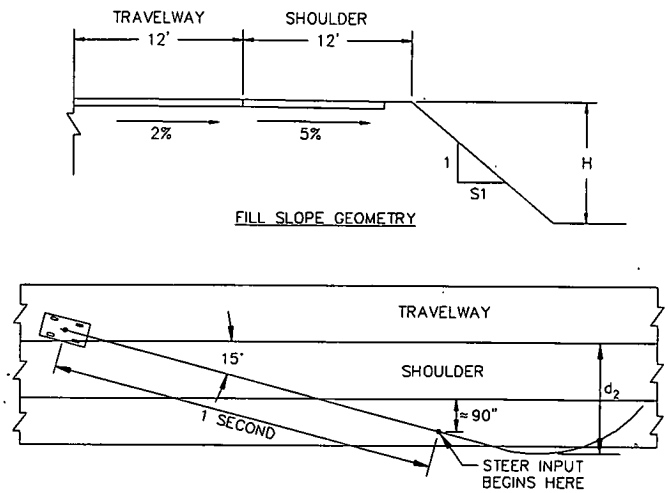

Figure 63. Encroachment parameters.

Table 18. HVOSM simulation of fill sections, Daihatsu Domino.

FILL SLOPE PARAMETERS[a]		VEHICLE RESPONSE				
FORESLOPE S1:1	DEPTH H (ft)	MAXIMUM LATERAL MOVEMENT[b] d_2 (ft)	MAXIMUM ROLL ANGLE (deg)	MAXIMUM PITCH ANGLE (deg)	MAXIMUM RESULTANT ACCELERATION (G's)	REMARKS
6:1	5	51.51	14.09	5.48	1.1	Stable
4:1	5	50.10	10.23	10.23	1.3	Stable
3:1	5	52.58	26.97	24.64	2.5	Sideslip
6:1	10	58.02	13.96	5.95	0.4	Sideslip
4:1	10	60.14	20.97	10.62	1.3	Sideslip
3:1	10	60.76	23.82	16.23	1.9	Sideslip
6:1	20	58.02	13.90	7.03	0.4	Sideslip
4:1	20	70.40	18.42	6.44	0.4	Sideslip
5:1	20	80.57	23.08	11.62	1.8	Sideslip

[a] See Figure 8
[b] See Figure 63

Table 19. HVOSM simulation of fill sections, Chevrolet Sprint.

FILL SLOPE PARAMETERS[a]		VEHICLE RESPONSE				
FORESLOPE S1:1	DEPTH H (ft)	MAXIMUM LATERAL MOVEMENT[b] d_2 (ft)	MAXIMUM ROLL ANGLE (deg)	MAXIMUM PITCH ANGLE (deg)	MAXIMUM RESULTANT ACCELERATION (G's)	REMARKS
6:1	5	51.88	13.09	5.27	0.9	Stable
4:1	5	49.84	18.31	8.28	1.2	Stable
3:1	5	51.55	25.46	22.15	5.1	Spinout
6:1	10	52.17	12.93	7.67	0.5	Sideslip
4:1	10	61.01	19.72	6.42	1.5	Stable
3:1	10	60.27	23.72	12.27	3.9	Stable
6:1	20	58.79	12.93	9.04	0.5	Sideslip
4:1	20	73.88	17.48	11.67	0.4	Sideslip
3:1	20	81.00	26.82	11.81	1.2	Sideslip

[a] See Figure 8
[b] See Figure 63

Table 20. HVOSM simulation of fill sections, Fiat Uno.

FILL SLOPE PARAMETERS[a]		VEHICLE RESPONSE				
FORESLOPE S1:1	DEPTH H (ft)	MAXIMUM LATERAL MOVEMENT[b] d_2 (ft)	MAXIMUM ROLL ANGLE (deg)	MAXIMUM PITCH ANGLE (deg)	MAXIMUM RESULTANT ACCELERATION (G's)	REMARKS
6:1	5	49.0	16.0	4.9	1.2	Stable
4:1	5	48.3	19.6	9.2	1.4	Stable
3:1	5	51.8	23.9	6.8	1.6	Spinout
6:1	10	55.6	13.4	7.1	0.4	Sideslip
4:1	10	59.9	21.4	7.7	1.3	Stable
3:1	10	62.7	24.2	6.8	1.8	Sideslip
6:1	20	55.6	13.4	7.1	0.4	Sideslip
4:1	20	71.5	18.5	10.7	0.9	Sideslip
3:1	20	80.2	23.9	6.9	1.7	Sideslip

[a] See Figure 8
[b] See Figure 63

Table 21. HVOSM simulation of fill sections, Ford Fiesta.

FILL SLOPE PARAMETERS[a]		VEHICLE RESPONSE				
FORESLOPE S1:1	DEPTH H (ft)	MAXIMUM LATERAL MOVEMENT[b] d_2 (ft)	MAXIMUM ROLL ANGLE (deg)	MAXIMUM PITCH ANGLE (deg)	MAXIMUM RESULTANT ACCELERATION (G's)	REMARKS
6:1	5	52.16	14.04	5.52	0.6	Stable
4:1	5	52.92	17.10	10.64	1.8	Stable
3:1	5	52.92	17.70	10.64	1.8	Sideslip
6:1	10	52.20	14.04	8.56	0.5	Sideslip
4:1	10	55.31	18.91	7.41	0.8	Stable
3:1	10	62.65	25.50	15.30	2.9	Stable
6:1	20	58.89	14.02	7.20	0.4	Sideslip
4:1	20	73.63	18.39	10.42	0.6	Sideslip
3:1	20	81.95	23.25	9.02	1.7	Sideslip

[a] See Figure 8
[b] See Figure 63

Table 22. HVOSM simulation of cut sections, Daihatsu Domino. Footnotes a and b in the table refer to Figures 8 and 63, respectively.

CUT SLOPE PARAMETERS[a] BACKSLOPE S2:1	VEHICLE RESPONSE: MAXIMUM LATERAL MOVEMENT[b] d_2 (ft)	MAXIMUM ROLL ANGLE (deg)	MAXIMUM PITCH ANGLE (deg)	MAXIMUM RESULTANT ACCELERATION (G's)	REMARKS
3:1	31.33	-28.29	-15.81	3.1	Spinout
2:1	** VEHICLE OVERTURNED **				
1:1	** VEHICLE OVERTURNED **				

Table 23. HVOSM simulation of cut sections, Chevrolet Sprint. Footnotes a and b in the table refer to Figures 8 and 63, respectively.

CUT SLOPE PARAMETERS[a] BACKSLOPE S2:1	VEHICLE RESPONSE: MAXIMUM LATERAL MOVEMENT[b] d_2 (ft)	MAXIMUM ROLL ANGLE (deg)	MAXIMUM PITCH ANGLE (deg)	MAXIMUM RESULTANT ACCELERATION (G's)	REMARKS
3:1	32.94	-26.07	-16.76	8.1	Spinout
2:1	52.13	-37.04	22.48	5.6	Sideslip
1:1	** VEHICLE OVERTURNED **				

Table 24. HVOSM simulation of cut sections, Fiat Uno. Footnotes a and b in the table refer to Figures 8 and 63, respectively.

CUT SLOPE PARAMETERS[a] BACKSLOPE S2:1	VEHICLE RESPONSE: MAXIMUM LATERAL MOVEMENT[b] d_2 (ft)	MAXIMUM ROLL ANGLE (deg)	MAXIMUM PITCH ANGLE (deg)	MAXIMUM RESULTANT ACCELERATION (G's)	REMARKS
3:1	29.2	29.0	15.9	7.7	Spinout
2:1	** VEHICLE OVERTURNED **				
1:1	** VEHICLE OVERTURNED **				

Table 25. HVOSM simulation of cut sections, Ford Fiesta. Footnotes a and b in the table refer to Figures 8 and 63, respectively.

CUT SLOPE PARAMETERS[a] BACKSLOPE S2:1	VEHICLE RESPONSE: MAXIMUM LATERAL MOVEMENT[b] d_2 (ft)	MAXIMUM ROLL ANGLE (deg)	MAXIMUM PITCH ANGLE (deg)	MAXIMUM RESULTANT ACCELERATION (G's)	REMARKS
3:1	31.59	-29.39	15.97	2.3	Spinout
2:1	27.17	-41.47	-18.53	3.2	Spinout, Marginal
1:1	19.40	-70.50	-16.05	16.0	Spinout, Marginal

cases investigated. However, in most cases the vehicle either sideslipped or spun out. If the slopes are not smooth and well compacted as assumed, the probability of overturn increases for these nontracking conditions. Note that in a "spinout" condition the vehicle is out of control, increasing the probability of the vehicle striking a fixed object within or outside the right-of-way.

Results of the above-described slope studies were not significantly different from similar studies of larger vehicles on slopes (*21, 43, 44*). The ability of HVOSM to simulate encroachments on embankments and ditches to a reasonable degree of accuracy has been demonstrated in earlier studies (*21, 22*) and in the present study as discussed in Appendix E, "Roadside Features."

Results of the recent studies (*11, 23*) of small car encroachments on slopes tend to agree with the foregoing findings. Further, the referenced studies point out the sensitivity of vehicle stability to the conditions of the embankment. As the soil becomes weaker and less stabilized, tires begin to rut and the probability of overturn increases, especially if the vehicle is skidding sideways. These studies have also determined that small cars tend to overturn more readily under these soft-soil conditions than do the larger cars. This is corroborated to some extent by a rather limited accident data base (*11*).

Cut slopes of 3:1, 2:1, and 1:1 were investigated and the results are summarized in Tables 22 through 25. This analysis indicates that certain minicars will overturn on 2:1 or steeper cut slopes. For these steeper slopes the bumper of the car penetrates the backslope creating a tripping action that overturns the vehicle.

A limited number of computer runs was also made to evaluate vehicle response for a "nontracking" encroachment. In these runs the vehicle was given a 15-deg/sec yaw rate as it was directed off the travelway at a 15-deg encroachment angle at 60 mph. The Fiat Uno was simulated in each run. Analysis was made of a 3:1 fill slope with heights of 10 ft and 20 ft. Runs were made with the vehicle yawing both positively and negatively, and in no case did rollover occur. A nontracking encroachment was also made for a 3:1 cut slope, and rollover did not occur.

It is not clear what, if anything, should be done to current design standards for fill and cut slopes if the minicar becomes a design vehicle. According to AASHTO (*24*), "Foreslopes steeper than 4:1 are not desirable because their use severely limits the choice of backslopes. Slopes 3:1 or steeper are recommended only where site conditions do not permit flatter slopes. When slopes steeper than 3:1 must be used, consideration should be given to the use of a roadside barrier."

From all indications a minicar's behavior on a smooth, well-compacted slope is not significantly different from a larger car. On the other hand it can be shown that the stability of a minicar is much more sensitive to terrain surface conditions, such as soft soil or a mound of dirt. For these reasons, if the current design standards and construction and maintenance practices for slopes are not changed, more overturns can be expected as the minicar population increases. Further study of the problem would be warranted if the minicar becomes a design vehicle.

Ditches

Shown in Figure 9 are the variables investigated for roadside ditches. All ditch analyses reported herein were made by use of the HVOSM computer program. The simulated vehicles were directed off the road and steered in the same way as that previously described in the section on "Fill and Cut Slopes." Both tracking and nontracking departures from the travelway were studied. The matrix of parameters examined included foreslopes of 6:1, 4:1, and 3:1; backslopes of 6:1, 4:1, and 3:1; and ditch depths of 5 ft and 10 ft. The ditches were assumed to be com-

posed of dry, well-stabilized soil. A tire-soil friction coefficient of 0.5 was assumed.

Results of the ditch runs are summarized in Tables 26 through 29. It can be seen that the behavior of the respective minicars on ditch sections is quite similar to their behavior on fill slopes. Again, no overturns are predicted, but in most cases the car either sideslips or spins out. As previously discussed, a vehicle (a small vehicle in particular) is more prone to overturn under these conditions if the soil is soft or if there are irregularities in the ditch surfaces.

The foregoing results are not significantly different from similar studies with larger cars (*21, 43*), and a more recent study with small cars (*23*). These studies have also shown that the overturn problem can be controlled to a large extent by rounding of slope junctures and by avoiding sharp "V-bottom" ditches.

Based on results of the present study and the above-referenced studies, there is no compelling reason for major changes in current AASHTO ditch standards (*24*) to accommodate minicars. Cautions previously cited with regard to fill and cut sections would also apply to ditch sections.

One nontracking encroachment was simulated for a ditch having a 3:1 foreslope, 6:1 backslope, and a 10 ft depth. The vehicle remained upright in this run. Reference should be made to the previous section on "Fill and Cut Slopes" for a description of the nontracking simulation procedures.

Driveways

Driveways and similar geometric features, such as median crossovers, are very common along nonfreeway roads. Previous studies have clearly shown the hazard these features pose to errant motorists (*26, 27*). Untreated culvert ends add to the hazard of many driveways that abut thruways.

Analysis of the driveway feature for minicars was made by use of the HVOSM computer program and two full-scale vehicular tests with a minicar. Reference should be made to Appendix E, under "Roadside Features," for a discussion of calibration of HVOSM for these two tests.

Driveway parameters investigated are shown in Figure 10. Two encroachment paths were used in the analysis, as illustrated in Figure 64. The encroachment speed was 60 mph in each case, and the vehicle was assumed to be in a coast mode (no traction or braking) on leaving the travelway. The vehicle was assumed to be free-wheeling, i.e., no steer input.

Results of the driveway simulations are summarized in Tables 30 through 32. The Ford Fiesta was not simulated because its response in the slope and ditch runs was similar to the Chevrolet Sprint. Very similar results are predicted for the path 1 traversals by all three cars. The Fiat Uno experiences higher resultant accelerations than the other two cars. Analysis of the simulations shows that the Fiat impacts the terrain, after crossing the drive-

Table 26. HVOSM simulation of ditch sections, Daihatsu Domino. Footnotes a and b refer to Figures 9 and 63, respectively.

DITCH PARAMETERS[a]			VEHICLE RESPONSE				
FORESLOPE S1:1	BACKSLOPE S2:1	DEPTH H (ft)	MAXIMUM LATERAL MOVEMENT[b] d_2 (ft)	MAXIMUM ROLL ANGLE (deg)	MAXIMUM PITCH ANGLE (deg)	MAXIMUM RESULTANT ACCELERATION (G's)	REMARKS
6:1	6:1	5	50.06	15.18	4.41	1.0	Stable
6:1	4:1	5	49.23	14.95	5.38	1.3	Sideslip
6:1	3:1	5	48.91	15.11	6.28	1.5	Sideslip
6:1	6:1	10	58.01	13.90	7.03	0.4	Sideslip
6:1	4:1	10	58.01	13.90	7.03	0.4	Sideslip
6:1	3:1	10	58.01	13.90	7.03	0.4	Sideslip
4:1	6:1	5	45.62	20.84	9.10	1.6	Stable
4:1	4:1	5	44.52	17.36	9.03	2.0	Stable
4:1	3:1	5	44.03	20.71	10.40	2.1	Stable
4:1	6:1	10	59.12	19.00	8.54	1.3	Sideslip
4:1	4:1	10	58.70	19.00	9.18	1.3	Sideslip
4:1	3:1	10	58.32	19.00	9.87	1.3	Sideslip
3:1	6:1	5	45.75	26.97	19.92	2.5	Sideslip
3:1	4:1	5	43.56	26.97	18.82	2.6	Sideslip
3:1	3:1	5	41.95	26.97	17.25	2.9	Stable
3:1	6:1	10	56.14	26.97	13.99	2.2	Stable
3:1	4:1	10	54.77	23.08	11.93	1.9	Sideslip
3:1	3:1	10	52.62	24.33	13.94	1.9	Sideslip

Table 27. HVOSM simulation of ditch sections, Chevrolet Sprint. Footnotes a and b refer to Figures 9 and 63, respectively.

DITCH PARAMETERS[a]			VEHICLE RESPONSE				
FORESLOPE S1:1	BACKSLOPE S2:1	DEPTH H (ft)	MAXIMUM LATERAL MOVEMENT[b] d_2 (ft)	MAXIMUM ROLL ANGLE (deg)	MAXIMUM PITCH ANGLE (deg)	MAXIMUM RESULTANT ACCELERATION (G's)	REMARKS
6:1	6:1	5	50.35	16.61	7.12	0.6	Sideslip
6:1	4:1	5	49.73	14.30	7.58	1.3	Sideslip
6:1	3:1	5	49.31	13.89	7.85	1.5	Sideslip
6:1	6:1	10	58.79	12.93	9.04	0.5	Sideslip
6:1	4:1	10	58.79	12.93	9.04	0.5	Sideslip
6:1	3:1	10	58.79	12.93	9.04	0.5	Sideslip
4:1	6:1	5	45.84	17.77	8.51	1.7	Stable
4:1	4:1	5	45.21	18.72	9.19	2.0	Stable
4:1	3:1	5	44.38	21.63	8.14	2.2	Sideslip
4:1	6:1	10	59.75	20.96	13.33	1.2	Sideslip
4:1	4:1	10	59.26	20.94	10.28	1.2	Sideslip
4:1	3:1	10	58.77	20.65	13.33	1.2	Sideslip
3:1	6:1	5	45.07	25.46	24.09	7.1	Spinout
3:1	4:1	5	43.78	25.46	24.69	7.1	Spinout
3:1	3:1	5	42.67	25.46	25.22	7.1	Spinout
3:1	6:1	10	55.82	25.46	11.85	4.0	Spinout
3:1	4:1	10	54.56	25.46	13.33	4.0	Sideslip
3:1	3:1	10	53.20	25.46	16.63	4.0	Sideslip

Table 28. HVOSM simulation of ditch sections, Fiat Uno. Footnotes a and b refer to Figures 9 and 63, respectively.

DITCH PARAMETERS[a]			VEHICLE RESPONSE				
FORESLOPE S1:1	BACKSLOPE S2:1	DEPTH H (ft)	MAXIMUM LATERAL MOVEMENT[b] d_2 (ft)	MAXIMUM ROLL ANGLE (deg)	MAXIMUM PITCH ANGLE (deg)	MAXIMUM RESULTANT ACCELER-ATION (G's)	REMARKS
6:1	6:1	5	47.6	15.2	7.3	1.2	Sideslip
6:1	4:1	5	46.9	14.6	8.1	1.1	Sideslip
6:1	3:1	5	46.4	14.4	8.1	1.3	Sideslip
6:1	6:1	10	55.6	13.4	7.1	0.4	Sideslip
6:1	4:1	10	55.6	13.4	7.1	0.4	Sideslip
6:1	3:1	10	55.6	13.4	7.1	0.4	Sideslip
4:1	6:1	5	44.6	21.1	10.1	1.8	Stable
4:1	4:1	5	43.8	20.6	10.2	1.9	Stable
4:1	3:1	5	42.9	23.9	9.4	2.3	Stable
4:1	6:1	10	57.9	20.6	8.2	1.3	Sideslip
4:1	4:1	10	57.3	21.3	10.3	1.2	Sideslip
4:1	3:1	10	56.7	21.2	10.6	1.2	Sideslip
3:1	6:1	5	43.9	23.9	26.1	2.4	Spinout
3:1	4:1	5	41.5	25.9	25.5	2.3	Spinout
3:1	3:1	5	38.9	26.6	24.7	2.3	Spinout
3:1	6:1	10	55.5	28.4	15.6	1.9	Stable
3:1	4:1	10	53.8	28.3	14.0	2.0	Stable
3:1	3:1	10	51.9	25.0	12.3	1.8	Sideslip

Table 29. HVOSM simulation of ditch sections, Ford Fiesta. Footnotes a and b refer to Figures 9 and 63, respectively.

DITCH PARAMETERS[a]			VEHICLE RESPONSE				
FORESLOPE S1:1	BACKSLOPE S2:1	DEPTH H (ft)	MAXIMUM LATERAL MOVEMENT[b] d_2 (ft)	MAXIMUM ROLL ANGLE (deg)	MAXIMUM PITCH ANGLE (deg)	MAXIMUM RESULTANT ACCELER-ATION (G's)	REMARKS
6:1	6:1	5	50.56	14.04	6.77	0.6	Sideslip
6:1	4:1	5	49.91	14.67	7.01	1.1	Sideslip
6:1	3:1	5	49.51	14.04	7.33	1.4	Sideslip
6:1	6:1	10	58.89	13.96	8.56	0.5	Sideslip
6:1	4:1	10	58.89	13.96	8.56	0.5	Sideslip
6:1	3:1	10	58.89	13.96	8.56	0.5	Sideslip
4:1	6:1	5	46.29	18.04	6.93	1.6	Stable
4:1	6:1	5	45.35	18.69	8.33	1.8	Stable
4:1	3:1	5	44.84	17.24	8.61	2.0	Stable
4:1	6:1	10	60.21	19.74	10.27	1.3	Sideslip
4:1	4:1	10	59.63	19.61	11.02	1.3	Sideslip
4:1	3:1	10	59.10	19.69	9.20	1.3	Sideslip
3:1	6:1	5	46.53	25.50	18.69	2.3	Sideslip
3:1	4:1	5	44.46	25.50	16.27	2.8	Stable
3:1	3:1	5	43.14	25.50	14.53	2.8	Stable
3:1	6:1	10	57.46	25.50	13.71	3.0	Sideslip
3:1	6:1	10	55.96	25.50	11.73	3.0	Sideslip
3:1	4:1	10	54.26	25.50	11.35	3.0	Sideslip

Table 30. HVOSM simulation of driveways, Daihatsu Domino. Footnotes a and b refer to Figures 10 and 64, respectively.

DRIVEWAY PARAMETERS[a]			VEHICLE RESPONSE PARAMETERS		
FORESLOPE S2:1	DRIVEWAY SLOPE S1D:1	ENCROACHMENT[b] PATH	MAXIMUM ROLL ANGLE (deg)	MAXIMUM PITCH ANGLE (deg)	RESULTANT ACCELER-ATION (G's)
10:1	10:1	1	7.3	17.8	5.7
10:1	8:1	1	11.4	36.8	7.2
10:1	6:1	1	** VEHICLE OVERTURNED **		
8:1	10:1	1	10.2	20.5	5.8
8:1	8:1	1	18.1	38.3	17.5
8:1	6:1	1	** VEHICLE OVERTURNED **		
6:1	10:1	1	20.8	22.7	7.1
6:1	8:1	1	32.8	38.7	9.2
6:1	6:1	1	** VEHICLE OVERTURNED **		
---	10:1	2	0	10.4	4.8
---	8:1	2	0	20.2	27.6
---	6:1	2	** VEHICLE OVERTURNED **		

Table 31. HVOSM simulation of driveways, Chevrolet Sprint. Footnotes a and b refer to Figures 10 and 64, respectively.

DRIVEWAY PARAMETERS[a]			VEHICLE RESPONSE PARAMETERS		
FORESLOPE S2:1	DRIVEWAY SLOPE S1D:1	ENCROACHMENT[b] PATH	MAXIMUM ROLL ANGLE (deg)	MAXIMUM PITCH ANGLE (deg)	RESULTANT ACCELER-ATION (G's)
10:1	10:1	1	11.0	15.1	9.9
10:1	8:1	1	14.7	23.8	11.1
10:1	6:1	1	** VEHICLE OVERTURNED **		
8:1	10:1	1	13.1	17.3	16.4
8:1	8:1	1	19.5	27.4	18.1
8:1	6:1	1	** VEHICLE OVERTURNED **		
6:1	10:1	1	16.2	25.4	8.4
6:1	8:1	1	25.7	38.4	11.4
6:1	6:1	1	** VEHICLE OVERTURNED **		
---	10:1	2	0	11.0	19.6
---	8:1	2	** VEHICLE OVERTURNED **		
---	6:1	2	** VEHICLE OVERTURNED **		

Table 32. HVOSM simulation of driveways, Fiat Uno. Footnotes a and b refer to Figures 10 and 64 respectively.

DRIVEWAY PARAMETERS[a]			VEHICLE RESPONSE PARAMETERS		
FORESLOPE S2:1	DRIVEWAY SLOPE S1D:1	ENCROACHMENT[b] PATH	MAXIMUM ROLL ANGLE (deg)	MAXIMUM PITCH ANGLE (deg)	RESULTANT ACCELERATION (G's)
10:1	10:1	1	8.9	18.6	24.9
10:1	8:1	1	10.0	29.4	27.0
10:1	6:1	1	** VEHICLE OVERTURNED **		
8:1	10:1	1	12.4	20.1	23.4
8:1	8:1	1	13.8	30.4	17.4
8:1	6:1	1	** VEHICLE OVERTURNED **		
6:1	10:1	1	13.6	17.8	14.4
6:1	8:1	1	24.7	30.6	15.8
6:1	6:1	1	** VEHICLE OVERTURNED **		
---	10:1	2	0	10.5	4.8
---	8:1	2	** VEHICLE OVERTURNED **		
---	6:1	2	** VEHICLE OVERTURNED **		

way and becoming airborne, in a nose down configuration. This causes the front bumper to contact the terrain with subsequent high impact forces. The Daihatsu and the Chevrolet return to the terrain in a nose up configuration and reduced impact forces.

Analysis of the results in Tables 30 through 32 indicates that a foreslope of 6:1 or flatter in combination with a 10:1 or flatter driveway slope is needed to avoid overturn by these vehicles for the given encroachment conditions. These findings are similar to results of driveway studies with larger cars (*26, 27, 43*).

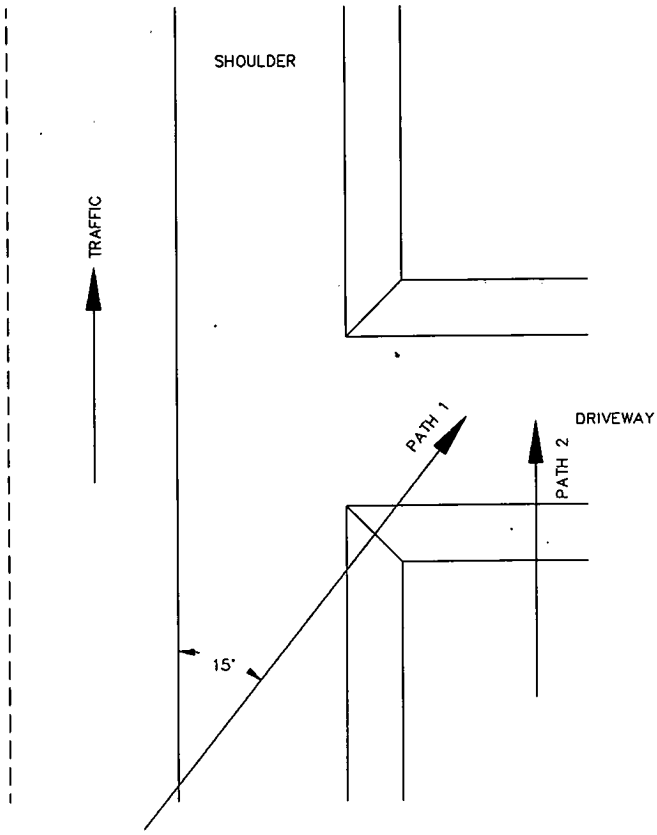

Figure 64. Driveway encroachment paths.

Curbs

Analysis of selected curbs was made by use of the HVOSM program and by a series of full-scale vehicular tests. Reference should be made to Appendix E, under "Roadside Features," for a discussion of the calibration of HVOSM for curbs when traversed by a minicar.

A series of HVOSM runs was made to examine minicar behavior when traversing two curb types. All of the runs were made with the vehicle approaching the curb in a tracking condition. Also, as discussed in Appendix E, the version of HVOSM used in the present study cannot accurately simulate shallow angle or brush hits with curbs due to limitations of the tire model. Thus, approach angles of 15 deg and greater were used in the analysis. Important measures of vehicle behavior include the roll and pitch angles, decelerations, and vehicle trajectory. The trajectory of a vehicle after crossing a curb can degrade the impact performance of safety devices located behind the curb, such as a breakaway sign or luminaire support of a roadside barrier.

A summary of the minicar response for traversals of the AASHTO type "B" curb is given in Tables 33 and 34. Dimensions of the curb and its idealized shape as used in HVOSM

Table 33. HVOSM study of minicar impacts with AASHTO type B curb.

Vehicle	Encroachment Conditions Speed (mph)	Angle (deg)	Max. Roll Angle (deg)	Max. Pitch Angle (deg)	Max. 50 ms Resultant Acc. (g's)
Daihatsu Domino	40	25	5.3	2.2	1.3
	60	15	7.9	1.7	1.4
	60	25	6.2	2.2	1.8
	60	35	5.4	5.1	1.7
Fiat Uno	40	25	4.4	1.8	1.2
	60	15	6.8	1.3	1.1
	60	25	4.7	1.4	1.5
	60	35	3.1	1.8	1.5
Chevrolet Sprint	40	25	5.3	2.2	1.5
	60	15	8.3	1.7	1.8
	60	25	6.6	2.6	1.8
	60	35	5.1	2.9	1.7

Table 34. Bumper trajectory data for impacts with AASHTO type B curbs.

Vehicle	Impact Conditions Speed (mph)	Impact Conditions Angle (deg)	ΔH max[a] (in.)	L max[a] (in.)
Daihatsu Domino	40	25	3.0	68
	60	15	2.7	46
	60	25	4.9	92
	60	35	3.7	114
Fiat Uno	40	25	3.8	98
	60	15	3.3	75
	60	25	3.9	107
	60	35	3.7	144
Chevrolet Sprint	40	25	4.1	90
	60	15	4.0	50
	60	25	5.6	103
	60	35	5.0	130

[a] See Figure 65 for definition

are given in Figure E-35, Appendix E. Reference should be made to Figure 65 for a definition of terms used in Table 34. The point that is tracked on the bumper is located at the mid-height of the front bumper (approximately 17 in. above ground) on the side of the car that crosses the curb first. Very stable behavior of each of the minicars is indicated for all conditions investigated.

An AASHTO type A curb was also investigated. Dimensions of the curb and its idealized shape as used in HVOSM are given in Figure 66. It will be noted that this curb is 6 in. from the travel surface, while the type B as used in the present study is effectively about 5 in. above the travel surface. The type A was selected because the results could be compared with results of previous studies of larger cars.

Bumper trajectory data for three minicars and for two larger cars are given in Table 35. Data for the two larger cars were taken from Ref. 10. These results suggest that a minicar does not climb as high as a larger car after crossing a curb. It is noted that the above-mentioned data from Ref. 10 was derived from a TTI study of curbs (*42*). It was one of the first studies that used HVOSM to study vehicular behavior on impact with curbs. A closer review of the results in Ref. 42 shows that, in general, the HVOSM overpredicted vehicular climb following a curb impact. This is believed to be the main reason for the differences indicated in Table 35.

It can be seen that minicars can traverse 6-in. curbs with little or no adverse response for tracking conditions. Unfortunately, many run-off-the-road accidents occur with the vehicle in a nontracking or spinning condition. The researchers were unable to address this problem with current versions of HVOSM. However, recent changes to the tire model by others (*23, 36*) offer promise in improving simulations of shallow-angle impacts and nontracking impacts with curbs. Reference should be made to the discussion (in Chapter Two, under "Modifications to Selected Roadside Safety Elements to Accommodate Minicars," "Roadside Features") on "Curbs" concerning a recent study of nontracking impacts with curbs.

SPECIALIZED ANALYTICAL PROCEDURES

Crash Cushions

Formulas used to estimate the impact performance of the sand-filled plastic barrel crash cushion are presented in this section. The basic relationships used for this purpose, taken from Appendix D of Ref. 10, are as follows:

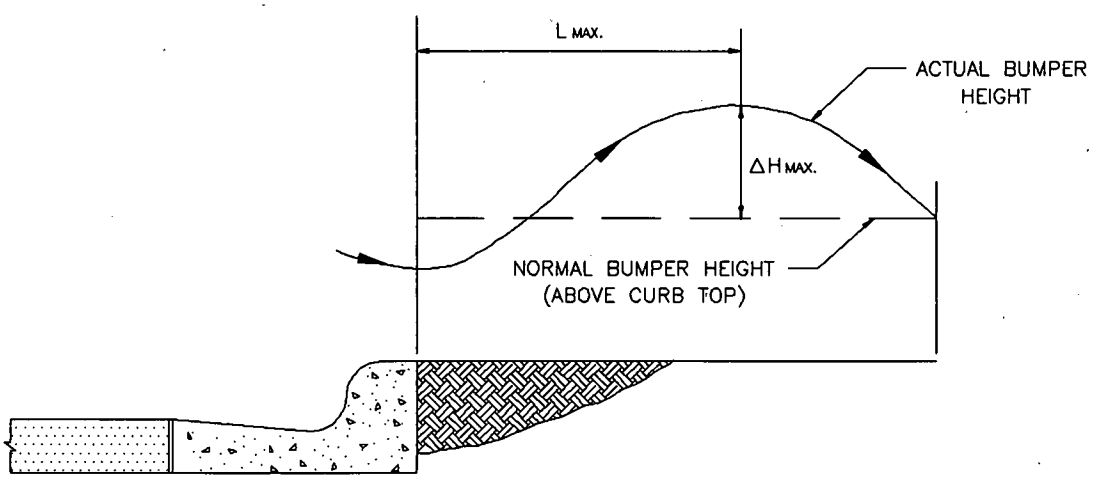

Figure 65. Bumper trajectory parameters.

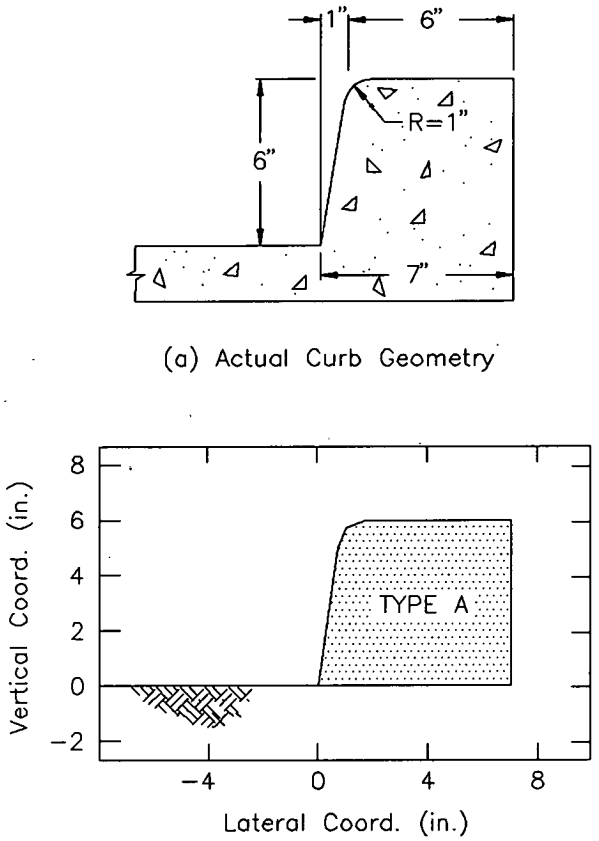

Figure 66. Curb type A geometry.

$$V_{i+1} = \frac{V_i W_v}{W_v + W_s} \quad (1)$$

$$\Delta V = V_i - V_{i+1} \quad (2)$$

$$t = \frac{2D}{V_i + V_{i+1}} \quad (3)$$

$$a_v = \frac{V_i^2 - V_{i+1}^2}{2D} \quad (4)$$

where: V_i = velocity of vehicle on impacting a module(s); V_{i+1} = velocity of vehicle after impacting a module(s); W_v = weight of vehicle; W_s = weight of sand in module(s); a_v = average deceleration of vehicle; t = time of deceleration; and D = diameter of module.

Use of the foregoing equations is illustrated in the analysis of the crash cushion shown in Figure 35, for impact by a 1,350-lb vehicle at 60 mph (88 ft/sec). The plastic barrels have a nominal diameter, D, of 3 ft.

First 200-lb module:

$$V_{i+1} = \frac{88(1{,}350)}{1{,}350 + 200} = 76.6 \text{ ft/sec}$$

Table 35. Bumper trajectory data for impacts with AASHTO type A curbs.

Vehicle	Impact Conditions Speed (mph)	Impact Conditions Angle (deg)	ΔH max[a] (in.)	L max[a] (in.)
Daihatsu Domino	40	25	4.7	74
	60	25	8.3	103
Fiat Uno	40	25	4.8	86
	60	25	7.0	101
Chevrolet Sprint	40	25	5.1	73
	60	25	8.3	97
Compact Car[b]	40	25	8.2	80
	60	25	9.5	115
Full-Size Car[b]	40	25	7.0	108
	60	25	7.5	132

[a] See Figure 65 for definition
[b] Results taken from Table F-11 of Reference 10

$$\Delta V = 88.0 - 76.6 = 11.4 \text{ ft/sec}$$

$$t = \frac{2\,(3)}{88.0 + 76.6} = 0.036 \text{ sec}$$

$$A_v = \frac{(88.0)^2 - (76.6)^2}{2\,(3)} = 312.7 \text{ ft/sec}^2$$

$$A_v = \frac{312.7}{32.2} = 9.7 \text{ g}$$

Second 200-lb module:

$$V_{i+1} = \frac{76.6\,(1{,}350)}{1{,}350 + 200} = 66.7 \text{ ft/sec}$$

$$\Delta V = 76.6 - 66.7 = 9.9 \text{ ft/sec}$$

$$t = \frac{2\,(3)}{76.6 + 66.7} = 0.042 \text{ sec}$$

$$A_v = \frac{(76.6)^2 - (66.7)^2}{2\,(3)} = 236.4 \text{ ft/sec}^2$$

$$A_v = \frac{236.4}{32.2} = 7.3 \text{ g}$$

The procedure is repeated for each succeeding module(s) until the velocity is near zero. Values thusly computed are as follows:

Module	V_{i+1} (ft/sec)	ΔV (ft/sec)	t (sec)	A_v (ft/sec^2)
200	76.6	11.4	0.036	312.7
200	66.7	9.9	0.042	236.4
200	58.2	8.6	0.048	179.3
400	44.9	13.3	0.058	228.2
700	29.5	15.3	0.081	189.9
1,400	14.5	15.0	0.136	110.4
2,800	4.7	9.8	0.312	188.0

The average deceleration during the impact is

$$A_{\text{ave}} = \frac{(88)^2 - (4.7)^2}{2[(3)(7)]} = 183.8 \text{ ft/sec}$$

$$A_{\text{ave}} = \frac{183.8}{32.3} = 5.7 \text{ g}$$

To estimate the occupant impact velocity in the longitudinal direction according to *NCHRP Report 230* procedures, one must first determine the point at which the "occupant" has moved 2 ft longitudinally with respect to the vehicle. This is accomplished as follows:

Occupant movement, d_o, after impact with first module

$$d_o = V_{\text{ave}}(t) \tag{5}$$

where V_{ave} = average velocity of the occupant relative to the vehicle during impact with module. $d_o = \frac{11.4}{2}(0.036) = 0.20$ ft.

Occupant movement after impact with second module

$$d_o = 0.20 + \frac{11.4 + 11.4 + 9.9}{2}(0.042)$$

$$d_o = 0.20 + 0.6 = 0.88 \text{ ft}$$

Occupant movement after impact with third module

$$d_o = 0.88 + \frac{21.3 + 21.3 + 8.6}{2}(0.048) = 2.11 \text{ ft}$$

It can be seen that the occupant would have moved 2 ft with respect to the vehicle slightly before the vehicle had moved through the third module. From previous calculations, the vehicle's velocity after moving through the third module was 58.2 ft/sec. Hence, the occupant impact velocity would be slightly less than 88.0 − 58.2 = 29.8 ft/sec.

Since this is less than the *NCHRP Report 230* recommended 30 ft/sec value, the cushion is satisfactory for vehicles in the 1,350-lb to 4,500-lb weight range, assuming the intrusion criteria would not be violated. It can be shown by the above procedure that the design in Figure 35 satisfies *NCHRP Report 230* for all vehicles in this weight range.

The design in Figure 35 and other inertial crash cushions do not offer complete protection to motorists if the cushion is struck on its side. If the 1,350-lb car struck the cushion on the side and engaged one of the larger modules first, the occupant impact velocity could easily exceed the 40-ft/sec limit. For example, if the 1,350-lb vehicle struck the 700-lb module first, it can be shown by the above procedure that the occupant impact velocity would exceed 46 ft/sec. Care should be exercised in the use of an inertial crash cushion in locations where side hits may be prevalent.

Breakaway Supports

Luminaire Supports

A procedure for analyzing impacts with breakaway base luminaire supports was developed to determine appropriate design parameters for these systems for impacts with small automobiles. The procedure is broken into three phases of impact. During the first phase, the impacting vehicle crushes into the luminaire support until the force on the pole reaches a level sufficient to activate the breakaway mechanism. Energy is dissipated only through crushing of the vehicle. It was assumed that the crush force was proportional to the crush distance. Using conservation of energy, the velocity at the end of this phase was calculated from the vehicle's stiffness and slip-base activation force as shown in Eq. 6.

$$V_a = \sqrt{V_i^2 \text{ ms } F_s^2/(k_v m_v)} \tag{6}$$

where V_i = initial impact velocity; V_a = velocity at activation of slip-base mechanism; F_s = slip-base or fracture mechanism activation force; k_v = ratio of crush force to crush distance; and m_v = mass of impacting vehicle.

Note from Eq. 6 that as a vehicle's stiffness is reduced, its velocity at the activation of the slip-base mechanism is reduced. This effect arises from an increase in vehicle crush and the accompanying energy dissipation associated with the reduction in vehicle stiffness. Vehicle stiffness effects on slip-base performance are discussed in greater detail later in this section.

After the lateral force on the luminaire support reaches the activation force of the slip-base or fracture mechanism, energy is assumed to be dissipated because of two events: (1) the mechanism slips and/or fractures, and (2) momentum is transferred to the support. There may be some additional vehicular crush during these two events, but it was assumed to be negligible. The question is which of the two events occurs first or do they occur simultaneously? The velocity change arising from momentum transfer is proportional to the vehicle's velocity at the start of momentum transfer. Conversely, the velocity change arising from energy dissipation by the breakaway mechanism increases as the vehicle's velocity at the start of energy dissipation decreases. Because the sequence of these two events is not well known, it was conservatively assumed that momentum is transferred prior to energy dissipation associated with the breakaway mechanism. As such, the predicted velocity change after both events will be higher than if the two events occurred simultaneously or in reverse order. Consequently, the second phase of impact was assumed to involve only momentum transfer from the vehicle to the support as the base of the support was accelerated. The laws of conservation of linear and angular momentum were used to determine the velocity change of an impacting vehicle due to momentum transfer to the support. The results of this formulation are shown in Eq. 7. This equation gives the predicted vehicular velocity at the end of phase two.

$$V_b = V_a \frac{d^2 + r^2 - er^2 m_s/m_v}{d^2 + r^2 + r^2 m_s/m_v} \tag{7}$$

where: V_a = vehicle velocity at beginning of phase two; V_b = vehicle velocity after momentum transfer to support; d = distance from vehicle bumper (or contact point) to center of gravity of luminaire support; r = radius of gyration of support; m_s = mass of support; m_v = mass of vehicle; and e = coefficient of restitution for vehicle.

The third phase of impact was then assumed to involve only energy dissipation as the slip-base or fracture mechanism released. The law of conservation of energy was used to determine the velocity of the vehicle after losing contact with the pole. To simplify the analysis, the force-deflection relationship associated with the breakaway mechanism was assumed to vary linearly as shown in Figure 67. The energy associated with failure of the breakaway mechanism can then be calculated if the travel distance during fracture can be estimated. Equation 8 gives vehicle velocity at the end of the impact event.

$$V_c = \sqrt{V_b^2 - F_s\delta_s/m_v} \qquad (8)$$

where: V_c = vehicle's velocity at end of impact, δ_s = distance traveled by base of support during slippage or fracture of breakaway mechanism.

Equations 6 to 8 were incorporated into a computer program for the purpose of developing design charts and conducting parametric studies of important variables for the improvement of slip-base luminaire supports. The objective was to develop design criteria for slip-base installations that can safely accommodate minicars. The luminaire analysis program gives the user two options for inputting the support properties. Option 1 uses input properties for the individual components of the luminaire support, namely, the pole, mast arm, luminaire, and base plate, to calculate the total mass, c.g. height, and mass moment of inertia for the entire structure. While most components of the luminaire support have standard shapes with properties that can be readily defined, the properties of the luminaire arm are more difficult to quantify. Therefore, for ease of implementation, some simplifying assumptions for the mast arm were incorporated into option 1 of the program. The arm was assumed to consist of a single tapered tubular section with twice the cross-sectional area at its connection to the pole than at its free end. The vertical projection of the arm was calculated using the pole height and mounting height of the luminaire. Based on these assumptions, the inertia and c.g. location of the arm were determined and referenced to the support system. Figure 68 shows the geometry of a typical luminaire support. The input format used for option 1 is given in Figure 69.

Option 2 of the luminaire analysis allows the direct input of properties for the entire support. The required input properties are total weight, c.g. location, and mass moment of inertia of the support system. When these properties are known, use of this option eliminates the need for the approximations that were used in option 1. The input format for option 2 is given in Figure 70. Table 36 summarizes the input variables required for each option.

In addition to the geometric and material properties of the support system, it was necessary to define vehicle properties and slip-base characteristics. These include vehicle stiffness, effective bumper height, slip-base activation force, and slip-base travel distance.

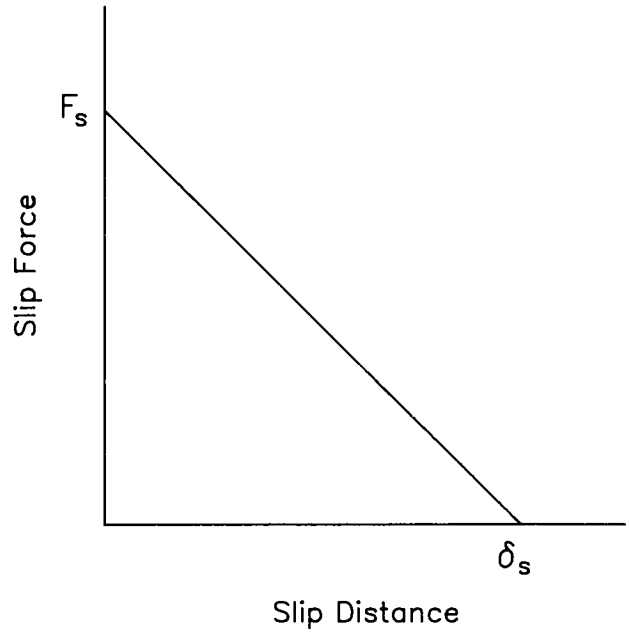

Figure 67. Force versus deflection relationship for breakaway mechanism.

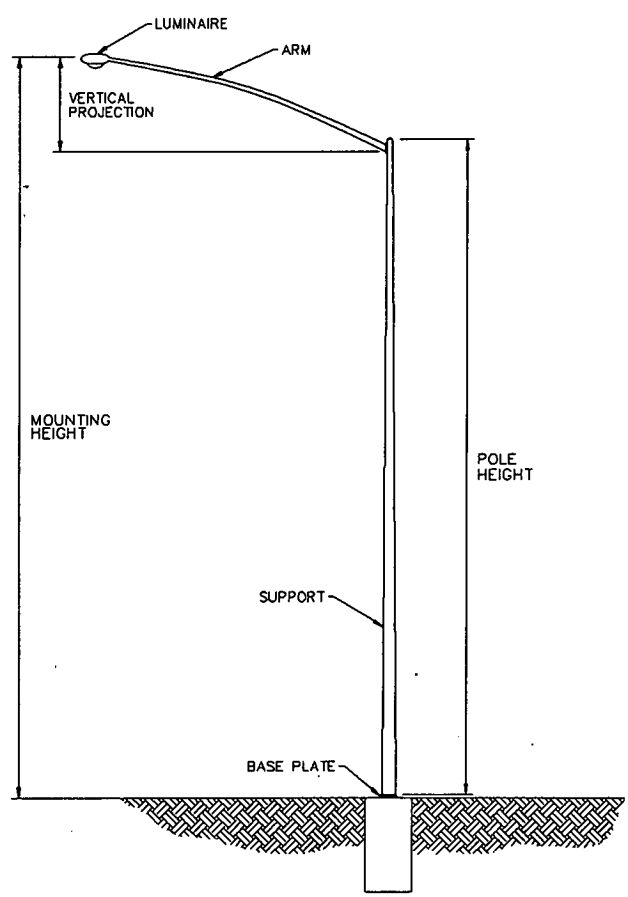

Figure 68. Typical luminaire support.

```
Do you wish to analyze a luminaire support or sign support?
(1 = Luminaire; 2 = Sign Support): 1

The Luminaire support analysis has two options:

Option 1 - Program calculates system properties (i.e. cg. location,
           inertia, radius of gyration) from user supplied dimensions
           and weights.

Option 2 - User inputs properties for entire support system (i.e.
           total weight, cg. location, total inertia).
           System includes pole, arm, luminaire, and base plate.

Please enter number of option desired (1 or 2): 1

Please input the following values :

 1. Initial Velocity (mph)                        : 60
 2. Vehicle Weight (lbs)                          : 1500
 3. Effective Vehicle Bumper Height (in)          : 14.5
 4. Vehicle Stiffness (lb/in) (-1 = default)      : -1
 5. Slip Force (lbs)                              : 12000
 6. Slip Base Slip Distance (in)                  : 1
 7. Pole Weight (lbs)                             : 285
 8. Pole Height (in)                              : 420
 9. Radius at Top of Pole (in)                    : 1.938
10. Radius at Bottom of Pole (in)                 : 4.375
11. Arm Weight (lbs)                              : 120
12. Luminaire Weight (lbs)                        : 50
13. Luminaire Height (in)                         : 474
14. Base Plate Weight (lbs)                       : 34

 EDIT SCREEN - The current values are :

 1. Initial Velocity (mph)                        :      60.000
 2. Vehicle Weight (lbs)                          :    1500.000
 3. Effective Vehicle Bumper Height (in)          :      14.500
 4. Vehicle Stiffness (lb/in)                     :    1500.000
 5. Slip Force (lbs)                              :   12000.000
 6. Slip Base Slip Distance (in)                  :       1.000
 7. Pole Weight (lbs)                             :     285.000
 8. Pole Height (in)                              :     420.000
 9. Radius at Top of Pole (in)                    :       1.938
10. Radius at Bottom of Pole (in)                 :       4.375
11. Arm Weight (lbs)                              :     120.000
12. Luminaire Weight (lbs)                        :      50.000
13. Luminaire Height (in)                         :     474.000
14. Base Plate Weight (lbs)                       :      34.000

Choice to edit 1-14 (0 = quit editing) :
```

Figure 69. Input format for luminaire analysis option 1.

```
Do you wish to analyze a luminaire support or sign support?
(1 = Luminaire; 2 = Sign Support): 1

The Luminaire support analysis has two options:

Option 1 - Program calculates system properties (i.e. cg. location,
           inertia, radius of gyration) from user supplied dimensions
           and weights.

Option 2 - User inputs properties for entire support system (i.e.
           total weight, cg. location, total inertia).
           System includes pole, arm, luminaire, and base plate.

Please enter number of option desired (1 or 2): 2

Please input the following values :

 1. Initial Velocity (mph)                        : 60
 2. Vehicle Weight (lbs)                          : 1500
 3. Effective Vehicle Bumper Height (in)          : 14.5
 4. Vehicle Stiffness (lb/in) (-1 = default)      : -1
 5. Slip Force (lbs)                              : 12000
 6. Slip Base Slip Distance (in)                  : 1.0
 7. Total Weight of Luminaire Support System (lbs)  : 489
 8. Vert. Dist. from Slip Plane to CG. of System (in): 262.4
 9. Total Inertia of Luminaire System (in-lb-sec^2)  : 36424.9

 EDIT SCREEN - The current values are :

 1. Initial Velocity (mph)                        :      60.000
 2. Vehicle Weight (lbs)                          :    1500.000
 3. Effective Vehicle Bumper Height (in)          :      14.500
 4. Vehicle Stiffness (lb/in)                     :    1500.000
 5. Slip Force (lbs)                              :   12000.000
 6. Slip Base Slip Distance (in)                  :       1.000
 7. Total Weight of Luminaire Support System (lbs)  :     489.000
 8. Vert. Dist. from Slip Plane to CG. of System (in):    262.400
 9. Total Inertia of Luminaire System (in-lb-sec^2)  :   36424.900

Choice to edit 1-9 (0 = quit editing) :
```

Figure 70. Input format for luminaire analysis option 2.

Table 36. Variables for luminaire analysis.

Option 1	Option 2	Options 1 & 2
pole weight	total weight	initial velocity
pole height	c.g. height	vehicle weight
top radius	total inertia	vehicle stiffness
bottom radius		vehicle bumper height
arm weight		slip force
luminaire weight		slip distance
luminaire height		
base plate weight		

Vehicle Stiffness

As discussed earlier, the ratio of crush force to crush distance or the stiffness of impacting vehicle was assumed to be a constant. Table 37 gives a summary of vehicular crush stiffness for various small cars obtained from the results of rigid pole impact tests (6). Stiffness values shown in this table were approximated from force-deflection curves. The crush distances used in the estimation of these values were representative of impacts with breakaway structures. It is evident from Table 37 that vehicle stiffness to weight ratios, K/W, vary significantly among different vehicle makes and models. This is important, and unfortunate, because a vehicle's stiffness has a direct influence on its change in velocity when impacting a breakaway structure. Figure 71 was developed by use of the program just described to illustrate the effect of frontal crush stiffness on change in velocity for a vehicle impacting a 1,000-lb luminaire support mounted on a triangular slip base. As indicated by this figure, a vehicle's change in velocity may differ by more than 6 ft/sec over a reasonable range of frontal stiffnesses. As a vehicular stiffness decreases, the change in velocity of the vehicle increases. This reduction in velocity results from an increase in energy dissipation due to additional vehicular crush.

On the basis of Figure 71 and Table 37, it was concluded that a vehicle's crush stiffness is an important parameter in the impact performance of breakaway structures. The K/W ratio not only varies for different vehicle makes and models, but also depends on the location of impact along the front of the vehicle. For the parametric studies described in this section and in Chapter Two, a K/W ratio of 1.0 was selected for use in simulating the frontal crush stiffness of minicars. This value is likewise used as the default value in the program unless otherwise specified by the user.

Table 37. Summary of rigid pole impact tests (*6*).

Test No.	Test Vehicle	Vehicle Weight, W, (lb)	Crush Stiffness, K, (lb/in.)	K/W (1/in.)
1	1974 Chevrolet Vega	2,474	2,000	0.83
2	1981 Honda Civic	1,764	1,600	0.91
3	1981 Dodge Colt	1,934	810	0.92
4	1981 Volkswagen Rabbit	2,178	1,980	0.91
5	1981 Volkswagen Rabbit	1,832	1,200	0.66
6	1981 Volkswagen Rabbit	1,847	1,410	0.76
7	1981 Dodge Colt	1,828	512	0.28
8	1981 Honda Civic	1,754	2,300	1.32
9	1973 Chevrolet Vega	2,230	850	0.38
10	1973 Chevrolet Vega	2,323	480	0.21
11	Micro-Mini Vehicle	1,370	2,000	1.18
12	Micro-Mini Vehicle	1,273	1,330	1.04

K/W Range 0.21 - 1.32

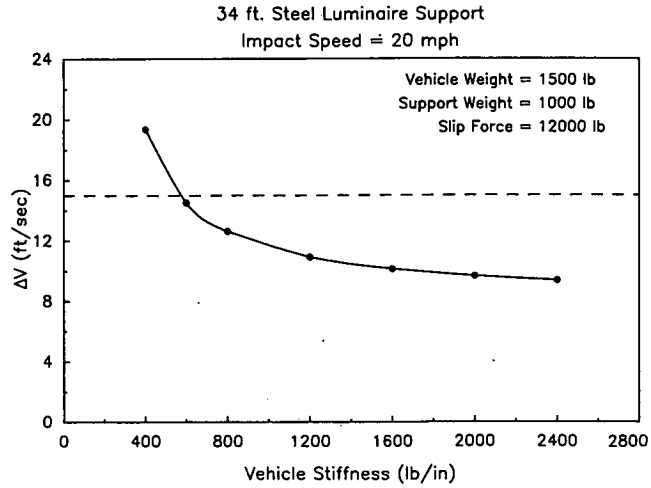

Figure 71. Effects of vehicle stiffness on change in velocity.

Coefficient of Restitution

Although it is known that restitution occurs for vehicles striking breakaway installations, little data are available for quantifying this value for such impacts. A coefficient of restitution of 0.5 was found to give good correlation for four full-scale crash tests simulated by the program. Therefore, this value was used for the parametric studies described in this report and was internally built into the program.

Effective Vehicle Bumper Height

The base plates of most slip-base installations are typically mounted 3 to 4 in. above grade. This distance must be considered when locating the vehicle's point of impact along the pole. The program indirectly accounts for the height of the slip base by means of an effective bumper height. A vehicle's effective bumper height is defined as the distance from the slip plane to the point of action of the imparted vehicle force (Figure 72). Simply stated, it is the height of the base plate subtracted from the vehicle's bumper height measured from the midpoint of the bumper. For example, a typical minicar has an average bumper height of approximately 17.5 in. When impacting a slip-base installation with a base plate mounted 3 in. above grade, such a vehicle would have an effective bumper height of 14.5 in.

Base Activation Force

The base activation force is defined as the force required to activate the slip-base mechanism or to fracture a frangible base. This activation force, or slip force, is dependent on a wide variety of factors. These factors include bolt diameter, bolt torque, surface treatment and finish, friction coefficient between the sliding surfaces (including bolts against notches), and notch geometry. Further, it is noted that triangular slip-base configurations are somewhat directional in nature (*40*). That is, the

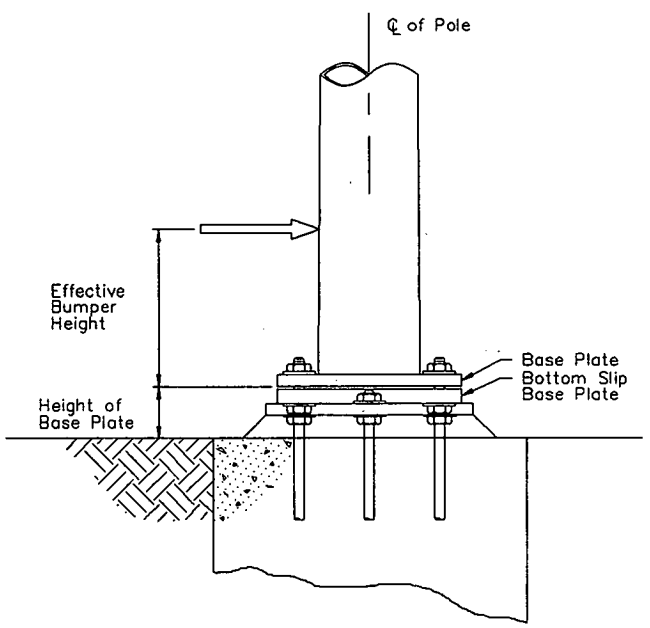

Figure 72. Effective vehicle bumper height.

angle of incidence (the orientation of the resultant impact force with respect to the breakaway base) has a direct influence on the base activation force. The slip force is also dependent on the height at which the vehicle contacts the pole above the slip plane.

In addition to the frictional forces that develop during impact, many of the foregoing factors contribute to a mechanical interlocking of slip-base components. The forces generated because of this mechanical interlocking must also be overcome before the breakaway mechanism will activate. Because of the complexities of these interactions, it is difficult to define the activation force through analytical means.

In a previous study (*40*), an empirical relationship was developed between bolt torque T (in.-lb) and bolt tension N (lb) in which the tension in a single bolt was given by

$$N = (K_t)\,(T) \tag{9}$$

where K_t depends on the bolt diameter. The total tensile force is thus the tensile force in a single bolt N multiplied by the number of bolts in the slip-base mechanism. The slip force, F_s, is then calculated by the following equation: $F_s = (\mu_e)N_T$, where μ_e = "effective" friction coefficient for slip base and N_T = total tension in bolts.

In addition to the normal friction between the sliding surfaces, the effective friction coefficient accounts for the forces generated by the various interactions described above. An analytical procedure developed in a previous study (*112*) was used to bracket this effective coefficient of friction for a typical three-bolt, multidirectional slip base under typical impact conditions. Using a typical metal-on-metal friction coefficient of 0.17-0.20, μ_e was found to vary from approximately 0.49 to 0.83.

Using the previously described model, a parametric study was conducted to determine the optimal value of μ_e for use in the validation and simulation efforts. In this parametric study all important vehicle and pole properties were known, and thus the effects of μ_e could be accurately assessed. It was found that an effective friction coefficient of 0.5 gave the best correlation with measured values. This value was therefore used for the validation rims and parametric studies described in this report.

Slip Distance

As previously described, the change in vehicular velocity for the third phase of impact is dependent on the travel distance of the slip base or fracture mechanism. Based on static tests of slip-base mechanisms, slip distances in the range of 1 in. to 3 in. are common. Furthermore, the associated force-deflection curves were approximately linear in form (*60*), supporting the assumption made in development of Eq. 8.

Figure 73, developed by use of the aforementioned program, indicates that the breakaway model is not extremely sensitive to small changes in slip distance. Over a reasonable range of slip-base force, the total change in vehicular velocity for a 1-in. and 3-in. slip distance differed by approximately 2 ft/sec. A slip distance of 1 in. was used in this study for both the validation and design simulations.

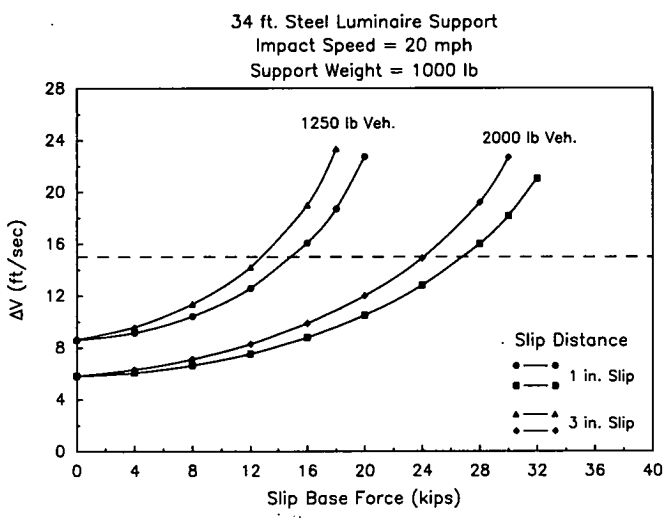

Figure 73. Effects of slip distance on change in velocity.

The reader should note that implied in Eq. 8 is a specified amount of energy dissipation due to the activation of the breakaway mechanism. The energy loss is given by Eq. 10:

$$E = \tfrac{1}{2}\,F_s S_s \tag{10}$$

If E is known for a given breakaway feature, such as a slip base or a frangible transformer base, one can input an activation force given by Eq. 11.

$$F_s = \frac{2E}{S_s} \tag{11}$$

In the present computer program F_s should equal $2E$ because $S_s = 1$.

Validation

The foregoing analysis and computer program were validated by comparing predicted velocity changes with results of a number of pendulum tests and full-scale bogie tests from Refs. 61, 62, and 63. The initial phase of the validation effort involved the pendulum tests. Table 38 gives predicted and measured velocity changes for each of the three phases of impact. The analysis procedure proved to give reasonably accurate velocity change predictions for each of the five pendulum tests evaluated. The only exception was for phase one of tests 201–204. The pendulum used in these tests incorporated a highly nonlinear crushable nose and, therefore, the assumption used in the de-

Table 39 gives predicted and measured velocity changes for six full-scale bogie tests (*62, 63*). These tests were selected because of the accurate control that existed over vehicle and slip-base parameters. The bogie test vehicle had a crushable nose of known stiffness, and use of load sensing bolts in the slip base permitted the accurate determination of preload across the slip plane.

The installation for tests B101–B103 consisted of a 34-ft steel pole mounted on a multidirectional slip base. Mast arms and/or surrogate luminaires were not included in the test installation. The total weight of the pole and slip base was 1,003 lb. The slip base used three 1-in. diameter bolts which were tightened to produce a clamping force of approximately 14,000 lb per bolt. Thus, the slip force was estimated to be: (3)(14,000)(0.5) = 21,000 lb.

The installation for tests 504, 509, and 515 consisted of a 28-ft steel pole mounted on a triangular slip base. Again, mast arms or luminaires were not included in the test installation. The combined weight of the system was 292 lb and the slip force was estimated to be 21,000 lb. These installations were assumed to bracket the size and weight of many common luminaire supports. The weight of the test bogie was 1,905 lb, and its measured frontal crush stiffness was approximately 1,450 lb/in.

As shown in Table 39, the model simulated the bogie crash tests with reasonably good accuracy. The predicted velocity changes were within ± 2 ft/sec of the average measured values.

Table 38. Measured and predicted velocity changes during slip-base pole impacts (fps).

Test #	PHASE I Measured	PHASE I Predicted	PHASE 2 Measured	PHASE 2 Predicted	PHASE 3 Measured	PHASE 3 Predicted	TOTAL ΔV Measured	TOTAL ΔV Predicted
201-204*	2.54**	1.24	1.70	1.30	0.60	0.70	4.84	3.54
4	N/A	0	2.54	2.78	--	0.47	2.99	3.25
10	--	5.38	2.49	2.78	--	1.61	9.39	9.30
9	--	2.02	2.49	2.61	--	0.88	5.55	5.51

* - Average of 4 tests

** - Nonlinear crushable nose used in this test

Sign Supports

A procedure similar to that developed for the luminaire supports was developed for analyzing impacts with breakaway sign supports. Effort was directed toward determining appropriate design parameters for impacts with minicars. The breakaway sign installation is characterized by the presence of a hinge at the level of the sign blank created by cutting the flange and web of the sign post. A fuse plate is spliced over the weakened post to transfer wind loads to the base. On impact, the sign post rotates about the hinge, allowing the vehicle to pass beneath the sign.

During the first phase of impact, the vehicle crushes into the sign support until the force on the sign post reaches a level sufficient to activate the breakaway features. Energy is dissipated only through crushing of the vehicle. In contrast to the luminaire support, both slip-base and fuse plate forces must be overcome during this phase.

Figure 74 shows a free body diagram for the sign post during phase one. Using equilibrium considerations, the vehicle force was equated to an equivalent slip force as shown in Eq. 12:

$$F_v = \frac{F_F D_b + F_s h}{d} = F_{se} \qquad (12)$$

Table 39. Slip-base pole impacts with bogie test vehicles.

Test #	Impact Speed (mph)	Change in Velocity (ft/sec) Measured[a]	Change in Velocity (ft/sec) Predicted
B101	20	11.0 - 12.9	13.7
B102	40	14.2 - 16.4	15.6
B103	60	17.2 - 19.2	20.2
504	20	10.9 - 11.6	11.1
509[b]	60	6.4 - 9.7	9.8
515	60	7.2 - 8.7	9.6

[a] Range of values measured from film, speed trap, and accelerometers

[b] Off-center impact

where: F_v = vehicle force; F_F = force required to activate fuse plate; F_s = slip-base activation force; D_b = depth of sign post; h = distance from slip base to hinge; d = distance from vehicle bumper to hinge; and F_{se} = effective slip-base activation force.

Using conservation of energy, the velocity at the end of this phase was then formulated in terms of the effective slip force as shown in Eq. 13.

$$V_a = \sqrt{V_i^2 - F_{se}^2/(k_v m_v)} \qquad (13)$$

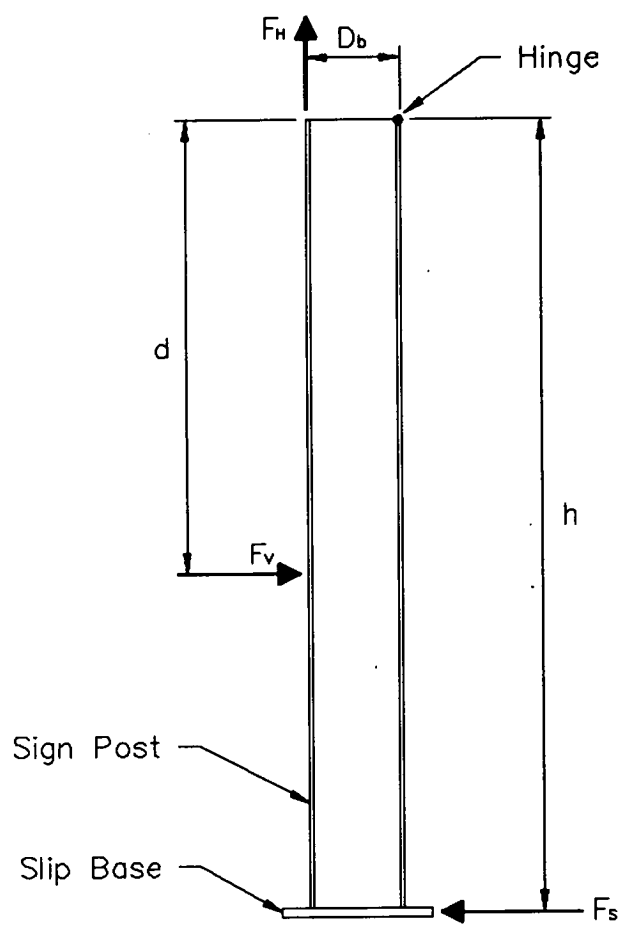

Figure 74. Free body of breakaway sign post.

where: V_i = initial impact velocity; V_a = velocity at activation of breakaway mechanism; F_{se} = effective slip-base activation force; k_v = frontal stiffness of impacting vehicle; and m_v = mass of impacting vehicle.

The second phase of impact was assumed to involve only momentum transfer from the vehicle to the sign post as the base was accelerated and the post rotated about the hinge. Conservation of angular momentum was used to determine the velocity change of the impacting vehicle due to momentum transfer to the support. Equation 14 gives the predicted vehicular velocity at the end of the second phase.

$$V_b = V_a \frac{m_v d^2 - eI_s}{m_v d^2 + I_s} \tag{14}$$

where: V_a = vehicle velocity at beginning of phase two; V_b = vehicle velocity after momentum transfer to support; d = distance from vehicle bumper to hinge; I_s = mass moment of inertia of sign support; m_v = mass of vehicle; and e = coefficient of restitution for vehicle.

The third phase of impact was assumed to involve only energy dissipation as the fuse plate and slip-base mechanisms released. To simplify the analysis, the force-deflection relationships associated with the slip base and fuse plate were assumed to vary linearly. Conservation of energy was used to determine the velocity of the vehicle at the end of the impact event. The energy associated with failure of the breakaway articles was formulated in terms of the slip distance of the base. The vehicle's terminal velocity is given by Eq. 15 below.

$$V_c = \sqrt{V_v^2 - \left(\frac{F_F D_b}{h} + F_s\right) \delta_s / m_v} \tag{15}$$

where: V_b = vehicle velocity at beginning of phase three; V_c = vehicle velocity at end of impact; and δ_s = failure distance of slip-base mechanism.

In terms of the effective slip force defined b Eq. 12, Eq. 15 becomes

$$V_c = \sqrt{V_b^2 - F_{se}\, \delta_s \left(\frac{d}{h}\right) \Big/ m_v} \tag{16}$$

where: F_{se} = effective slip-base activation force.

Equations 13, 14, and 16 were incorporated into a computer program to conduct parametric studies of important sign support parameters. The objective of this task was to improve the safety performance of breakaway sign supports for impacts with minicars. Figure 75 gives input parameters required for the sign support analysis as prompted for by the program. A typical breakaway sign-support installation is shown in Figure 28.

For impacts in which the hinge is activated, the effective slip-base activation force is calculated using Eq. 12. Bolt tension for the slip base and fuse plate is calculated using the empirical relationship given by Eq. 9. The slip force F_s (lb) and fuse plate force F_F (lb) are then determined using an appropriate effective coefficient of friction. The post height is taken to be the distance from the slip base to the hinge, and the post weight is calculated based on this length.

In instances when the hinge does not activate during impact, the input parameters are slightly modified. Under these circumstances, the effective slip force is assumed to be equivalent to the slip-base activation force, and the post height becomes the distance from the slip base to the point of rotation of the sign post. When the hinge does not activate, additional energy may be dissipated in the form of tearing the support away from the sign. This phenomenon may be accounted for in the program by converting the energy dissipated to an equivalent force at the base acting over 1 in. of deformation. In this way an effective slip force may be determined and input into the program.

Effective Friction Coefficient

The majority of breakaway sign supports are mounted on rectangular or unidirectional slip bases. Because of the basic differences in base geometry, bolt orientation, and notch geometry, the rectangular slip base has an effective friction coefficient different from the triangular or multidirectional base.

In a previous study (*113*), the effect of bolt torque on the transverse load required to activate a unidirectional slip base was investigated. Using a K_T value of 3.2 for a 1¾ in. bolt, the effective friction coefficient for a rectangular base was found to be approximately 0.26. This value was subsequently used in the validation runs and parametric studies performed with the sign support model.

Validation

The preceding analysis technique was validated by comparing predicted velocity changes with results of four full-scale crash tests from Refs. 13 and 15. Table 40 gives predicted and measured velocity changes for the selected tests. The installation in tests 1009 and 1010 consisted of a 12 ft by 24 ft sign blank supported on 12WF45 steel beams mounted on unidirectional slip bases. The slip base used four 1-in. diameter strain-sert bolts that were tightened to 5,000 lb per bolt. A hinge was located

```
Do you wish to analyze a luminaire support or sign support?
(1 = Luminaire; 2 = Sign Support): 2

Please input the following values :

1. Initial Velocity (mph)                          : 20
2. Vehicle Weight (lbs)                            : 1800
3. Effective Vehicle Bumper Height (in)            : 15.0
4. Vehicle Stiffness (lb/in) (-1 = default)        : -1
5. Effective Slip Force (lbs)                      : 12000
6. Slip Base Slip Distance (in)                    : 1
7. Distance from Slip Plane to Hinge (in)          : 99
8. Sign Post Weight (lbs)                          : 371
9. Base Plate Weight (lbs)                         : 30

 EDIT SCREEN - The current values are :

 1. Initial Velocity (mph)                         :      20.000
 2. Vehicle Weight (lbs)                           :    1800.000
 3. Effective Vehicle Bumper Height (in)           :      15.000
 4. Vehicle Stiffness (lb/in)                      :    1800.000
 5. Effective Slip Force (lbs)                     :   12000.000
 6. Slip Base Slip Distance (in)                   :       1.000
 7. Distance from Slip Plane to Hinge (in)         :      99.000
 8. Sign Post Weight (lbs)                         :     371.000
 9. Base Plate Weight (lbs)                        :      30.000

Choice to edit 1-9 (0 = quit editing) :
```

Figure 75. Input format for sign support analysis.

in the legs at a height of 8½ ft above the ground line. Two ¾-in. diameter hinge bolts were tightened to 28,000 lb each. Using an effective friction coefficient of 0.26, the hinge and base activation forces were estimated to be 14,560 lb and 5,200 lb, respectively. Using Eq. 12, the effective slip force was estimated to be $F_{se} = \frac{(14{,}560)(12) + (5{,}200)(99)}{84.5} = 8{,}160$ lb.

The test vehicle for each test was a Honda Civic weighing 1,516 lb and 1,617 lb, respectively. Based on the information presented in Table 37, an average K/W ratio of 1.1 was used for the Honda. The vehicle crush stiffness for the two tests was thus estimated to be 1,668 and 1,779 lb/in., respectively. It should be noted that the upper hinge did not activate in test 10 although the slip base broke away as designed. An effective post length of 17.5 ft was used in the "no hinge" analysis although the total post length was 20 ft. This was done since the depth of the upper 5 ft of the support leg was tapered down to near zero. Because the hinge did not activate, the hinge activation force was neglected and the effective slip force was estimated to be 5,600 lb.

The installation for tests 7024-1 and 7024-2 used S4 × 7.7 posts to support an 8 ft by 5 ft sign panel. The hinge was placed at the midheight of the panel or 9.5 ft above ground level. The slip base used four ½-in. diameter bolts torqued to 17 ft-lb each. The hinge used two ½-in. diameter bolts torqued to 90 ft-lb each. Using a K_T value of 10.0 for a ½-in. diameter bolt, Eqs. 9 and 12 estimate the slip force to be 2,700 lb.

These installations were assumed to bracket the size and weight of most common breakaway sign supports. As shown in Table 40, the model predicted velocity changes with reasonable accuracy. One exception was for test 7024-1. During this test, the hinge did not fully activate and a considerable amount of energy was dissipated in twisting and buckling of the sign. In addition, the restoration forces in the sign carried the sign post back into the vehicle's path causing a secondary impact to occur. Determination of vehicle stiffness, slip force, and fuse plate force may also be a cause of deviation between predicted and measured values. It was difficult to extract required information from test reports, and in the absence of this information, approximations were made.

The luminaire and sign support models discussed in this section were combined into a single comprehensive program for analysis of breakaway structures.

An evaluation of key luminaire and sign support parameters was made by application of the program described in this section. Results of the parametric studies are given in Chapter Two, "Modifications to Selected Roadside Safety Elements to Accommodate Minicars." A copy of this program may be obtained upon request, by sending a floppy diskette to one of the TTI authors.

Others have also developed a model that is available for use as an analytical tool in the evaluation of various breakaway supports (*114*). However, because of the complexity of the program, it has not seen widespread use.

Table 40. Full-scale tests of breakaway sign supports.

Test #	Vehicle Weight (lb)	Impact Speed (mph)	Change in Velocity (ft/sec)	
			Measured	Predicted
1009	1,516	60	10.8	13.9
1010	1.617	20	9.9	9.6
7024-1*	1,820	20	4.9	1.2
7024-2	1,820	60	3.1	2.7

* Secondary impact with sign support occurred

Small Sign Supports

Because only one test of a small sign installation was conducted in the study, it was desirable that an estimate be made of the impact performance of other under 1,800-lb vehicles with other sign supports. A primary measure of impact performance is vehicular velocity change. Following is a methodology for estimating velocity change in small sign support impacts for small vehicles based on test results of other vehicles. It is consistent with a procedure contained in FHWA Technical Advisory T 5040.22 dated September 27, 1983. It is noted that the procedure in the referenced advisory was proposed to allow one to estimate vehicular velocity change for impacts with multiple sign supports given test results from a single post impact.

The reader is cautioned that the procedure presented herein is only an approximation to a very complex problem. Impacts with base-bending sign supports involve highly nonlinear behavior of the support, the soil, and the vehicle. Attempts to analytically model the system have met with little success (*59*). Studies are now under way by Federal Highway Administration officials at the Turner-Fairbank Highway Research Center, McLean, Virginia, to develop analytical and experimental methods of analysis for small, base-bending-type sign supports.

For many widely used small sign supports the critical velocity change of an impacting vehicle occurs at low rather than high impact speeds. High carbon, high strength steels exhibit this behavior. Supports with breakaway features such as the slip base or the lap-splice at ground level also exhibit this behavior. Brittle materials tend to fracture, and breakaway features tend to actuate more readily at the higher loading rates. Further, the mass of most small sign installations is relatively small in comparison to the impacting vehicle. The vehicular velocity change is due in large part to an energy loss (distortions in sign posts, soil displacements and damping, and vehicular crush) as opposed to a momentum transfer, especially for low-speed impacts. For purposes of estimating velocity change, it was assumed that energy loss is independent of vehicle mass. Based on this assumption, the velocity change of a given vehicle is estimated from that measured in a test of another vehicle as follows:

$$(\Delta KE)_T = \tfrac{1}{2} M_T (V_{IT}^2 - V_{FT}^2) \qquad (17)$$

where: $(\Delta KE)_T$ = change in kinetic energy of test vehicle during contact with support; M_T = mass of test vehicle; V_{IT} = impact velocity of test vehicle; and V_{FT} = final velocity of test vehicle after loss of contact with support.

Then, for a different size vehicle with mass M_V impacting at V_{IT},

$$(\Delta KE)_T = \tfrac{1}{2} M_V (V_{IT}^2 - V_{FV}^2) \qquad (18)$$

and

$$V_{FV} = \sqrt{V_{IT}^2 - \frac{2(\Delta KE_T)}{M_V}} \tag{19}$$

where V_{FV} = final velocity of vehicle.

The change in velocity, ΔV, is then computed as follows:

$$\Delta V_V = V_{IT} - V_{FV} \tag{20}$$

It is noted that for sign impacts, the occupant impact velocity will, in most cases, approximately equal the velocity change of the vehicle during impact. This is borne out by results of various tests.

The above procedure was used to estimate the impact performance of a 1,500-lb vehicle and a 1,250-lb vehicle for selected sign support systems now in use across the country. Equations 19 and 20 were used to compute the predicted vehicular velocity changes. Results are given in Chapter Two, "Modifications to Selected Roadside Safety Elements to Accommodate Minicars," under the subsection on "Base Bending Sign Supports."

Vehicular Stability Considerations

As alluded to in various sections of this report, accident data have shown that the propensity for vehicular overturn in single vehicle, run-off-the-road accidents increases as the size of the vehicle decreases. This observation is true for all run-off-the-road accidents involving barrier, sign and luminaire supports, ditches, embankments, driveways, and so forth. Attempts to isolate specific vehicular properties that are critical to the overturn problem have not been successful (*11*). According to McHenry (*11*), "The lack of a detailed definition of the properties of each vehicle undermines any definitive conclusion with respect to identification of specific vehicle characteristics which affect the overall vehicle resistance to rollover."

Studies of accident data show that many, if not most, overturn accidents occur while the vehicle is in a nontracking or skidding-sideways condition. Simulations of nontracking encroachments on roadside slopes and ditches were made in the present study using the HVOSM program. However, because of the limitations of the tire-terrain models in the versions of HVOSM used in the present study, the results of the simulations were not very discerning. Those limitations include a smooth, impenetrable terrain surface and a tire incapable of generating sidewall forces. Recent changes to HVOSM to remedy some of these limitations show promise for improved simulations of soft-soil conditions and irregular terrain (*23, 36*).

It is apparent that a discontinuity on the roadway surface (such as a curb) or terrain irregularity (such as a mound of dirt, a large rock, a washout) poses a greater risk for a minicar than for a larger car, especially if the car slides broadside onto the object.

To better quantify the "stability threshold" factor and to develop reasons for this occurrence, a first-order approximation of the overturn problem was developed. Consider a car sliding sideways encountering a terrain irregularity such as a rut or a mound of soil. Depending on the mass and inertia properties, a vehicle sliding sideways into a mound of soil can either plough through it or be tripped by it. Even if the vehicle pushes through the mound, the impulse can cause it to overturn. To demonstrate this, conservation of momentum and conservation of energy were used to estimate the impulse required to overturn a vehicle. The vehicle was assumed to be a rigid body having a track equal to T and height of the center of gravity above ground equal to h, as shown in Figure 76. If the horizontal impulse due to the mound of earth is P_y, by conservation of momentum, it can be shown that the angular velocity ϕ just after impact is given by:

$$\dot{\phi} = \frac{hP_y}{\left|I_x + \frac{W}{g}(T/2)^2\right|} \tag{21}$$

where: I_x = roll moment of inertia; W = weight of the vehicle; and g = acceleration due to gravity.

If this angular velocity is large enough to rotate the vehicle such that its center of gravity is directly above the pivoting point

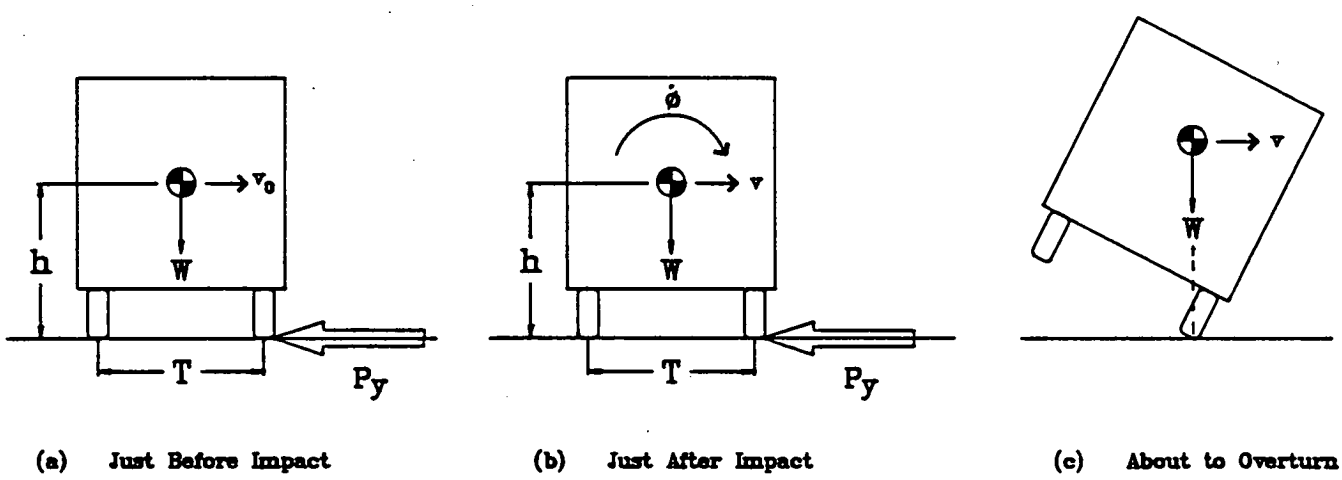

Figure 76. Schematic of a vehicle overturning due to a side impact with a mound of earth.

(see Figure 76), the vehicle will overturn. Considering the conservation of energy during the post impact motion, the angular velocity $\dot{\phi}$ required to rotate the vehicle into the position shown in Figure 76 can be shown to be given by:

$$\dot{\phi}^2 = \frac{2W\left[\sqrt{h^2 + (T/2)^2} - h\right]}{\left[I_x + \frac{W}{g}(T/2)^2\right]} \tag{22}$$

Now, by eliminating $\dot{\phi}$ from Eq. 21 and Eq. 22, the impulse required to overturn a vehicle P_y is given by:

$$P_y = \frac{1}{h}\left\{2W\left[I_x + \frac{W}{g}(T/2)^2\right]\left[\sqrt{h^2 + (T/2)^2} - h\right]\right\}^{1/2} \tag{23}$$

To plot P_y as a function of W, the value of h was assumed to be equal to 20.4 in. for W less than 1,800 lb (Honda Civic), and it was assumed to change linearly between 1,800 lb and 5,000 lb with a value 23.6 in. at 4,500 lb (Plymouth Fury). The track T was found by assuming that the ratio $T/2h$ is constant and equal to 1.38 for all vehicles between 1,000 lb and 5,000 lb. The roll moment of inertia was found as a function of W by the use of empirical relationship given below (*3*):

$$I = 4.752\,\frac{(0.889W - 126.6)}{g}\,W^{0.546}\ \text{lb-sec}^2\text{-in.} \tag{24}$$

where $g = 386.4$ in./sec.

The impulse P_y was then plotted as a function of weight W as shown in Figure 77. The plot shows that P_y varies almost linearly with the weight of the vehicle. Based on this simplified theory, a 610 lb-sec impulse will overturn a 1,500-lb vehicle compared to a 1,870 lb-sec impulse to overturn a 4,000-lb vehicle. Transient behavior of the vehicle just prior to the impulse, suspension compliance, and many other factors can alter the overturning impulse. Although the actual impulse values required to overturn a vehicle may differ considerably from those of Figure 77, it is believed that the relative differences indicated by these results are reasonably indicative of real world values.

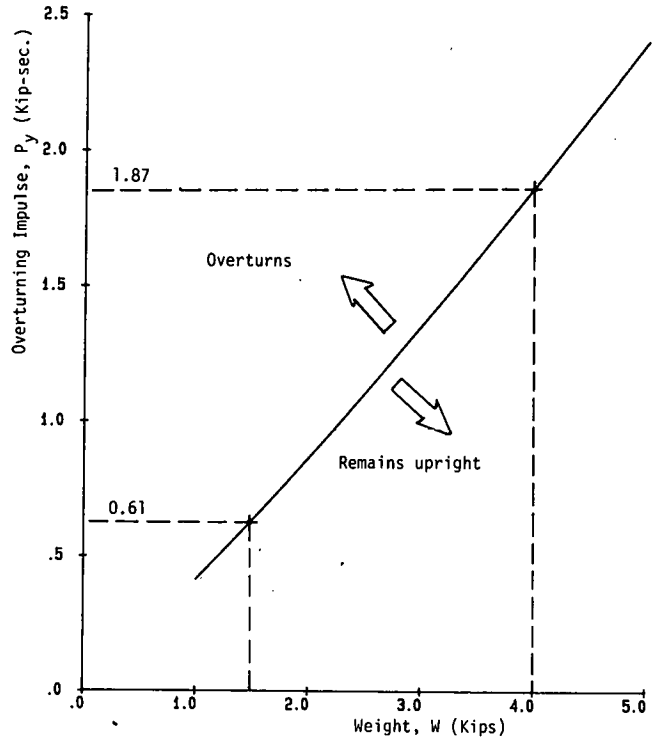

Figure 77. Plot of overturning impulse vs. weight of the vehicle in a side impact with a mound of earth.

CHAPTER FOUR

CONCLUSIONS AND RECOMMENDATIONS

CONCLUSIONS

This project had two basic objectives; (1) to evaluate the impact performance of widely used roadside safety elements for a 1,500-lb vehicle using *NCHRP Report 230* performance guidelines, and (2) to identify potential modifications that would be necessary for existing roadside safety elements to accommodate a design vehicle weighing as little as 1,250 lb. A full-scale crash test program coupled with an extensive computer analysis study was used to accomplish the objectives. Computer programs HVOSM and GUARD were calibrated with the tests of the minicars prior to their use in a comprehensive parametric study.

Specific roadside safety elements analyzed and conclusions reached about each follow.

ROADSIDE HARDWARE

Rigid Longitudinal Barriers

On the basis of five full-scale crash tests and a series of computer simulations, the performance of the concrete safety shaped barrier (CSSB) is acceptable for cars weighing as little as 1,250 lb for *NCHRP Report 230* criteria. However, it was determined that overturns can be expected for nontracking and/or high angle impacts with the CSSB by small cars. It is estimated that approximately 50 percent of inadvertent run-off-the-road vehicle encroachments occur in a nontracking mode. It was shown that a barrier with a constant-slope face or a vertical wall will greatly reduce the overturn problem. A retrofit design for the CSSB consisting of a longitudinal member placed on the side of the barrier near the top also shows promise in reducing the overturn problem. Full-scale crash tests of the constant-slope design are planned for the summer of 1988 at TTI on another project.

A modified version of the HVOSM computer program was used in studying the performance of the CSSB and the designs mentioned above. Extensive changes and improvements were made to the vehicular crush routines. The modified HVOSM program was subjected to an extensive calibration effort and found to produce reasonably accurate results in most cases.

Flexible Longitudinal Barriers

On the basis of two full-scale crash tests and a series of computer simulations by the GUARD program, the performance of the G4(1S) roadside barrier is acceptable for cars weighing as little as 1,250 lb. Since the G4(1S) is essentially a vertically faced barrier, overturn problems associated with nontracking impacts are not anticipated, at least to the degree seen in CSSB impacts. Minor modifications may be needed to minimize wheel snag for the higher angle impacts. This could be accomplished by increasing the depth of the blockout.

Breakaway Luminaire Supports

Studies have shown that most supports with transformer bases are not in compliance with current AASHTO performance guidelines for an 1,800-lb car. A 35-ft pole supported by a cast-aluminum transformer base was tested in the present project with a 1,500-lb car at 20 mph. The base fractured but did not breakaway and the car came to an abrupt stop. It is doubtful that the transformer base can be modified to accommodate a vehicle weighing 1,500 lb. It is estimated that moderate size steel or aluminum supports (in the 35-ft range weighing 500 lb or less) with the slip-base design comparable thereto will be acceptable for a 1,500-lb car. For taller supports acceptable performance can be achieved if the support is aluminum or of a light weight material, provided a slip base is used.

Breakaway Sign Supports

With few exceptions all sign supports with the slip-base design or a design comparable thereto will accommodate a 1,500-lb car.

A computer program was developed to assist in the analysis and design of breakaway sign and luminaire supports. It was written for use on a microcomputer, and it has a user-friendly input format. The program was used to study the sensitivity of impact performance to key vehicular and support parameters. It was shown that although most slip-base supports can be designed for minicars, care will be needed in construction and maintenance practices. If either the base bolts or the hinge bolts (in a sign post) are overtorqued, the system may not perform in an acceptable manner and this becomes more critical as the design vehicle size decreases. The point at which vehicular contact is made with the support is also an important factor, particularly with smaller cars. It was also shown that the crush stiffness of the impacting vehicle is an important factor in the performance of a breakaway support.

Base-Bending Sign Supports

On the basis of a full-scale crash test and computer simulations, a 4-lb/ft rail steel, single U-post is marginally acceptable for a 1,500-lb car. Improvement in the performance of the U-post can be achieved by the use of a two-piece support with a short bolted splice at ground level. Estimates were made of the performance of other widely used small sign supports for impacts with under 1,800-lb cars. Most widely used small single-post systems are predicted to be acceptable for a 1,500-lb car. However, very few could accommodate a 1,250-lb car, the notable exception being supports with a slip-base design or a design comparable thereto.

Crash Cushions

On the basis of an evaluation by analytical procedures, none of the current crash cushions would be acceptable for a 1,500-lb car. The sand-filled plastic barrel system can easily be designed to accommodate a 1,300-lb car. The GREAT and Hi-Dri systems could be modified to accommodate a 1,500-lb car. Modifications would involve the addition of more bays extending the length of the cushion. Moderate cost increases would ensue.

Estimates of crash cushion performance were based on analytical procedures that have been developed over a period of time and proven reliable for current vehicular designs. In light of the response of the 1,500-lb car during the eccentric loader test, these procedures may require further evaluation and calibration.

Guardrail Terminals

Based primarily on a full-scale crash test, it was the opinion of the researchers that the performance of the eccentric loader BCT was not acceptable for a 1,500-lb car because of excessive ridedown accelerations and intrusions and deformations of the passenger compartment. Performance can be improved by reducing the mass of the nose and by further reducing forces needed to buckle or collapse the W-beam. A new guardrail extruder terminal (GET) shows promise as a cost-effective end treatment, and it could possibly be designed for under 1,800-lb cars. The SENTRE system could be modified to accommodate a 1,500-lb car.

In the test of the eccentric loader the occupant impact velocity was actually below the 30-ft/sec recommended limit of *NCHRP Report 230.* However, damage to the 1,500-lb car was extensive due to a relatively low crush stiffness. This result is believed to be indicative of potential problems that may arise in other safety features if the under 1,800-lb car becomes a design vehicle. (See recommendation 3.)

ROADSIDE FEATURES

Analysis of roadside safety features was made by a limited test program in combination with a comprehensive computer simulation study. Two full-scale vehicular tests of a driveway configuration and a series of five tests of an AASHTO type B curb were conducted. The HVOSM computer program was calibrated with these tests of a 1,500-lb car.

Slopes, Ditches, and Driveways

It was found that the behavior of under 1,800-lb cars on these features is similar to larger cars for encroachments on smooth, well-compacted terrain. However, soft terrain or terrain irregularities, such as large rocks or eroded areas, pose an increased risk to occupants of a small car. Seemingly innocuous vegetation would also pose an increased risk. It was shown that terrain objects that would not trip a large vehicle would trip and overturn a smaller one. It is not clear if current design guidelines for the above feature should be changed to accommodate under 1,800-lb vehicles. At a minimum more care would have to be exercised in their construction and maintenance to avoid an increase in overturn accidents. Further studies of slopes, ditches, and driveways would be warranted should the minicar become a design vehicle.

Curbs

Six-inch high curbs can easily be traversed by a 1,250-lb car if it impacts the curb in a tracking (nonskidding) condition. For nontracking impacts a small car will overturn more easily than a larger car. To minimize overturn accidents of nontracking minicars, the face of the curb should be sloped as flat as possible. AASHTO curb types C, E, and G or similarly sloped designs are preferred.

Finally, as has been alluded to, much of the information in this project was developed through the application of computer programs HVOSM, GUARD, and other specialized programs. To the extent possible the programs were calibrated against full-scale tests to evaluate their accuracy and applicability. Impacts with most of the elements evaluated in the project involve complex and highly nonlinear vehicular and appurtenance response that often exceed the limitations of the respective programs. In some cases the programs were used to study "atypical" impact conditions such as nontracking and/or high angle impacts with a barrier. Since these impacts are outside the range of the tests used in the calibration, results should be viewed as preliminary in nature subject to experimental verification. The above limitations notwithstanding, the programs have provided valuable insight on the performance of minicar impacts with a wide array of roadside safety elements.

RECOMMENDATIONS

1. At the time this project was conceived (1984) there were no 1,500-lb cars on the U.S. market. The project was intended as a "what if" study. At the time of this writing there are at least two models being sold with curb weights near 1,500 lb and it is likely that others will soon be on the market. This should be carefully considered in future changes to *NCHRP Report 230* and other nationally recognized performance standards.

2. Evidence from accident data strongly indicates that small cars are overrepresented in run-off-the-road overturn accidents. Further, a large portion of these are believed to occur with the vehicle in a nontracking condition. Based on the computer simulations conducted in the present project, overturns are much more likely to occur if a small car impacts the CSSB in a nontracking mode as opposed to a tracking mode. Simulation studies by others of nontracking traversals of curbs and slopes with soft terrain have produced similar results. In accordance with *NCHRP Report 230* roadside safety features are evaluated for tracking conditions. Further changes to *NCHRP Report 230* and other nationally recognized performance standards should consider the need and feasibility of including nontracking impact tests. Further studies of the stability of minicars traversing curbs, slopes, and ditches are probably warranted to include simulation studies, crash test studies, and accident analysis studies.

3. As demonstrated in this and other studies, the crush properties of a vehicle is an important element in the impact performance of many roadside safety devices. The small cars studied in this project all had a relatively light-weight, integral, shell body as opposed to the more rigid frame construction of the past. In effect, they are much softer than older models. More research is needed to better define the range of crush properties of these vehicles and the effect these properties have on the design of roadside safety features. Updates to *NCHRP Report 230* and other nationally recognized performance standards need to strongly consider this factor in selecting test vehicles.

4. A major effort was made to improve the barrier impact routines in HVOSM for simulation of impacts with a multifaced rigid barrier. The CSSB is one such barrier. While these changes were a major step forward in barrier simulation, an effort is needed to improve the "thin-disk" tire model in HVOSM. Tire/barrier interaction is a major factor in vehicular response, and the present model can produce inaccurate and extraneous tire forces depending on the impact conditions. An effort has been made by others to improve the tire model, but it was limited in scope. Researchers at Texas A&M University are currently developing a sophisticated finite element model of a tire. It may be feasible to incorporate the model or certain features of the model into the HVOSM program.

5. On the basis of a computer program developed in the project, it was shown that the point of impact on a breakaway support is an important factor in its impact performance. Supports placed behind a curb or on a slope can be impacted above the desired point of impact. As the design vehicle gets smaller, this factor becomes more acute. Consideration should be given to further evaluations of this potential problem.

6. *NCHRP Report 230* presents a recommended procedure for computing the velocity at which a pseudo-occupant would impact the vehicle's interior for crash tests evaluation. An alternate and more exact procedure was developed and presented. It was shown that impact velocities can be significantly different

and higher when computed by the improved procedure. It may be desirable to incorporate the improved procedure in future changes to *NCHRP Report 230* and other nationally recognized performance standards.

REFERENCES

1. MICHIE, J. D., "Recommended Procedures for the Safety Performance Evaluation of Highway Appurtenances." *NCHRP Report 230* (Mar. 1981) 42 pp.
2. WELCH, R. E. and CHIAPETTA, R. L., "Validation and Application of the GUARD Computer Program." Four volumes, final report, Contract DOT-FH-11-9460, Federal Highway Administration (Jan. 1984).
3. SEGAL, D. J., "Highway-Vehicle-Object-Simulation-Model—1976." Four volumes, Federal Highway Administration, report numbers FHWA-RD-75-162 through 165 (Feb. 1976).
4. ROSS, H. E., JR., and SICKING, D. L., "Roadside Safety Design for Small Vehicles." Phase I Interim Report Draft, NCHRP Project 22-6 (May 1986).
5. "Standard Specifications for Structural Supports for Highway Signs, Luminaires and Traffic Signals." American Association of State Highway and Transportation Officials (1985).
6. CARLSON, L. E. and LEONARD, P., "Improved Performance of Small Sign Supports." Final report, Contract DTFH61-80-C-00170, Mobility System and Equipment Co. (Aug. 1985).
7. BUTH, C. E., ET AL., "Performance Limits of Longitudinal Barrier Systems." Final report, Contract DTFH61-82-C-00051, Texas Transportation Institute, Texas A&M University (May 1985).
8. POWELL, G. H., "BARRIER VII: A Computer Program for Evaluation of Automobile Barrier System." FHWA Report No. FHWA-RD-73-51 (Apr. 1973).
9. IWANKIW, N. W., HAHN, E. E., CHIAPETTA, R. L., WALGRAVE, S., and JOYCE, R. P., "Modelling the Interaction of Heavy Vehicles with Protective Barriers: Development and Validation of the 'CRUNCH' Program." Illinois Institute of Technology Research Institute (Mar. 1980).
10. "Guide for Selecting, Locating, and Designing Traffic Barriers." American Association of State Highway and Transportation Officials (1977).
11. COUNCIL, F. M., ET AL., "Safe Geometric Design for Minicars." FHWA Report No. FHWA/RD-87/047 (Mar. 1987).
12. HANSEN, A. G. and HOTT, C. R., "Summary of Luminaire Support Capability Testing." Report No. FHWA-RD-87-104 (Mar. 1988).
13. BLOOM, J. A. and HINCH, J. A., "Laboratory Evaluation of Existing Breakaway Structures." Three Volumes, Report No. FHWA-RD-79-140, Federal Highway Administration, Washington, D.C. (June 1980).
14. ROSS, H. E., JR., ET AL., "State of the Practice in Supports for Small Highway Signs." Technology Sharing Report 80-222, Federal Highway Administration, Washington, D.C. (Apr. 1980).
15. ROSS, H. E., JR., ET AL., "Small Sign Support Analysis: Phase I—Crash Test Program." Research Report 7024-1, Texas Transportation Institute, Texas A&M University (Jan. 1986).
16. Energy Absorption Systems, Inc., One East Worker Drive, Chicago, Illinois, 60611.
17. FIBCO, Inc., One Boston Place, Boston, Massachusetts, 02108.
18. BRONSTAD, M. E. and MICHIE, J. E., "Development and Crash Test Evaluation of Traffic Barrier Terminals." Final report on Project 03-3291, Southwest Research Institute (1973).
19. HIRSCH, T. J. and BUTH, C. E., "Improved End Treatment for Texas Guardrail." Research Report No. 189-1(F), Texas Transportation Institute, Texas A&M University (Oct. 1976).
20. BRONSTAD, M. E., ET AL., "Crash Test Evaluation of Eccentric Loader Guardrail Terminals." *Transportation Research Record 1065,* Transportation Research Board (1986).
21. WEAVER, G. D., MARQUIS, E. L., and OLSON, R. M., "The Relation of Side Slope Design to Highway Safety." *NCHRP Report 158* (1975) 57 pp.
22. ROSS, H. E., JR., and POST, E. R., "Full-Scale Embankment Tests and Comparisons with a Computer Simulation." *Highway Research Record No. 488,* Highway Research Board (1974).
23. DELEYS, N. J. and PARADA, L. O., "Rollover Potential of Vehicles on Embankments, Sideslopes, and other Roadside Features." Final report, Contract No. DTF61-83-C-00060, Calspan Corp. (Aug. 1986).
24. "A Policy on Geometric Design of Highways and Streets." American Association of State Highway and Transportation Officials (1984).
25. ROSS, H. E., JR., and ROSCHKE, P. N., "Effectiveness of Sloped End Sections." Research Report 407-1F, Texas Transportation Institute, Texas A&M University (Nov. 1987).
26. ROSS, H. E., JR., ET AL., "Safety Treatment of Roadside Drainage Structures." *Transportation Research Record No. 868,* Transportation Research Board (1982).
27. ROSS, H. E., JR., and POST, E. R., "Tentative Criteria for

the Design of Safe Sloping Culvert Grates." *Highway Research Record No. 386,* Highway Research Board (1972).

28. BRONSTAD, M. E., ET AL., "Performance of Longitudinal Traffic Barriers." *NCHRP Report 289* (June 1987) 169 pp.
29. MORGAN, J. R., ET AL., "Small Sign Support Analysis: Phase II-Development of a New Small Sign Support System." Two Volumes, Research Report 7024-2, Texas Transportation Institute, Texas A&M University (Aug. 1987).
30. ROSS, H. E., JR., ET AL., "Evaluation of Bolted Base Steel Channel Signpost." *Transportation Research Record No. 736,* Transportation Research Board (1978).
31. ZEGEER, C. V., HUMMER, J., REINFURT, D. W., HEIF, L., and HUNTER, W. W., "Safety Éffects of Cross-Section Design for Two-Lane Roads." Federal Highway Administration, Washington, D.C. (Dec. 1986).
32. ROSS, H. E., JR., "Analysis and Design of Safety Appurtenances by Computer Simulation." *Proc.,* ASCE Specialty Conference on the Role of the Civil Engineer in Highway Safety, New Orleans, Louisiana (Sept. 1983).
33. YOUNG, R. D., POST, E. R., ROSS, H. E., JR., and HOLCOMB, R. M., "Simulation of Vehicle Impact with the Texas Concrete Median Barrier." Research Report 140-5, Texas Transportation Institute, Texas A&M University (June 1972).
34. BRONSTAD, M. E., CALCOTE, L. R., and KIMBALL, C. E., "Concrete Median Barrier Research." Volumes I and II, Final report, Contract DOT-FH-11-8130, Southwest Research Institute (June 1976).
35. BUTH, C. E., ET AL., "Development of a High-Performance Median Barrier." Final report on Work Order No. 2, Contract DOT-FH-11-9485, Texas Transportation Institute, Texas A&M University (Apr. 1983).
36. MCHENRY, B. G., "Final Report on the Investigation of Pavement/Shoulder Dropoffs." Contract No. DTFH61-80-C-00146 (Nov. 1982).
37. BETZ, J. F., "Three-Dimensional Response of an Automobile to a Generalized Impulse." Master of Science Thesis, Texas A&M University (Dec. 1979).
38. SICKING, D. L., ET AL., "Development of New Guardrail End Treatments." Research Report 404-1F, Texas Transportation Institute, Texas A&M University (Jan. 1988).
39. "Standard Plans." State of California, Department of Transportation (July 1984).
40. CHISHOLM, D. B. and VINER, J. G., "Dynamic Testing of Luminaire Supports," Report No. FHWA-RD-73-55, Federal Highway Administration (July 1973).
41. SICKING, D. L., ET AL., "An End Treatment for Concrete Barriers Used in Work Zones." Research Report 2262-2, Texas Transportation Institute, Texas A&M University (Aug. 1982).
42. OLSON, R. M., ET AL., "Effect of Curb Geometry and Location on Vehicle Behavior." *NCHRP Report No. 150,* Transportation Research Board (1974) 88 pp.
43. DELEYS, N. J., "Safety Aspects of Roadside Cross Section Design." Final report, FHWA Contract DOT-FH-11-8189, Report No. FHWA-RD-75-41 (Feb. 1975).
44. JAMES, M. E., JR., and ROSS, H. E., JR., "HVOSM User's Manual." Research Report 140-9, Texas Transportation Institute, Texas A&M University (Aug. 1974).
45. PERERA, H. S., "Simulation of Vehicular Impacts with Safety-Shaped Barrier." Ph.D. Dissertation, Texas A&M University (Dec. 1987).
46. MCHENRY, R. R., SEGAL, D. J., AND DELEYS, N. J., "Determination of Physical Criteria for Roadside Energy Compression Systems." *Technical Report, Cal No. VJ-2251-V-1,* Cornell Aeronautical Laboratory, Inc., Buffalo, N. Y. (1967).
47. HARGENS, R. L., and DAY, T. D., "Vehicle Crush Stiffness Coefficients." Engineering Dynamics Corporation, Ref. No. 1042 (Undated).
48. SCHUMAKER, L. L., "Fitting Surfaces to Scattered Data." *Approximation Theory II, Symposium on Approximation Theory,* University of Texas, Austin, Tex, 203-268 (1976).
49. RENKA, J. R., "Triangulation of Bivariate Interpolation for Irregularly Distributed Data Points." Dissertation presented to the University of Texas, Austin, Texas, in partial fulfillment of the requirements for the degree of Doctor of Philosophy (1981).
50. LANG, H. H., "A Study of the Characteristics of Automotive Hydraulic Dampers at High Stroking Frequencies." Dissertation presented to the University of Michigan, Ann Arbor, Michigan, in partial fulfillment of the requirement for the degree of Doctor of Philosophy (1977).
51. CAMPBELL, C., *New Directions in Suspension Design.* Robert Bently, Inc., Cambridge, Mass (1981).
52. SMILEY, R. F., and HORNE, W. B., "Mechanical Properties of Pneumatic Tires with Special Reference to Aircraft Tires." *Technical Report NASA TR R-64,* National Aeronautics and Space Administration (1960).
53. BUTH, C. E., ARNOLD, A., CAMPISE, W. L. HIRSCH, T. J., IVEY, D. L., and NOEL, J. S., "Safer Bridge Railings." Report No. FHWA-RD-82-074.2 Vol. 4, App. C, Part 2, Federal Highway Administration, 255–359 (1984).
54. IVEY, D. L., ET AL., "Barriers in Construction Zones." Final report, three volumes, Contract DOT-FH-11-9485, Texas Transportation Institute, Texas A&M University (Mar. 1984).
55. ROSS, H. E., JR., Post, E. R., 'Warrants for Guardrail on Embankments." *Highway Research Record No. 460,* Highway Research Board (1973).
56. ROSS, H. E., JR., and Post, E. R., "Dynamic Behavior of an Automobile Traversing Selected Curbs and Medians." Research Report 1406, Texas Transportation Institute and Texas Highway Department (Jan. 1975).
57. DUNLAP, D. F., "Curb-Guardrail Vaulting Evaluation." *Highway Research Record No. 460,* Highway Research Board (1973).
58. SEGAL, GRIFFITH, "Studies of Curb Impacts Using the HVOSM." Contract DTFH61-83-C-00086 (Mar. 1985).
59. ALLEN, D. H., "Dynamic Response of Small Roadside Signs to Vehicle Impacts." Master of Engineering Report, Texas A&M University (June 1977).
60. IVEY, D. D., ET AL., "Safety Provisions for Support Structures on Overhead Sign Bridges." Volume 4 (Technical Memo 605-4), Final report, project HPR-2(107), Texas Transportation Institute, Texas A&M University (Sept. 1970).
61. OWENS, R. P., ET AL., "Safer Sign and Luminaire Supports: Task K—Correlation of Full-Scale, Laboratory, An-

alytical and Computer-Simulated Results." FHWA Report RD-76-35, Federal Highway Administration (Mar. 1976).

62. HINCH, J., ET AL., "Laboratory Procedures to Determine the Breakaway Behavior of Luminaire Supports in Mini-Sized Vehicle Collisions." Task D report, Contract DTFH61-81;-C-00036, ENSCO, Inc. (May 1985).
63. HINCH, J., ET AL., "Laboratory Procedures to Determine the Breakaway Behavior of Luminaire Supports in Mini-Sized Vehicle Collisions." Task E report, contract DTFH61-81-C-00036, ENSCO, Inc. (July 1985).
64. MAK, K. K., SICKING, D. L., and LOCK, J. R., "Rollover Caused by Concrete Safety Shaped Barrier." Final report, FHWA Contract DTFH-61-85-C-00129 (Aug. 1988).
65. BUTH, C. E., ET AL., "Safer Bridge Railing." Summary report on Contract DOT-FH-11-9181, Texas Transportation Institute, Texas A&M University (May 1983).
66. HIRSCH, T. J., "Bridge Rail to Restrain and Redirect Buses." Research Report 230-3, Texas Transportation Institute, Texas A&M University (Feb. 1981).
67. HIRSCH, T. J., STOCKER, A. J., and IVEY, D. L., "Energy-Absorbing Bridge Rail (Fragmenting Tube)." Texas Transportation Institute, Texas A&M University (Jan. 1970).
68. MICHIE, J. D., BRONSTAD, M. E., KIMBALL, C. E., JR., and WILES, E. O., "Upgrading Safety Performance in Retrofitting Traffic Railing Systems." Southwest Research Institute (Sept. 1976).
69. KIMBALL, C. E., JR., BRONSTAD, M. E., and MICHIE, J. D., "Heavy-Vehicle Tests of Tubular Thrie-Beam Retrofit Bridge Railing." *Transportation Research Record No. 796,* Transportation Research Board (1981).
70. BRONSTAD, M. E., KIMBALL, C. E., JR., and MCDEVITT, C. F., "Crash Test Evaluation of Barriers Installed on a Curved Off Ramp." *Transportation Research Record No. 868,* Transportation Research Board (1982).
71. STOUGHTON, R. L., ET AL., "Vehicle Impact Tests of a See-Through Collapsing Ring, Structural Steel Tube, Bridge Barrier Railing." Report No. FHWA-CA-TL-83-05, California Department of Transportation, Sacramento, Calif. (June 1983).
72. BRYDEN, J. E. and PHILLIPS, R. G., "Performance of Thrie-Beam Steel-Post Bridge-Rail System." *Transportation Research Record 1024,* Transportation Research Board (1985).
73. BEASON, W. L., ET AL., "A Low-Maintenance, Energy-Absorbing Bridge Rail." *Transportation Research Record No. 1065,* Transportation Research Board (1986).
74. HANCOCK, K. L., ET AL., "Crash Test Evaluation of Selected Bridge Rails." *Transportation Research Record,* Transportation Research Board (Jan. 1987).
75. "Testing of New Bridge Rail and Transition Designs." Contract DTFH61-86-C-00071, being performed by Texas Transportation Institute, Texas A&M University (in progress).
76. JEHU, V. J., and LAKER, I. B., "The Cable and Chain-Link Crash Barrier." *Rep. L R 105,* British Road Research Laboratory (1967).
77. MICHIE, J. D., CALCOTE, L. R., and BRONSTAD, M. E., "Guardrail Performance and Design." *NCHRP Report 115* (1971) 70 pp.
78. DAVIS, S., ET AL., "Test and Evaluation of Heavy Vehicle Barrier Concepts—Technical Report." Final report on Contract DOT-FH-11-9115, Dynamic Science, Inc., Phoenix, Ariz. (July 1981).
79. JEHU, V. J. and PEARSON, L. C., "Impacts of European Cars and a Passenger Coach Against Shaped Concrete Barriers." TRRL Report 801, Transport and Road Research Laboratory, Crowthorne, Berkshire, U.K. (1977).
80. GROB, H., "Anfahrversuche An Varianten Der Seilleitschranke System (British Ropes)." Mitterlung Nr. 43, Institut fur Strassen-, Eisenbahn-und Felsbau an der Eidgenossichen Technischen Hochschule Zurich, Zurich (Sept. 1979).
81. GROB, H., "Anfahrversuche Gladu-Planke." Schlussbericht, Institut fur Strassen-, Eisenbahn-und Felsbau an der Eidgenossichen Technischen Hochschule Zurich, Zurich (Mar. 1973).
82. IVEY, D. L., ET AL., "Tests and Evaluation of W-Beam and Thrie-Beam Guardrails." Final report on Contract DOT-FH-11-9485, Texas Transportation Institute, Texas A&M University (Mar. 1982).
83. BRONSTAD, M. E., KIMBALL, C. E. JR., and MCDEVITT, C. F., "SERB: A New High-performance Self-Restoring Traffic Barrier." *Transportation Research Record No. 796,* Transportation Research Board (1981).
84. ARNOLD, A., CAMPISE, W., and BUTH, E., "Thrie-Beam Weak-Post Guardrail System-Test Report No. 1." Texas Transportation Institute, Texas A&M University (June 1982).
85. BRYDEN, J. E. and PHILLIPS, R. G., "Roadside Barriers for Bridge-Pier Protection." *Transportation Research Record 1024,* Transportation Research Board (1985).
86. BRONSTAD, M. E., ET AL., "W-Beam Approach Treatment at Bridge Rail Ends Near Intersecting Roadways." *Transportation Research Record,* Transportation Research Board (1987).
87. HERRING, D. G., and BRYDEN, J. E., "W-Beam Guiderail Transition from Light to Heavy Posts." *Transportation Research Record,* Transportation Research Board (1988).
88. HIRSCH, T. J., DOLF, T., and ARNOLD, A., "Maryland Turned-Down Guardrail Terminal." Contract AW080-237-046, Texas Transportation Institute, Texas A&M University (Aug. 1982).
89. KIMBALL, C. E., ET AL., "Evaluations of Guardrail Breakaway Cable Terminals." Report No. FHWA/RD-82/057, Technical Report on Contract DOT-FH-11-9486, Southwest Research Institute, San Antonio, Tex. (May 1982).
90. "SENTRE—NCHRP 230 Certification Report." Energy Absorption Systems, Inc., One East Wacker Drive, Chicago, Ill. 60601 (May 1983).
91. HINCH, J. A., ET AL., "Safety Modification of Turned-Down Guardrail Terminals." Three volumes, Contract DOT-FH-11-9614, Report No. FHWA/RD-84/035 (June 1984).
92. BRONSTAD, M. E., and MAYER, J. B., JR., "Crash Test Evaluation of the Vehicle Attenuating Terminal (V-A-T)." Final report, Southwest Research Institute Project 06-1004 (May 1986).
93. WHITE, M. C., and HIRSCH, T. J., "Corrugated Steel Pipe Crash Cushion—Crash Tests and Evaluation." Contract No. DOT-FH-11-7840, Texas Transportation Institute, Texas A&M University (Nov. 1971).

94. WHITE, M. C., and HIRSCH, T. J., "Highway Crash Cushions." Special report on Contract No. CPR-11-5851, Texas Transportation Institute, Texas A&M University (Nov. 1971).
95. "Development of Impact Attenuators Utilizing Waste Materials." Final report on Task Order 6-1, NCHRP Project 20-7, Texas Transportation Institute, Texas A&M University (Oct. 1973).
96. HAYES, G. G., HIRSCH, T. J., and IVEY, D. L., "Dragnet Vehicle Arresting System." Texas Transportation Institute, Texas A&M University (Jan. 1970).
97. "Impact Attenuators—A Current Engineering Evaluation." Test reports for FHWA Contract DTFH61-83-C-00140, ENSCO, Inc. (1984–85).
98. CARNEY, J. E., III, ET AL., "The Connecticut Impact-Attenuation System." *Transportation Research Record 1024,* Transportation Research Board (1985).
99. "Hex-Foam Cell Sandwich Test Report." Energy Absorption Systems, Inc., One East Wacker Drive, Chicago, Ill. 60601 (May 1984).
100. "Crash Test Results of Hex-Foam Cartridges in GREAT Attenuators." Energy Absorption Systems, Inc., 860 South River Road, West Sacramento, Calif. 95691 (Mar. 1981).
101. STRIZKI, R., POWERS, J., JAGANNATH, M., and REILLY, E., "U-Post Investigation." *Transportation Research Record No. 488,* Transportation Research Board (1974).
102. CAMPISE, W. L., and ROSS, H. E., JR., "Performance Evaluation of the Post-Mate Punched Square Tube Signpost." Texas Transportation Institute, Texas A&M University (May 1984).
103. SZALAJ, W. M., and HOLLINGER, R. L., "New Jersey Breakaway Sign Testing." *Transportation Research Record 1024,* Transportation Research Board (1985).
104. NORDLIN, E. F., ET AL., "Dynamic Tests of Wood Post and Timber Pole Supports for Roadside Signs." Series XV, Materials and Research Department, California Department of Transportation, Report 635398 (Dec. 1967).
105. "Laboratory Procedures to Determine the Breakaway Behavior of Luminaire Supports in Mini-Sized Vehicle Collisions." ENSCO, Inc., Contract DTFH61-81-C-00036 (July 1985).
106. BEASON, W. L., and ROSS, H. E., JR., "A Truck-Mounted Portable Maintenance Barrier." *Transportation Research Record No. 1024,* Transportation Research Board (1985).
107. MORGAN, J. R., ET AL., "Emergency Opening System for Authorized Vehicle Lanes." *Transportation Research Record No. 1024,* Transportation Research Board (1985).
108. CAMPISE, W. L., and ROSS, H. E., JR., "Test and Evaluation of Neighborhood Mailbox." Research Report 343-2, Texas Transportation Institute, Texas A&M University (Mar. 1984).
109. NORDLIN, E. F., "Crash Test Evaluation of a Movable Concrete Construction Barrier." *Transportation Research Record,* Transportation Research Board (1987).
110. FALLER, R. K., ET AL., "Full-Scale Vehicle Crash Tests on Nebraska Rural Mailbox Designs." *Transportation Research Record,* Transportation Research Board (1988).
111. IVEY, D. L., and MORGAN, J. R., "Timber Pole Safety By Design." *Transportation Research Record No. 1065,* Transportation Research Board (1986).
112. EDWARDS, T. C., ET AL., "Development of Design Criteria for Safer Luminaire Supports," *NCHRP Report 77,* Highway Research Board (1969) 82 pp.
113. IVEY, D. L., ET AL., "Safety Provisions for Support Structures on Overhead Sign Bridges, Volume 4—Testing Program." Technical Memorandum 605-4, Contract No. FH-11-7032, Texas Transportation Institute, Texas A&M University (1970).
114. OWINGS, R. P., ET AL., "Safer Sign and Luminaire Supports—Task L, Final Report." FHWA Report No. FHWA-RD-76-36, ENSCO, Inc. (Oct. 1975).

APPENDIXES—A THROUGH H

Appendixes A through H are not published herewith, but are contained in a separate volume, as submitted by the research agency to the sponsors. Volume II, Final Report Appendices, "Roadside Safety Design for Small Vehicles," November 1988, is available for purchase at a nominal cost, upon written request to the NCHRP. The contents are listed here for the reader's convenience.

TABLE OF CONTENTS—VOLUME II

THE TRANSPORTATION RESEARCH BOARD is a unit of the National Research Council, which serves the National Academy of Sciences and the National Academy of Engineering. It evolved in 1974 from the Highway Research Board which was established in 1920. The TRB incorporates all former HRB activities and also performs additional functions under a broader scope involving all modes of transportation and the interactions of transportation with society. The Board's purpose is to stimulate research concerning the nature and performance of transportation systems, to disseminate information that the research produces, and to encourage the application of appropriate research findings. The Board's program is carried out by more than 270 committees, task forces, and panels composed of more than 3,300 administrators, engineers, social scientists, attorneys, educators, and others concerned with transportation; they serve without compensation. The program is supported by state transportation and highway departments, the modal administrations of the U.S. Department of Transportation, the Association of American Railroads, the National Highway Traffic Safety Administration, and other organizations and individuals interested in the development of transportation.

The National Academy of Sciences is a private, nonprofit, self-perpetuating society of distinguished scholars engaged in scientific and engineering research, dedicated to the furtherance of science and technology and to their use for the general welfare. Upon the authority of the charter granted to it by the Congress in 1863, the Academy has a mandate that requires it to advise the federal government on scientific and technical matters. Dr. Frank Press is president of the National Academy of Sciences.

The National Academy of Engineering was established in 1964, under the charter of the National Academy of Sciences, as a parallel organization of outstanding engineers. It is autonomous in its administration and in the selection of its members, sharing with the National Academy of Sciences the responsibility for advising the federal government. The National Academy of Engineering also sponsors engineering programs aimed at meeting national needs, encourages education and research, and recognizes the superior achievements of engineers. Dr. Robert M. White is president of the National Academy of Engineering.

The Institute of Medicine was established in 1970 by the National Academy of Sciences to secure the services of eminent members of appropriate professions in the examination of policy matters pertaining to the health of the public. The Institute acts under the responsibility given to the National Academy of Sciences by its congressional charter to be an adviser to the federal government and, upon its own initiative, to identify issues of medical care, research, and education. Dr. Samuel O. Thier is president of the Institute of Medicine.

The National Research Council was organized by the National Academy of Sciences in 1916 to associate the broad community of science and technology with the Academy's purpose of furthering knowledge and advising the federal government. Functioning in accordance with general policies determined by the Academy, the Council has become the principal operating agency of both the National Academy of Sciences and the National Academy of Engineering in providing services to the government, the public, and the scientific and engineering communities. The Council is administered jointly by both Academies and the Institute of Medicine. Dr. Frank Press and Dr. Robert M. White are chairman and vice chairman, respectively, of the National Research Council.